Kokate Rutika A., Formulation, characterization and validation of CpG functionalized PLGA bacteriomimetic nanoparticles for breast cancer immunotherapy. Doctor of Philosophy (Biomedical Sciences), April, 2015, 147 pp., 6 tables, 32 figures, bibliography, 143 titles.

Targeted Immunotherapy represents a potential and innovative means to combat cancer. Cancer vaccines designed against a specific tumor antigen have been efficiently utilized to trigger immune responses against tumor cells. Despite the preliminary evidence in animal models, low immunogenicity is one of the major hurdles in the development of vaccines in humans. Several approaches including the use of an “ideal” tumor antigen, appropriate delivery techniques, immune boosting strategies with co-stimulatory molecules are being explored to surmount this obstacle. The goal of this dissertation project was to utilize polymeric nanoparticles (NPs) as a vehicle to deliver Tumor Associated Antigen (TAA) that would elicit a strong antitumor immune response. In the present study, we successfully formulated CpG surface functionalized Tag encapsulating PLGA nanoparticles (CpG-NP-Tag) and tested their efficacy using *in vivo* and *ex vivo* experimental models. Specifically, we developed and characterized NPs for physicochemical properties including particle size, surface charge, surface morphology, Polydispersity index (PDI), encapsulation efficiency and CpG ligand binding efficiency. CpG-NP-Tag NPs were found be of desired size (220-230 nm) and surface charge (negative zeta potential). Particles were non agglomerated, spherical in shape and uniform in size with PDI in the range of 0.03-0.1. Due to the hydrophobic nature of the encapsulated entity (Tag), the encapsulation efficiency was limited to 30-40%. CpG ligand conjugation on the surface of NPs

was confirmed using Fluorescence Correlation Spectroscopy (FCS). CpG ligand binding efficiency was found to be around 10-14%. We also found that CpG-NP-Tag NP formulation had desired properties (size, charge and morphology) for efficient uptake by phagocytic antigen presenting cells (APCs) such as dendritic cells (DCs).

The major aim of our studies was to test the antitumor efficacy of NPs. Using a prophylactic syngenic Balb/c mice model, we demonstrated that CpG-NP-Tag can serve as an efficient tool to bolster antitumor immunity and thus could be used as a platform for the development of NP based immunotherapeutic interventions in future. We found that CpG-NP-Tag NP immunization attenuated tumor growth, proliferation, angiogenesis and induced apoptotic tumor cell death. These NPs indicated immunostimulatory potential by enhancing tumor $CD4^+$ and $CD8^+$ T cell infiltration as well as local IFN-γ production. Overall, from these *in vivo* studies we concluded that CpG-NP-Tag promotes IFN-γ secretion which possibly mediates the inhibited tumor growth, angiogenesis and enhanced T cell mediated immunity which facilitates tumor cell death via apoptosis.

To understand the mechanism by which CpG-NP-Tag imparts antitumor effects we used *ex vivo* model of APCs. Studies were conducting using Bone Marrow Derived Dendritic Cells (BMDCs) isolated from female Balb/c mice. We demonstrated enhanced NP uptake, preferential Endosomal localization, and increased population of CD80/86 expressing BMDCs in case of CpG-NP-Tag pulsed BMDCs indicating these NPs could serve as candidates for DC based vaccines in future.

In summary, both *ex vivo* and *in vivo* studies conducted with CpG-NP-Tag NPs provide insight in the development of particulate vaccines in cancer immunotherapy.

FORMULATION, CHARACTERIZATION AND VALIDATION OF CpG FUNCTIONALIZED PLGA BACTERIOMIMETIC NANOPARTICLES FOR BREAST CANCER IMMUNOTHERAPY

RUTIKA KOKATE, MS

APPROVED:

_____

Major Professor

_____

Committee Member

_____

Committee Member

_____

Committee Member

_____

Committee Member

_____

Dean, Graduate School of Biomedical Sciences

FORMULATION, CHARACTERIZATION AND VALIDATION OF CpG FUNCTIONALIZED PLGA BACTERIOMIMETIC NANOPARTICLES FOR BREAST CANCER IMMUNOTHERAPY

PhD THESIS

Presented to the Graduate Council of the

Graduate School of Biomedical Sciences

University of North Texas

Health Science Center at Fort Worth

in Partial Fulfillment of the Requirements

For the Degree of

DOCTOR OF PHILOSOPHY

By

RUTIKA KOKATE, MS

Fort Worth, Texas

April 10, 2015

ACKNOWLEDGEMENTS

I strongly believe that this exciting PhD journey would not be completed successfully without the support and blessings of my parents, husband, friends and family who have always been there with me through thick and thin situations in my career.

Firstly, I would like to thank my mentor, guide, Dr. Harlan Jones, Department of Molecular and Medical Genetics, University of North Texas Health Science Center (UNTHSC), Fort Worth for keeping patience and giving me unconditional support and constant motivation throughout the last 4 years. I would also like to thank my co-mentor Dr. Jamboor Vishwanatha and all his lab members at UNTHSC for allowing me to use his lab facility. I would like to acknowledge and extend my heartfelt gratitude to few important people, who have made the completion of this practicum project possible; Dr. Sanjay Thamake, PhD, Scientist, RadioMedix Inc., Houston, TX for initiating this project and training me with nanoparticle formulation technology, animal handling and guiding me as a friend to take apt decisions and make right choices in tricky situations. Dr. Pankaj Chaudhary, PhD, Post-doctoral Fellow, in Dr. Vishwanatha's lab, for his immense help in confocal microscopy experiments and helpful discussions and tips regarding manuscript writing. Dr. Sangram Raut, PhD, Post-doctoral Fellow, Dr. Gryczynski's group, Center for Fluorescence Technology and Nanomedicine (CFTN), for his help as a co-author in analyzing some data, planning and executing important experiments through the CFTN group and also helping me with manuscript editing. I would also like to thank him for being very good friend and giving apt advice in crucial situations.

Lastly, I would like to thank my friends, roommate Ms. Bhuvaneshwari Koneru, my in laws, special thanks to my husband, Mr. Srinivas Patkar for bearing with me and being there for me in all stressful professional as well as personal situations.

LIST OF PUBLICATIONS

1. **Rutika Kokate**, Pankaj Chaudhary, Xiangle Sun, Sayantan Maji, Sanjay Thamake, Rahul Chib, Jamboor K. Vishwanatha and Harlan Jones. Rationalizing the use of functionalized PLGA nanoparticles for DC targeted anticancer therapy (Manuscript in preparation).
2. **Rutika Kokate**, Sanjay Thamake, Brittney Mott, Pankaj Chaudhary, Jamboor K. Vishwanatha and Harlan Jones. Tumor Antigen Encapsulated Nanoparticles Functionalized with CpG attenuates Tumor growth in Syngeneic Mouse Model of Breast Cancer. *Nanomedicine Future Medicine*. (In press March 2015).
3. Sangram Raut, Ryan Rich, Rafal Fudala, **Rutika Kokate**, Joe Kimball, Jamboor Vishwanatha, Zygmunt Gryczynski, Ignacy Gryczynski. BSA Au Clusters as a Probe for Enhanced Fluorescence Detection Using Multi-pulse Excitation Scheme. *Curr Pharm Biotechnol*. 2014 May; 14(13):1139-44.
4. Sangram Raut, Rafal Fudala, Ryan Rich, **Rutika Kokate**, Rahul Chib, Zygmunt Gryczynski, Ignacy Gryczynski. Long lived BSA Au clusters as a time gated intensity imaging probe. *Nanoscale*. 2014 March; 6(5):2594-7.
5. Sangram Raut, Ryan Rich, Rafal Fudala, Susan Butler, Rutika Kokate, Zygmunt Gryczynski, Rafal Luchowski, Ignacy Gryczynski. Resonance energy transfer between fluorescent BSA protected Au nanoclusters and organic fluorophores. *Nanoscale*. 2014 Jan; 6(1):385-91.
6. Badri P Maliwal, Rafal Fudala, Sangram Raut, **Rutika Kokate**, Thomas J Sørensen, Bo W Laursen, Zygmunt Gryczynski, Ignacy Gryczynski. Long-lived bright red emitting azaoxa-triangulenium fluorophores. *PloS One*. 2013 May; 8(5):e63043.

7. Sushil Kumar, **Rutika A**. **Kokate**, Mukesh Sahu, Pankaj Chaudhary, Rajendra Sharma, Sanjay Awasthi, Yogesh C. Awasthi. Inhibition of Mercapturic Acid Pathway-Mediated Disposal of 4-Hydroxynonenal Causes Complete and Sustained Remission of Human Cancer Xenografts in Nude Mice. *Indian J of Exp Biol*. 2011 November; 49(11):817-25.

TABLE OF CONTENTS

Page

ABBREVIATIONS

APC- Antigen Presenting Cell

BMDC- Bone Marrow Derived Dendritic Cells

BS3- Bis[sulfosuccinimidyl] suberate

CpG- Cytosine-phosphate-guanosine oligodeoxynucletide

DC- Dendritic Cell

EPR- Enhanced Permeability and Retention

NP- Nanoparticle

NPs- Nanoparticles

PLGA- Poly(lactic-co-glycolic acid)

PVA- Poly vinyl alcohol

PBS- Phosphate Buffered Saline

Tag- Tumor Antigen

TAP- Transporter associated with antigen processing

TEM- Transmission Electron Microscopy

SEM- Scanning Electron Microscopy

LIST OF TABLES

CHAPTER I

CHAPTER II

CHAPTER III

LIST OF ILLUSTRATIONS

CHAPTER II

CHAPTER III

CHAPTER IV

CHAPTER I

INTRODUCTION

Cancer Immunotherapy

Cancer is one of most common fatal diseases afflicting people globally. It is believed that cancer will become the leading cause of death across the US population in near future thus increasing the need for cancer therapeutics even more [1]. Cancer is a complex heterogeneous disease characterized by uncontrolled/unregulated division of cells "self" in nature [2]. Despite tremendous progress in the field of cancer biology, cancer remains one of the deadliest diseases to treat [3].

Conventional cancer treatment strategies including radiation, surgery and chemotherapy play a significant role in the treatment of primary tumors. However, what remains a significant challenge is cancer recurrence due to metastasis. The inherent ability of the immune defense system to recognize and destroy cancer cells is believed to hold promise toward the eradication of cancers. Researchers are therefore aggressively seeking novel ways to exploit immune function for cancer prevention.

William B. Coley, considered a pioneer in the field of cancer, introduced the concept of immunotherapy by identifying the potential of immune cells in treating cancers and designed a crude vaccine known as 'Coley's Toxin' consisting of killed bacteria that was administered to cancer patients. The patients presented with fever and chills but complete remission of their cancer in some cases [4,5]. His experiment served as a stepping stone for future cancer immunotherapy [6]. Progress toward advances in cancer immunotherapy however, was not without

initial setbacks. A significant hurdle was attributed to the difficulty of *in vitro* culturing immune cells, particularly lymphocytes *in vitro*. In 1976, interlukin-2 (IL-2), previously known as the T cell growth factor was cloned and was noted for its ability to support the growth of T lymphocytes *ex vivo*. Studies thereafter, were able to examine the role of T lymphocytes against cancer cells, leading to the first characterization of a cancer antigen in 1991 [7]. Based on this and other studies, it became widely accepted that the immune system could detect cancer cells and kill them [8]. Such observations also led to the concept that cancer cells express specific proteins (antigens) on their surface which may be specific or over expressed and may not be found or scarcely expressed in normal cells.

Tumor antigens are primarily characterized as two major types [9].Tumor Specific Antigens (TSAs) are unique to cancer cells and are not expressed on normal cells. TSAs may arise due to point mutations in genes. They may be unique to an individual or may be expressed in various tumors but not normal tissues. The second major type of tumor-antigens is termed Tumor Associated Antigens (TAAs). TAAs are expressed by both tumor and normal cells. They are not tumor specific and their use may result in autoimmunity against normal tissue expressing that Antigen. Examples include ~~MAGE, GAGE, and NY-ESO1~~ [10].

Despite the ability of our immune system to recognize unique antigens expressed by tumor cells, they also have the ability to avoid immune attack by employing several “tricks” termed “tumor immune escape”. The Tumor microenvironment for example, consisting of masses of tumor cells and surrounding stroma forms a barrier, limiting immune cell invasion of the primary tumor. In addition, cancer cells may secrete some immunosuppressive substances that may inhibit the immune response [11,12]. Furthermore, the immune system may consider cancer cells as “self” since they are of the same origin expressing very similar antigens. Most

noted is the ability to express self-antigen in the context of the Major Histocompatibility Class I (MHC I) complex expressed on the surface of tumor cells that is recognized by host immune cells as a non-threatening signal. Thus, the body's immune system behaves "blind" to cancer cells. This phenomenon is known as "tumor tolerance" [13]. There is also a possibility that the tumor cells expressing TSAs or TAAs, with MHC I are down regulated in their surface expression. Thus, allowing the tumor cell to hide from immune system by not displaying the antigenic peptide and thus fooling the immune system [14]. Together, these mechanisms of tumor escape make it difficult for the host's to initiate an optimal anti-tumor immune response. To recognize the full potential of immunotherapy, it will be necessary to develop novel approaches to elevate and/or complement immune-based vaccines. To this end, the ultimate goal of cancer immunotherapy must be: 1) To specifically target cancer cells; 2) To recruit efficient immune cells that are capable of generating a robust and long lasting response; and 3) most importantly prevent relapse [8].

Types of Cancer Immunotherapy

Cancer immunotherapy may involve passive or active immunotherapy alone or in combination with conventional cancer treatments.

1] Passive Immunotherapy:

Passive immunotherapy does not rely on the body's natural immune system to attack cancer cells but uses components of the immune system such as antibodies which can be made in the laboratory to target tumor antigens [13]. Some examples include Herceptin, Avastin, Rituxan, Campath, Zevalin [10].

Monoclonal Antibodies (mAb) are the most widely used form of targeted cancer immunotherapy in clinic today [15]. mAbs bind to a specific target (antigen) on tumor cell and their mode of action depends on their ability to engage with growth receptors or with proapoptotic targets inducing apoptosis of cancer cells. mAbs facilitate antigen presentation. As discussed before DCs are the major APCs of the immune system and play pivotal role in priming of tumor specific T cells. They express a variety of surface receptors and are capable of binding and internalizing Ag-Ab complexes, which eventually lead to their activation and maturation. Mature DCs present the antigenic peptide via MHC Class I or MHC Class II peptide complexes and thus are able to launch a T cell mediated response [16]. Herceptin and Cetuximab are examples of such mAbs that bind to HER2 and EGFR receptor respectively. These mAbs not only block the growth signaling cascade but also facilitate antigen presentation through formation of immune complexes which induces a potent T cell response. It was seen that the patients who received Herceptin treatment generated effective T cell responses. Additionally, mAbs may activate components of the immune system via Fc portion based interactions eventually promoting antibody-dependent cell-mediated cytotoxicity (ADCC) and complement-dependent cytotoxicity (CDC) by macrophages and NK cells [10]. Herceptin is known to mediate ADCC via NK cells and monocytes [16]. Likewise, cetuximab, the EGFR antibody also helps in DC priming and promotes antitumor responses. *In vitro* studies indicate that cetuximab augments DC opsonization of cancer cells and also helps in DC maturation. It also produces NK cell mediated ADCC and CDC which further enhances its tumoricidal activity. Currently, cetuximab is being tested in a phase II clinical trial in combination with a pancreatic cancer vaccine [16].

Cytokines such as *Interleukin 2 (IL-2) and Interferons (IFNs) and Interleukin-12 (IL-12) are also characterized as passive immunotherapy.* IL-2 is produced by activated T cells. ~~It~~ does

not primarily act on cancer cells; rather it acts as an adjuvant and stimulates immune reactions [17]. IL-2 therapy has been found to be effective in melanoma and metastatic renal cell carcinoma. ~~But it is~~ associated with a side effect known as vascular leak syndrome [18]. *IFNs* are inflammatory cytokines that are produced by the body in response to certain infections. It has been shown that IFN-α inhibits proliferation of tumor cells and also as anti-angiogenic activity against leukemia and lymphoma. It is used as an adjuvant therapy and facilitates activation of immune cells [19,20]. IL-12 is an interleukin that is involved in differentiation of naïve T cells into T-helper Th1 or Th2 cells. It activates CTLs, NK cells and supports growth and function of T cells. Combination of HER2 mAb with systemic IL-12 has shown to decrease tumor progression and increase tumor necrosis as compared to treatments given individually. Recently, a phase I clinical trial, using combination of IL-2 with Herceptin and paclitaxel has shown increased production of IFNs [16].

One obvious drawback with mAbs would be that the immune system may recognize these mAbs as foreign and may launch an immune response against them which may lead to several allergic reactions. But over the years, researchers have surmounted this obstacle by designing "chimeric" or humanized antibodies achieved by replacing some parts of the mouse antibody proteins with human proteins [1910]. Additional limitations of mAb therapy are listed in the Table 1.

Table 1. Limitations of Monoclonal Antibodies (mAb)
1. Change in expression level of target antigen due to mutations.
2. Use restricted to a subgroup of patients expressing the unique antigen.
3. Difficult to get a significant therapeutic response avoiding autoimmunity
4. Tumor microenvironment is particularly immunosuppressive limiting mAb success.

2] Active Immunotherapy

"Cancer vaccines" are considered as active immunotherapy as they boost the body's immune system to defend against cancer. Recently, active immunotherapy in the form of cancer vaccines has indicated some encouraging and promising results in many clinical trials [13]. Active Immunotherapy may be divided into to sub-categories, prophylactic or therapeutic.

Prophylactic Cancer Vaccines are aimed to prevent cancer in patients who may be at high risk of developing cancer due to genetic predisposition or environmental factors. These function as "traditional vaccines" like flu vaccine. Prophylactic cancer vaccines target infections that may lead to development of cancer. The US FDA has approved two vaccines namely- Gardesil and Cervarix against Human Papilloma Virus (HPV) which is responsible for 70 percent cases of cervical cancer [21]. Gardasil utilizes HPV antigens as proteins. These proteins are processed in the laboratory to synthesize four different types of 'virus like particles' or VLPs which are combined to form a cocktail that is effective against HPV infections of type 6, 11, 16 and 18. This is superior to traditional vaccines consisting of weak or inactivated whole microbes which may sometimes be infectious [13]. Similarly, Cervarix is composed of proteins from HPV type 16 and 18. US FDA has also approved vaccine against Hepatitis B virus (HBV) infection which is known to cause liver cancer. In all cases mentioned above the causative infectious agent is known. But the formulation of therapeutic vaccines in other types of cancer wherein the etiology is unclear would be a challenging task for future scientists [21].

Therapeutic vaccines are intended to treat existing tumor. Once cancer is diagnosed, solid accessible tumor may be removed by surgery, chemotherapy or radiation therapy. After surgery the patient is vaccinated to develop a specific immune response to kill residual cancer cells and thus prevent relapse [22,23]. Examples of therapeutic vaccines are listed in Table 2.

Table 2. Therapeutic Cancer vaccines	
➢ **Whole Cell based vaccines**	➢ **Synthetic protein antigen vaccines**
This approach uses inactivated whole tumor cells that display a variety of known or unknown oncogenic antigens on their surface against which the body's immune system develops an antitumor response.	These are synthetically produced tumor specific antigens that can generate immune response in body against cancer cells displaying this antigen.
This approach may overcome the problem of identifying specific tumor antigen, majority of which are unknown till today but is still associated with the risk of autoimmunity.	This therapy is will produce a more tumor specific immune response compared to whole cell approach.
Whole cell vaccines may be autologous or allogenic: • *Autologous:* If the tumor cells are obtained from patient itself then it is known as an autologous or self tumor cell vaccine [24]. • *Allogenic:* if tumor cells are obtained from another individual having the same cancer then it may be called as an allogenic or donor vaccine [25] • *Dendritic Cell (DC) based vaccines:* These may be either *ex vivo* or *in vivo* and are explained in detail in the next section.	Often combined with adjuvants that help to further enhance immune response [26]. Examples of synthetic protein antigen based vaccines include: Melanoma: MART-1, tyrosinase, gp-100 [27]. Breast and ovarian cancer: Sialyl-Tn (STn) [28] Pancreatic, Lung, Colorectal, Breast, and Ovarian Cancers: Carcinoembryonic antigen (CEA) [29]

DC based vaccines have become a very popular form of cancer vaccine therapy. These are safe for use in humans. Two approaches may be used to design such vaccines [30,31]: *Ex vivo* and *in vivo* which are outlined in Table 3.

Table 3: Dendritic Cell Based Vaccines	
Ex Vivo	***In Vivo***
In this approach, DCs may be loaded with antigen by culturing DCs obtained from patients with a tumor specific antigen and an adjuvant *(ex vivo)* that will induce DC maturation. These cells are injected back into the patient.	DCs may be induced to take up tumor antigen *in vivo*. Antitumor responses may take time to build but responses may be robust and long lasting.
This method involves ex vivo culture of the DCs in the laboratory and thus may have higher risk of endotoxin contamination.	Since DCs are induced in vivo to take up the tumor antigen considerable lesser risk of endotoxin contamination.
Cultured DCs should not loose migratory capacity to lymph nodes	No risk of loss of migratory capacity for in vivo based vaccines
Does not require targeting of DCs	This approach will require optimum *in vivo* targeting of DCs.
May be laborious and time consuming	Relatively less laborious and time consuming

Unfortunately, initial attempts to design cancer vaccines were not very successful as the actual mechanism of immunization was unclear. Now that the function of DCs in generating a potent T cell response is known, many clinical trials are exploiting this concept. DC based vaccines are being tested for a variety of cancers such as prostate, colorectal, kidney, breast cancer, melanoma, leukemia, lymphoma and other tumor malignancies [32,33].

Cancer vaccines are designed to target the cancer cells with the help of the immune system and so the success of cancer vaccines largely depends on the status of the individual's immune system receiving the vaccine. Factors affecting the immune system include: Age [34], Immune suppression due to tumor microenvironment [35], substances secreted by tumor or other immunosuppressive drugs like glucocorticoids or analgesic or anesthetic drugs [36], Nutritional supplements enhance the function of immune cells that play a key role in cancer immunotherapy. Previous studies in cancer patients indicate that nutritional supplements improve the immune system function that may be adversely affected due to existing tumor or surgery [37]. Despite of

tremendous research that is currently going on in the field of cancer vaccines, major hurdles still impedes the success of cancer vaccines (Table 4).

Table 4. Limitations of Cancer Vaccines	
1.	***Variable Antigen expression:*** Although a variety of tumor associated antigens have been identified still these antigenic peptides differ in their ability to generate an effective immune response. Lately, tumor specific antigens have been discovered which further facilitate a tumor specific response sparing the healthy cells and ruling out the possibility of autoimmunity [13,38].
2.	***Low immunogenicity:*** Often cancer vaccines are unable to generate a strong immune response. This problem may be solved by incorporation of "immune boosters" such as IL-2 and Granulocyte-macrophage colony stimulating factor (GM-CSF) which act as co-stimulatory molecules and facilitate immune reactions [38].
3.	***Tumor microenvironment:*** Even if immune response is generated tumor microenvironment may neutralize it. So some strategies must be employed to break the immune suppressive nature of the tumor microenvironment
4.	***Loss of efficacy:*** Vaccine may render desired response initially but over the time immune response may diminish which might lead to relapse.

Nanoparticles: a novel drug delivery system

Nanodevices have garnered a reputation globally as carriers for therapeutic agents and many such nanocarriers have sparked interest of many pharmaceutical industries due to unique physical and chemical properties. To date, a number of nano-based products have been successfully launched in market or in the pipeline [39] to treat a wide variety of diseases. NPs can be formulated using a variety of materials such as lipids (liposomes), organometallic compounds (narbon nanotubes), polymers (polymeric NPs, micelles, dendrimers) [40]. Polymeric NPs prepared from biodegradable polymers being non-toxic in nature are being widely explored as controlled release delivery vehicles for proteins, peptides, plasmid DNA and low molecular weight compounds [41]. Apart from facilitating sustained release, such NPs protect the

encapsulated cargo from enzymatic degradation, metabolism and filtration [42]. Size and surface characteristic of NPs can be manipulated to achieve both passive and active targeting explained elaborately in the following section. Surface functionalization of NPs with targeting ligands such as antibodies allows site specific targeted delivery [43]. The goal of such drug delivery systems are to reformulate existing therapeutics/drug entities in order to extend their lifetime, and thereby increase effectiveness, safety and continue to be cost effective. Among all the types of NPs, polymer-based NPs have the potential to realize the holistic view of targeting encompassing variables such as route of administration, molecular characteristics and the temporal control of drug delivery [44].

Targeted Nanoparticles for Cancer Therapy

Currently, chemotherapy is the backbone of cancer treatment. However, antineoplastic drugs have low therapeutic index, target "fast proliferating cells" and are thus associated with non-specific killing of healthy non-cancerous cells [3]. NP drug delivery system has the potential to solve this problem. To reduce the non-specific toxicity, it is essential to deliver the drug at the site of tumor. Such preferential delivery can be achieved either by passive or active targeting. Passive targeting takes the advantage of "leaky" tumor vasculature and facilitates accumulation at tumor site due to enhanced permeability and retention (EPR) effect. But passive targeting lacks specificity to tumor cells as such and is accompanied with limitations such as low cellular uptake or decreased retention time at the tumor site which may compromise efficacy [43,45]. Active targeting on the contrary may prove to be a more beneficial route in such cases. Active route involves surface modifications of NPs to direct them to desired location. NPs can be surface

functionalized using chemical crosslinkers with monoclonal antibodies specific to tumor cell type which enhances cell specific delivery [43].

In the past decade researchers have tried to exploit all the unique properties of NPs for immunotherapeutic interventions. A number of studies have reported the use of surface functionalized NPs to target immune cell populations (particularly DCs) for cancer immunotherapy [46,47]. The last section sheds light on the details of how NPs (especially polymeric PLGA based NPs) could be utilized for the development of cancer vaccines in future.

PLGA nanoparticles and cancer vaccines

Literature suggests NPs have the ability to modulate cellular and humoral immune responses and could be potentially used as vaccine carriers for cancer therapy. Different types of NPs can be fabricated with unique properties based on their size, surface charge and composition to target a distinct immune cell population such as DCs and maximize the benefits of cancer vaccines [47]. Poly (lactide-co-glycolic acid) (PLGA) polymer based biodegradable and biocompatible micro/nano particles have been used as a platform for delivery of small drug molecules, proteins, peptides, oligonucleotides to a wide variety of cell populations including APCs of the immune system who are the keys players in the generation of both innate and adaptive immune responses. Many groups have demonstrated the capability of Ag-loaded PLGA NPs to induce both systemic and mucosal immunity in animal models [48-52]. Several studies also indicate these particles have inherent adjuvant properties comparable to alum compounds and can serve as synthetic adjuvants to activate DCs and induce Ag specific T cell immunity [48,49,53]. Encapsulation of Ag in PLGA NP offers distinct advantages over soluble Ag formulations: (i) Protection of Ag from preteolytic degradation and delivering Ag in a controlled fashion to

phagocytic cells (mainly DCs) in a targeted manner (ii) restricting entry of Ag in systemic circulation (iii) facilitate MHC Ag presentation and cross presentation better than soluble Ag (iv) most importantly provide co-delivery of Ag and immune stimulants such as Toll-like receptor (TLR) agonists to the same APC. Impaired DC function due tumor related immune suppression is one of the major hurdles in success of cancer vaccines. Vaccination models focusing on the simultaneous delivery of Tag and TLR ligands to the same APC (mainly DC) can provide both targeted delivery to DC as well as immune activation and thereby help in overcoming tumor resistance [54,55]. In the thesis project elaborated below, we have formulated PLGA NPs encapsulating breast Tag (membrane lysate of tumor cells) and surface functionalized them with TLR9 ligand, CpG, and tested their efficacy *in vivo* and *ex vivo* models.

Rationale and objectives of the proposed project

About 1 in 8 women in USA will develop invasive breast cancer over the course of their lifetime with death rates being higher than any other cancer besides lung cancer [56]. Although current treatment strategies such as radiation, chemotherapy, or a combinatorial approach have been partially successful in limiting primary breast tumors, the five year recurrence rates for breast cancer are still around 20-30%. Thus, there is a need to develop alternative treatment modalities that could be used in conjunction with the existing therapies to reduce the probability of relapse [57].

Identification of tumor antigens at the molecular level has provided a large stimulus for the development of targeted cancer vaccines. However, because tumor antigens are not immunogenic by themselves; low immunogenicity is one of the major hurdles in the

development of cancer vaccines in humans. A better understanding of the interaction between the immune system and the tumor microenvironment has led to an emerging field of cancer immunotherapy [16]. The objective of cancer immunotherapy is essentially to harness the body's immune system to specifically target cancer cells, provide robust and long lasting immune responses that reduces the rate of relapse [58]. To combat this problem, various approaches such as use of an "ideal" tumor antigen, appropriate delivery techniques and the use of costimulatory molecules like granulocyte macrophage-cell stimulating factor (GM-CSF) are being explored to overcome obstacles associated with tumor immune evasion [59].

One major obstacle in the success of cancer vaccines is the development of safe, non-toxic and clinically relevant delivery vehicle or system. NPs made from a biocompatible polymer such as poly (lactic-co-glycolic acid) (PLGA) have been successfully utilized to deliver anticancer drugs (e.g. chemotherapeutic agents) at the tumor site [60]. NP-based delivery systems in general offer several benefits such as improved pharmacokinetic profile, targeted delivery and improved stability. Encapsulating Tag within NPs could overcome the inefficient delivery of Tag to the APCs by preventing the degradation of Tag by extracellular proteolytic enzymes; thereby increasing Tag uptake by APCs. Secondly, NP-encapsulation of Tag provides sustained release, all of which has a role to play in potent activation of APCs [61]. Tumor lysates, peptides and antigens encapsulated within NPs have been shown to induce specific antitumor responses [57,62,63]. Another concern in the success of cancer vaccines is generating an immune response that can overcome the immunosuppressive tumor microenvironment [64]. Escape mechanisms by tumors such as the release of immune-suppressive cytokines promote an overall inhibitory effect on the antitumor immune response [64,65]. Tumors are also capable of recruiting immune cells such as tumor-associated macrophages (TAMs) and regulatory T cells (Tregs) that promote tumor

development [66]. TLR agonists including CpG ODN have been effectively used to counter mechanisms of immune tolerance by improving the function of professional APCs (plasmacytoid dendritic cells and B cells in particular) [67]. CpG-ODNs are synthetic oligodeoxynucleotides containing CpG motifs predominantly found in bacterial DNA as compared to mammalian DNA. CpG ODN is a TLR-9 agonist that binds specifically to TLR-9 present on the endosomes of the APCs. TLR-9 CpG binding leads to the activation of NF-κB via a MyD88 mediated signaling pathway that mediates the release of pro-inflammatory cytokines such as type I interferons (IFNs) that orchestrate innate and adaptive immune responses [68-71]. Specifically, it has been found that type I IFNs produced by host APCs play a critical role in generating potent antitumor immunity [72]. To date, clinical trials have shown CpG ODNs possess a good safety profile and enhance the immunogenicity of cancer vaccines as adjuvants [73]. Based on current findings, we believe that CpG coated Tag containing NPs (CpG-NP-Tag) is attractive approach to elicit immune activation by mimicking bacterial infection ("bacteriomimetic") and by preferentially being recognized and processed by APCs to generate a potent antitumor immune response.

Previous studies have shown that antibody coated NPs can be engineered using a homo-bifunctional chemical cross-linker, bis (sulfosuccinimide) suberate (BS3) for targeted delivery of curcumin to breast cancer cells [43]. Taking advantage of this technology, the overall goal of this study was to formulate; characterize and evaluate the efficacy of "bacteriomimetic NPs (CpG-NP-Tag)"as a therapeutic option for immune-based strategies against breast cancer. Outlined below are the objective, hypothesis and the specific aims laid down to test the hypothesis for this project:

Objective: The objective of this study was to synthesize "bacteriomimetic" NPs by cytosine-phosphate-guanosine oligodeoxynucletide (CpG) surface functionalization of tumor antigen encapsulating NPs and evaluate its efficacy in generating strong anti-tumor response.

Hypothesis: We hypothesize that CpG coated "bacteriomimetic" NPs encapsulated with breast Tag such as membrane lysate of breast tumor cells (CpG-NP-Tag) will enhance delivery of antigen to APCs which can launch a selective and strong immune response against breast tumor cells.

Specific Aims

Specific Aim 1:

Formulation and characterization of CpG coated NPs encapsulated with Tag (CpG-NP-Tag).

The **rationale** behind this specific aim is that NPs encapsulating a breast Tag, either dead tumor cells, membrane lysates or peptides, coated with a bacterial ligand such as CpG Oligodeoxynucleotide (ODN), which mimics bacterial infection and acts as an immune stimulant, will efficiently deliver the antigen to APC's and overcome the problem of tumor resistance due to immune surveillance escape.

Specific Aim 2: *In vivo* evaluation of the "bacteriomimetic NPs" to induce potential $CD4^+$ and $CD8^+$ T cell responses against breast cancer cells in a syngenic breast cancer BALB/c mice model.

The **rationale** supporting this specific aim is that CpG-NP-Tag NPs will induce a potent antitumor $CD4^+$ and $CD8^+$ T cell response against the 4T1 tumor cells. We will pre-immunize BALB/c mice with CpG followed by secondary immunization using respective NPs (CpG-Blank NP; NP-Tag and CpG-NP-Tag) 7 days before tumor challenge. Subsequently, mice will be

challenged with 4T1 tumor cells. Primary tumor size will be measured using vernier caliper. Tumors will be harvested at day 14 or day 28. $CD4^+$ and $CD8^+$ T cell response in the spleen will be quantified using flow cytometry. Immunohistochemistry will be conducted to observe $CD4^+$ and $CD8^+$ T cell infiltration of the primary tumor tissue.

Specific Aim 3: To investigate the mechanism through which "bacteriomimetic NPs" induce a potent cell mediated adaptive anti-tumor immune response.

The rationale supporting this specific aim is CpG-NP-Tag NPs will be endocytosed by the APCs such as the dendritic cells which will further process the antigen and present it to the T cells to generate a potent $CD4^+$ and $CD8^+$ T cell response against the Tag. For this aim we will conduct *ex vivo* experiments to evaluate the activation and maturation of NP pulsed APCs as well as some functional assays to indicate T cell activation.

Significance

Breast cancer is the second leading cause of death in American women after lung cancer [56]. Although the available treatment therapies have been partially successful to limit primary breast cancer but still the five year recurrence rates are around 20-30%. Thus, there is a need to develop alternative treatment modalities that could be used in conjunction with the existing therapies [57]. Cancer vaccines based on tumor associated antigens (TAA) have been effectively used as an adjuvant treatment for breast cancer. But low immunogenicity remains to be a major obstacle. To surmount this problem new approaches are being investigated. The use of CpG coated Tag containing "bacteriomimetic" NPs will serve as a novel technique to evoke a dual immune response – non-specific immune stimulation by the use of common bacterial/viral antigens such as CpG / HA peptide and Tag specific T cell mediated response eventually

providing a robust and a long-lasting immune response. Thus, “bacteriomimetic” NPs will serve as a platform for the development of immune based therapeutic vaccines in future which could be efficiently used as an adjuvant therapy along with surgery, radiation and chemotherapy. Validation of this system in mice model will be of translational importance for breast cancer therapy.

Innovation

There are two innovative aspects of this study; a) methodology of NP formulation for better encapsulation and rapid functionalization of bacterial antigen at NP surface and b) use of common antigens for pre-immunization, such as CpG in this model or influenza peptide in human model, to elicit memory response leading to enhanced uptake and consecutive antigen presentation. Based on our studies, we are confident that this innovative approach could be validated for tumor size regression and enhanced immunity against breast cancer. Thus, CpG coated tumor antigen containing NPs will function as a novel tool to deliver tumor antigen to the APCs and thereby boost body’s immunity against breast or other types of cancer. Overall, positive outcomes obtained from this study will serve as a stepping stone for the development of nanoparticle based therapeutic cancer vaccines in future which could be efficiently used as an adjuvant therapy along with surgery, radiation and chemotherapy.

CHAPTER II

ENHANCEMENT OF ANTITUMOR EFFECT OF PARTICULATE VACCINE DELIVERY SYSTEM BY "BACTERIOMIMETIC" CpG FUNCTIONALIZATION OF PLGA NANOPARTICLES

Rutika A. Kokate[1,2], Sanjay I. Thamake[1,2,#], Pankaj Chaudhary[1,2], Brittney Mott[1], Sangram Raut[1], Jamboor K. Vishwanatha*[1,2] and Harlan P. Jones*[1,2]

[1] *Department of Molecular and Medical Genetics, University of North Texas Health Science Center (UNTHSC), Fort Worth, TX 76107, USA*

[2] *Institute of Cancer Research, UNTHSC, Fort Worth, TX 76107, USA*

[#] *Current Address:*

RadioMedix Inc., Houston, TX 77042, USA

* Corresponding Authors: Department of Molecular and Medical Genetics, UNTHSC, 3500 Camp Bowie Blvd, Fort Worth, TX 76107, USA.

E-mail address: Harlan P. Jones (Harlan.Jones@unthsc.edu) and Jamboor K Vishwanatha (Jamboor.Vishwanatha@unthsc.edu). Phone: 817-735-2448/0494; Fax: 817-735-0180/0243

1. ABSTRACT

Low immunogenicity remains a major obstacle in realizing the full potential of cancer vaccines. In this study, we evaluated cytosine-phosphate-guanosine oligodeoxynucletide (CpG) coated tumor antigen (Tag) encapsulating “bacteriomimetic” nanoparticles (CpG-NP-Tag NPs) as an approach to enhance antitumor immunity. CpG-NP-Tag NPs were synthesized, characterized for their physicochemical properties and tested *in vivo.* We found CpG pre-dosing followed by intraperitoneal (IP) immunization with CpG-NP-Tag NPs significantly attenuated tumor growth in female BALB/c mice compared to respective controls. Histopathological and Immunofluorescence data revealed CpG-NP-Tag tumors had lower proliferation, higher apoptotic activity, greater $CD4^+$ and $CD8^+$ T cell infiltration as well as higher IFN-γ levels as compared to control groups. Our findings suggest CpG-NP-Tag NPs can enhance anti-tumor effect of nanoparticulate tumor vaccination system.

KEYWORDS: Breast Cancer, Immunotherapy, Antigen, Vaccines, Nanoparticle (NP).

2. INTRODUCTION

Nanoparticulate drug delivery systems for vaccines and immunotherapy are being widely studied [74]. Such systems have been tested in infectious disease models, viral infections as well as cancer [75]. Although cancer is a disease of self-cells, the immune system is capable of producing exquisite and specific response against it. However, such response is not enough for preventing the growth and spread of cancer [76]. NP mediated cancer immunotherapeutic approaches have shown promise in enhancement of host immune responses against cancer antigens and are being explored as a novel alternative approach for cancer treatment [77]. NPs made from a biocompatible polymer such as poly (lactic-co-glycolic acid) (PLGA) have been utilized to deliver antineoplastic drugs (e.g. chemotherapeutic agents), siRNA, peptide or DNA vaccines for treatment of cancer [60]. NP-based delivery systems in general offer several benefits such as improved pharmacokinetic profile, targeted delivery, protection of antigen from enzymatic degradation and improved stability of encapsulated cargo. Recent advances suggest that NPs can be efficiently used for vaccines and immunotherapeutic strategies [39].

Efficient delivery of Tag to antigen presenting cells (APCs) though a major challenge; is a promising approach in the development of immune-targeted tumor vaccines. NPs potentiate the intracellular delivery of antigen which enhances the immune response significantly. Tumor lysates, peptides and antigens encapsulated within NPs have been shown to induce specific antitumor responses. For example, several studies have reported enhancement of immune responses against cancer by encapsulation of tumor-associated antigens (TAA), which are aberrantly expressed on cancer cells but not on normal cells [62,63,78]. DNA vector encoding proteins overexpressed on tumor cells have also shown a similar effect [38]. In addition, studies have shown that non-specific immune activation by repeated administration of bacterial antigen

CpG-ODN controls tumor growth [37,79,80]. Administration of NPs encapsulating such antigens leads to activation of tumor specific T-cell responses as well as enhanced secretion of cytokines responsible for efficient function of cytotoxic T cells [81]. Among APCs, dendritic cells play a major role in antigen processing and presentation. Therefore, some studies have utilized ligands specific to dendritic cells to target delivery of antigen encapsulating NP cargo to these cells. This allows further enhancement of immune responses against the antigen, resulting in anti-tumor immunity [47].

CpG-ODNs have been successfully employed as adjuvants to enhance antitumor immune defenses [73]. However, its use has also been shown to elicit adverse responses [82]. In particular, repeated administration of CpG has been shown to cause pain at site of injections as well as frequent headaches in healthy volunteers [83]. Consideration of the multiple exposures of CpG and other potent adjuvants is a critical factor in vaccine efficacy. Thus, the dose of CpG is a critical factor in vaccine efficacy. In this study we engineered CpG-NP-Tag NPs using Bis (Sulfosuccinimidyl) suberate (BS3) as a bridge to dock the CpG on the surface of the NPs encapsulated with membrane lysate of 4T1 murine mammary carcinoma cells as the Tag (Fig. 1A) and tested its efficacy in generating anti-tumor immunity limiting CpG exposure. It is well known from literature that surface proteins of pathogens are primary antigens and are sensed as foreign by the host immunity system, which is very likely in tumor cells as well [84]. However, both tumor antigens and material used to make NPs is less immunogenic. Therefore, to enhance identification of NPs as foreign particles, we coated bacterial antigen CpG on surface to prepare "bacteriomimetic" NPs. The principle of booster dose is also very well known in vaccination. Therefore, we administered a pre-dose of CpG to the mice and CpG coated NP as a booster dose. The objective of this study was to synthesize "bacteriomimetic" NPs by CpG surface

functionalization of tumor antigen encapsulating NPs and evaluate its efficacy in generating strong anti-tumor effect.

3. MATERIALS AND METHODS

3.1 Materials

Poly (D,L-lactide-co-glycolide) 50:50; inherent viscosity 0.7-0.9 dL/g; mw 50,000 was purchased from Lakeshore Biomaterials (Birmingham, AL). Polyvinyl alcohol (PVA; mw 30,000–70,000; alcoholysis degree 88 ~ 99.9 (mol / mol) %) was purchased from Sigma Aldrich (St Louis, MO). (BS3) was purchased from Thermo Fisher Scientific (Indianapolis, IL). CpG-ODN 1826 (Class B CpG Oligonucleotide-Murine TLR9 ligand) was obtained from InvivoGen (San Diego, CA). RPMI 1640 media, Penicillin-Streptomycin (Pen-Strep), fetal bovine serum (FBS) were obtained from Invitrogen (Carlsbad, CA). Na^+/K^+ ATPase and Phosphoglycerate kinase (PGK) antibodies were purchased from Cell Signaling, Inc (Danvers, MA). $CD4^+$ /$CD8^+$ Alexa fluor 488 and IFN-γ Alexa fluor 488 conjugated anti-mouse antibodies as well as Ki67 eFluor® 615 conjugated anti-mouse antibody was purchased from ebioscience, Inc. (San Diego, CA). D-Luciferin - K+ Salt Bioluminescent Substrate for imaging was obtained from Perkin Elmer Inc. (Waltham, MA). In Situ Cell Death Detection Kit, Fluorescein for TUNEL assay was purchased from Roche Diagnostics (Indianapolis, Indiana).

3.2. Cell line

4T1 murine mammary carcinoma cell line was purchased from American Type Culture Collection (ATCC), [Manassas, VA] (refer supplementary section 1.2 for ATCC cell line characterization) and was grown until seventy percent confluent in RPMI media supplemented with 10% FBS and 1% Pen-Strep.

3.3. Membrane Lysate preparation:

4T1 cells were lysed using hypotonic buffer and dounce homogenizer followed by centrifugation at 5,000 x g at 4°C for 15 minutes to pellet cell debris. Supernatant was collected and further centrifuged at 100,000 g for 1 hr at 4°C using N55 rotor. After centrifugation, pellet (membrane fraction) was collected and washed with PBS followed by a second round of centrifugation. Final membrane fraction was resuspended in 100-150 µl of RIPA buffer. Protein estimation was performed using Pierce™ BCA protein assay kit (Thermo Scientific, Rockford, IL).

3.4. Formulation of CpG-NP-Tag NPs:

CpG-NP-Tag NPs were prepared using water-in-oil-in-water (w/o/w) double emulsion method employing solvent evaporation technique reported elsewhere [43,85,86] with slight modifications as described in section 1.1 of supplementary methods. CpG-NP-Tag NPs were further characterized and subsequently used for *in vivo* studies.

3.5. Characterization of NPs

3.5.1. Particle size, Polydispersity Index (PDI), Zeta Potential and Encapsulation efficiency:

Particle size was measured using Nanotrac ULTRA instrument by suspending NPs in PBS while PDI (i.e. the width of the particle size distribution) was calculated using the formula: $(\sigma / d)^2$ where σ represents the standard deviation and d indicates mean diameter. Zeta potential was measured using Zetasizer (Malvern Instruments Ltd.). A known amount of NPs (0.25- 0.5 mg) were resuspended in 1m distilled water and further diluted 10 times before measuring particle size and zeta potential. The quantity of Tag actually encapsulated was confirmed based

on the amount of Tag (protein) extracted after degrading a fixed amount of NPs. 5 mg of NPs were degraded using 100 mM NaOH + 0.05% SDS (Sigma-Aldrich, St. Louis, MO) by incubating at 37° C on a shaker. Samples were further centrifuged at 11,000 g at 4° C for 10 minutes and the supernatants were tested for their protein content [87]. Protein estimations were done in triplicate using Bicinchonic acid (BCA) protein assay kit (Thermo Scientific, Rockford, IL) as per manufacturer's instructions. Encapsulation efficiency was calculated as follows: Amount of protein encapsulated / amount of protein used in encapsulation * 100%.

3.5.2. Transmission electron microscopy (TEM):

Briefly, a known quantity of NPs (1mg) were resuspended in distilled water and deposited on a TEM grid employing uranyl acetate as negative stain. TEM images were taken using a Zeiss EM 910 Transmission Electron Microscope at 80 keV.

3.5.3. Fluorescence Correlation Spectroscopy (FCS):

For FCS, 0.25 mg of NPs were resuspended in distilled water and incubated with 7 µg of CpG-FITC for 60-90 min followed centrifugation and washing at 11,000 g for 15 min to remove excess CpG ligand. FCS measurements were done using Microtime 200 system from Picoquant GmbH (Berlin, Germany). NPs (approximately 0.25 mg) were diluted in distilled water and 30 µl of solution was dropped onto a 20 mm * 20 mm No. 1 coverslip (Menzel–Gläser). The focal height was adjusted to 20 µm above this coverslip using an Olympus i * 71 microscope and an Olympus 60 * 1.2 NA objective.

3.6. Syngenic breast cancer BALB/c mice model

BALB/c AnNHsd female mice were obtained from Harlan laboratories, Inc. (Indianapolis IN) and housed at UNTHSC animal facility and allowed to acclimatize for a week prior to experimentation. All procedures were in accordance with the guidelines of the Institutional Animal Care and Use Committee (IACUC) at UNTHSC at Fort Worth. Mice were pre-immunized intraperitoneally with CpG (600 µg/kg) followed by secondary immunization using respective NPs (Table 1) 7 days before tumor challenge. Dose of NPs (5mg) was calculated based on the encapsulation efficiency to deliver Tag equivalent to the amount of CpG used during preimmunization. Mice immunized with the CpG-NP-Tag NPs (n=5) comprised the test/treatment group while mice immunized with CpG-NP-Blank NPs (n=5) and NP-Tag (n=5) were considered as control groups. Subsequently, mice were challenged with $1*10^5$ 4T1-luciferase transfected cells. Primary tumor size was monitored over the course of 14 days following tumor challenge. Spleens and primary tumors were harvested for further studies (Fig. 1).

Figure 1

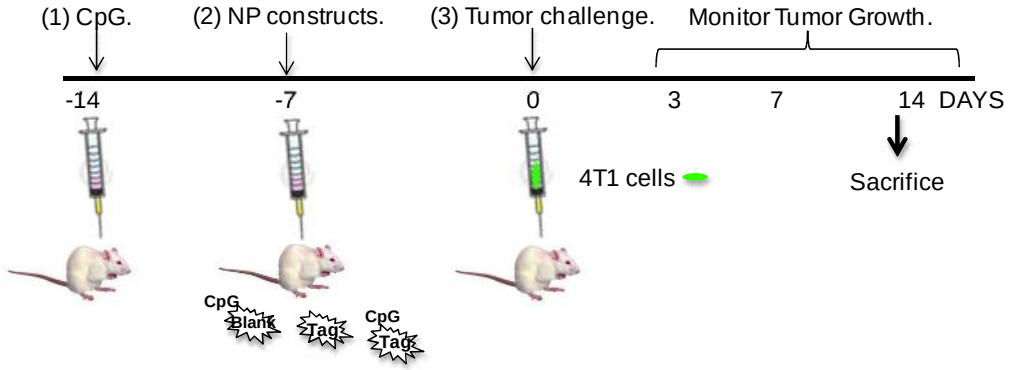
(1) CpG.
(2) NP constructs.
(3) Tumor challenge.
Monitor Tumor Growth.
-14
-7
0
3
7
14 DAYS
4T1 cells
Sacrifice
CpG
Blank
Tag
CpG
Tag

Figure 1: Schematic representation of the study timeline followed for the *in vivo* studies. 5-6 weeks female BALB/c mice (n=5) were preimmunized intraperitoneally (IP) with CpG 14 days before tumor challenge followed by IP immunization (7days after CpG preimmunization) with the respective groups of NPs. Mice were challenged subcutaneously (SC) with 10^5 4T1 luciferase transfected mammary carcinoma cells and the effect of NP immunization was evaluated on the rate of tumor growth and immune response for 14 days.

3.7.1. Rate of tumor growth and animal weight:

Tumor size and animal weight were measured using vernier caliper and weighing balance respectively at different time intervals till day 14. Tumor size was measured in three different dimensions (mm): length, breadth and height. Tumor volume (mm^3) was calculated using the below formula and the fold change in tumor volume was compared among the different groups of animals [88]. Tumor volume (mm^3) = $\pi/6$ (length *breadth*height)

3.7.2. Bioluminiscence Imaging:

Tumor growth was monitored using *in vivo* IVIS® Lumina bioluminescence imaging facility (Caliper Life Sciences Inc., MA). BALB/c mice were injected with D-luciferin (5mg/kg) via IP route 10 minutes before taking images using IVIS Lumina and analyzed using Living Image software 3.0.

3.7.3. Histological analysis of tumors:

For morphological examination, tissues were fixed in 4% paraformaldehyde, embedded in Optimum Cutting Temperature (O.C.T) compound (Tissue-Tek, Sakura Fine-Tek, Torrance, CA) and sectioned using cryostat to obtain 5-8 µm thin sections. Haematoxylin and Eosin (H & E) staining was performed using standard protocol. Images were captured using Olympus AX70 Provis microscope (Scotia, NY).

3.7.4. Proliferation rate:

For proliferation study, 5-7 µm OCT embedded tumor sections were used. Sections were stained for nuclear proliferation marker, Ki 67 and were further quantified for tumor proliferation activity using NIH Image J software.

3.7.5. TUNEL Assay

Apoptosis study was performed using fluorometric TUNEL (terminal deoxynucleotidyl transferase biotin dUTP nick end labeling) staining on 5-7 µm OCT embedded tumor sections. Data was further quantified for apoptotic activity using NIH Image J software.

3.8. Immunostimulatory efficacy of bacteriomimetic NPs

Immunostimulatory potential was evaluated by tumor quantification of $CD4^+$ and $CD8^+$ T cell infiltration and IFN-γ cytokine production using Immunofluorescence staining technique.

3.8.1. Immunohistochemical staining of primary tumors

To check the $CD4^+$ and $CD8^+$ T cell infiltration of primary tumor, 5-7 µm OCT embedded sections were stained with anti-$CD4^+$ and anti-$CD8^+$ alexa fluor 488 conjugated antibodies and immunofluorescence was observed using confocal microscopy. Confocal microscopy was conducted utilizing LSM 510 META (Carl Zeiss).

3.8.2. Intracellular IFN-γ staining of primary tumor

To evaluate the IFN-γ levels 5-7 µm tumor sections were permeabilized using 0.5% Triton-X and stained for IFN-γ using anti- IFN-γ antibody conjugated to Alexa fluor 488 and immunofluorescence was observed using confocal microscopy.

3.9. Statistical analysis

NP particle size characterization data was analyzed using Origin Pro 8.5 software. For evaluating biological assays GraphPad Prism 4.5 version was utilized. One way ANOVA ($p<0.05$) was used to analyze the *in vivo* tumor study data.

4. Results

4.1. Formulation of NPs

NPs were formulated employing a solvent evaporation method from a water/oil/water (w/o/w) emulsion as described in the materials and methods section (Fig. 2A). Binding of CpG onto the surface of NPs was established using BS3 crosslinker. This approach takes advantage of the avidity of amine groups associated with the nucleobases cytosine/guanine of CpG DNA, which interact with the free carbonyl groups of BS3 to form an amide linkage (Fig. 2B). We engineered three NP formulations: 1) CpG-linked NP devoid of membrane antigen (CpG-NP-Blank), 2) NPs encapsulating purified membrane fractions only (NP-Tag) and 3) NPs encapsulating purified membrane fractions with CpG linked to the outer surface (CpG-NP-Tag) (Table 1).

Table 1. Physicochemical Characterization of NPs

Sr.no.	NP-Construct	Particle Size (nm ± SD)	Zeta potential (mV ± SD)	PDI	Encapsulation efficiency (%)	PLC(µg/100 mg NP)
1.	CpG-NP-Blank	211.8 ± 79	-4.22 ± 0.2	0.137	-	-
2.	NP-Tag	221.3 ± 75	-3.62 ± 0.4	0.115	32.2 ± 2.1	183
3.	CpG-NP-Tag	227.4 ± 40	-6.73 ± 0.3	0.031	32.2 ± 2.1	183

NPs: Nanoparticles
NP-Construct: Nanoparticle Construct
PDI: Polydispersity Index
PLC: Protein (Tag) Loading Content

Figure 2

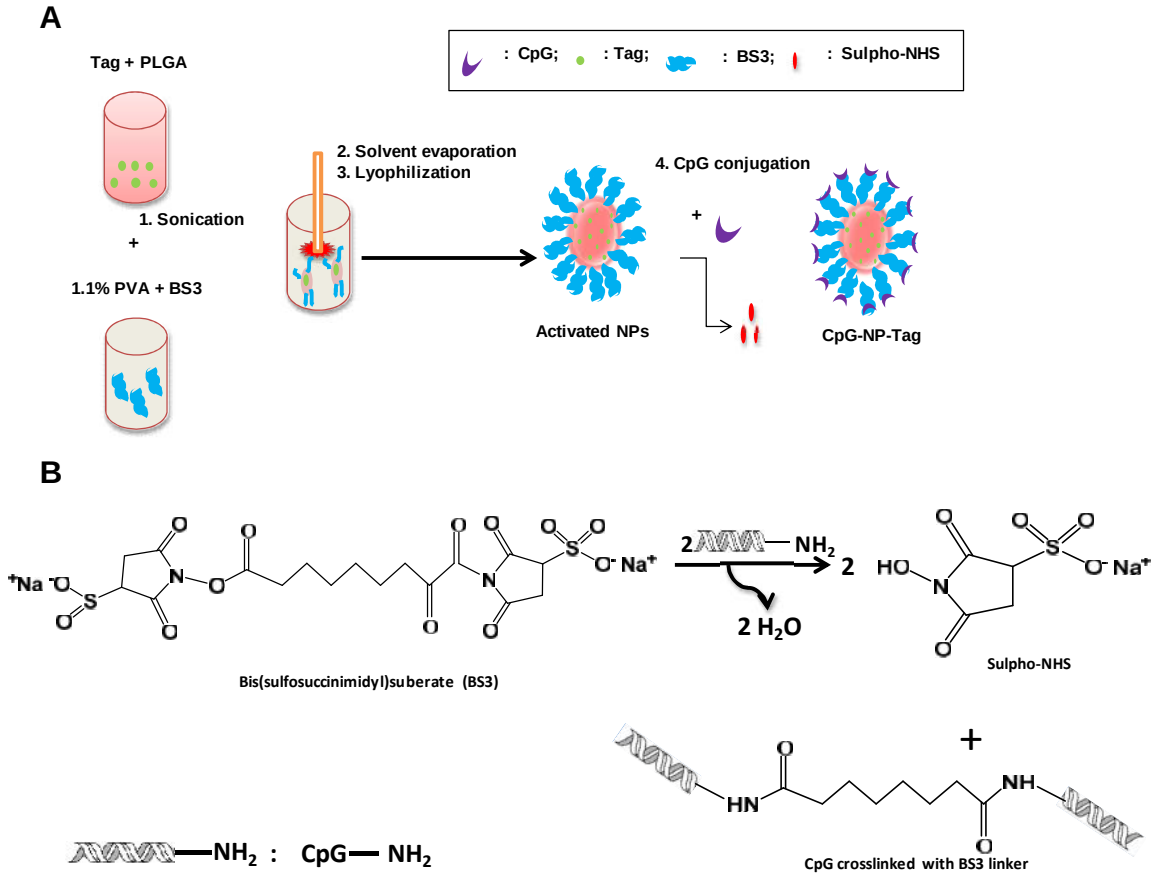
A
: CpG; : Tag; : BS3; : Sulpho-NHS
Tag + PLGA
1. Sonication
+
1.1% PVA + BS3
2. Solvent evaporation
3. Lyophilization
Activated NPs
4. CpG conjugation
+
CpG-NP-Tag
B
Bis(sulfosuccinimidyl)suberate (BS3)
2 NH2
2
2 H2O
Sulpho-NHS
NH2 : CpG NH2
+
CpG crosslinked with BS3 linker

Figure 2: A) Schematic of the steps involved in the formulation of CpG surface functionalized Tag encapsulated (CpG-NP-Tag) NP and components of the NP. **B)** Schematic of the chemical reaction involved in the surface conjugation of CpG ligand.

4.2. Assessment of 4T1 cell membrane fraction (Tag) purity

Membrane fractions of 4T1 cells (Tag) devoid of cytosolic protein were prepared to avoid non-specific immune stimulation. Purity of membrane fraction was confirmed by probing for the membrane marker, Na^+/K^+ ATPase as well as a cytosolic marker Phosphoglycerate kinase (PGK) using SDS-PAGE (Fig. 3A). Lane 1 shows unfractionated 4T1 cell lysate used as positive control for Na^+/K^+ ATPase and PGK. Lane 2 indicates purity of the membrane preparation demonstrated by the presence of Na^+/K^+ ATPase and the absence of PGK contamination within the membrane preparation.

4.3. Surface functionalization and Characterization of NPs

NP formulations were characterized for particle size, PDI, zeta potential, encapsulation efficiency, surface functionalization and surface morphology. The average particle size of the NPs was found to be in the range of 200-220 nm with PDI of 0.1 (Fig. 3B & Table 1) [89]. The zeta potential was found to be slightly positive for the uncoated NP-Tag NPs as compared to CpG-Blank or CpG-NP-Tag NPs as indicated in Table 1. Encapsulation efficiency of Tag was on average 32 ± 2% with protein (Tag) loading content (PLC) of 183 µg/100mg of NPs. Results from the TEM indicated that the particles were non-agglomerated, spherical and had a uniform size distribution (Fig. 3C). Surface functionalization of NP was confirmed via Fluorescence Correlation Spectroscopy (FCS) (Fig. 3D). FITC labeled CpG was used in these experiments. Fig 3D shows the FCS curves of free CpG (diffusion coefficient: 250 $\mu M^2/s$) and NP bound CpG (diffusion coefficient: 3 $\mu M^2/s$) clearly indicating slower diffusion of bound CpG proving successful conjugation of CpG to NPs.

Figure 3

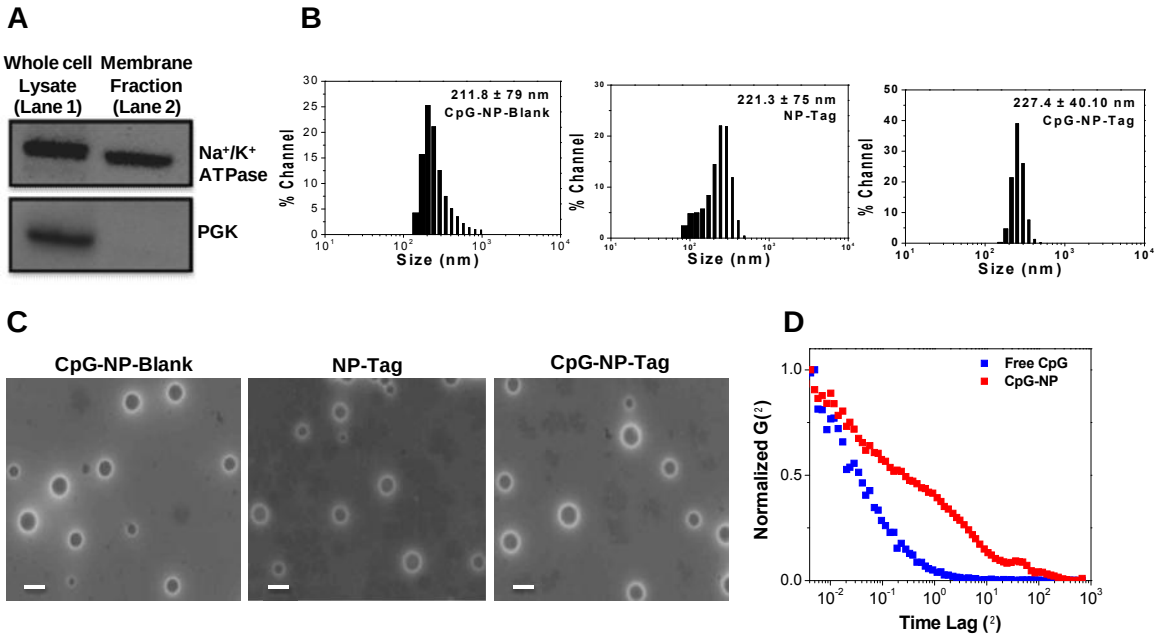
A
Whole cell Lysate (Lane 1)
Membrane Fraction (Lane 2)
Na+/K+ ATPase
PGK
B
211.8 ± 79 nm
CpG-NP-Blank
221.3 ± 75 nm
NP-Tag
227.4 ± 40.10 nm
CpG-NP-Tag
% Channel
Size (nm)
C
CpG-NP-Blank
NP-Tag
CpG-NP-Tag
D
Free CpG
CpG-NP
Normalized G(2)
Time Lag (2)

Figure 3: Physicochemical characterization of NPs. A) Evaluation of purity of membrane preparation as a tumor antigen (Tag) determined by immunoblotting for Na^+/K^+ ATPase and PGK. **B)** Particle size of CpG-Blank (i), NP-Tag (ii) and CpG-NP-Tag (iii) NPs as measured by dynamic light scattering. **C)** Transmission Electron Micrographs of CpG-Blank, NP-Tag and CpG-NP-Tag NPs (Scale, bar: 200nm). **D)** Fluorescence Correlation Spectroscopy (FCS) curves of bound and free CpG.

4.4. Effect of NP immunization on tumor growth and morphology

4.4.1. Rate of tumor growth

During and at the end of the study, tumor size was measured using digital vernier caliper and bioluminiscence imaging. Fold change in tumor size was found to be significantly smaller in mice immunized with "bacteriomimetic" CpG-NP-Tag NPs (test sample) as compared to mice immunized with CpG-NP-Blank NPs (control sample) ($p=0.0292$) which correlated with bioluminescence intensity of imaged primary tumors (Fig. 4).

The bioluminiscence was higher for CpG-NP-Blank [$8.77*10^6$ photons/ sec/cm2/steradian (p/sec/cm^2/sr)] and NP-Tag ($3.809*10^6$ p/sec/cm^2/sr) tumors as compared to CpG-NP-Tag tumors ($2.058*10^6$ p/sec/cm^2/sr).

Ex vivo examination of primary tumors 14 days post tumor challenge also demonstrated significantly smaller primary tumors in size and weight for CpG-NP-Tag immunized mice ($p= 0.0133$) as compared to NP-Tag and CpG-NP-Blank (Fig. 5).

Figure 4

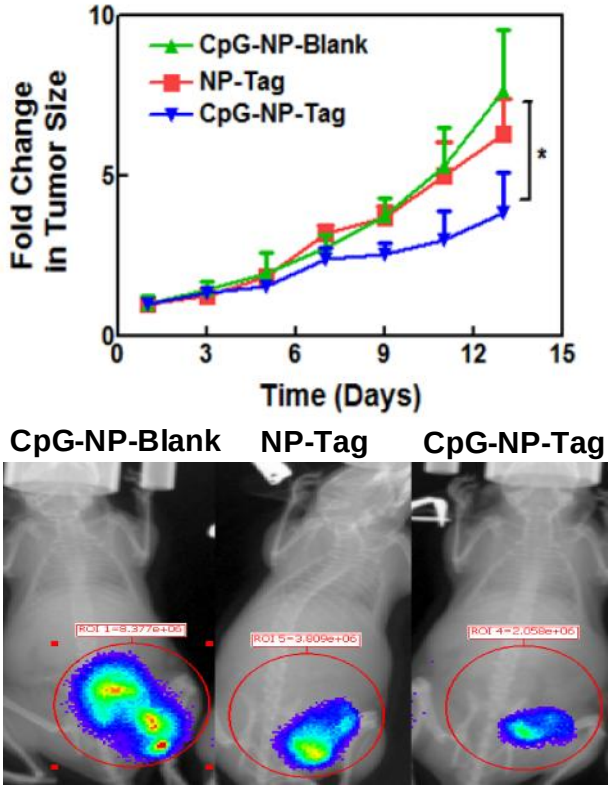
CpG-NP-Blank
NP-Tag
CpG-NP-Tag
Fold Change in Tumor Size
Time (Days)
0
3
6
9
12
15
0
5
10
*
CpG-NP-Blank
NP-Tag
CpG-NP-Tag

Figure 4: Effect of NP immunization on tumor growth rate. Fold change in tumor volume (mm^3) as compared to Day 1 post-tumor challenge, in mice treated with different NP formulation and its correlation with Bioluminiscence Imaging tracking tumor growth at day 12 after tumor challenge (*$p < 0.05$).

Figure 5

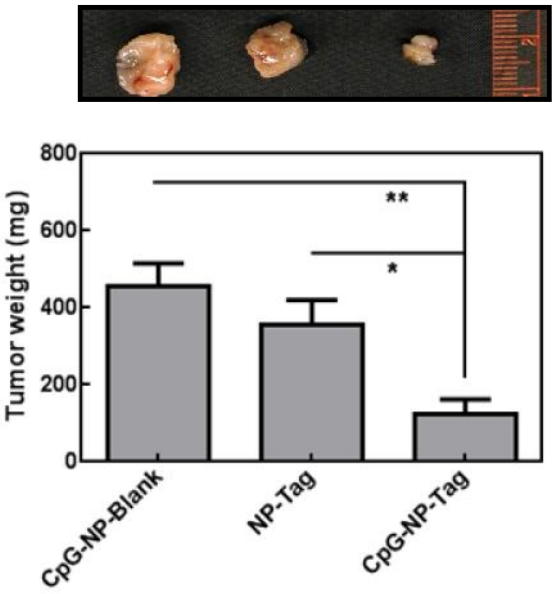

Figure 5: Effect of NP immunization on tumor size and weight. Tumor tissue of animals immunized with respective groups of NPs harvested on day 14 after tumor challenge and weight (mg) of isolated tumors of mice immunized with the respective groups of NPs harvested at day 14 after tumor challenge (*$p < 0.05$; **$p < 0.01$).

4.4.2. Gross Histopathological changes in breast tumor tissue

Tumor sections were stained with H & E dyes to study the histopathology features of tumor tissues. Tumors from mice administered with CpG-NP-Blank and NP-Tag NPs (i.e. control groups) showed polymorphic nuclei, decreased cellular organization and poor differentiation as compared to tumors from CpG-NP-Tag-administered mice. Additionally, tumors from CpG-NP-Blank and NP-Tag were intensely stained for the nuclear stain, haematoxylin relative to eosin in comparison to tumors from CpG-NP-Tag-treated mice indicative of higher proliferative activity and aggressive phenotype in control groups (Fig. 6) [90].

Figure 6

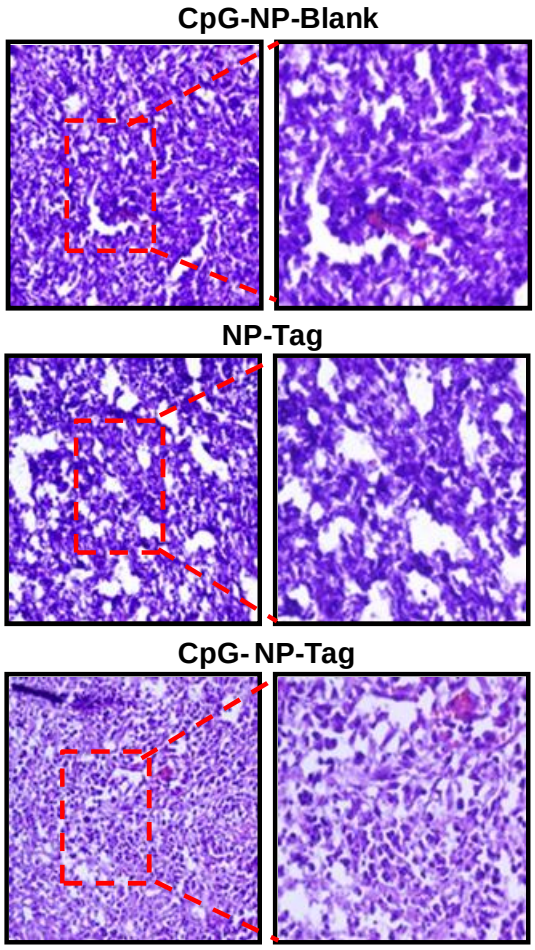

Figure 6: H & E staining of tumor tissues isolated from different groups. Frozen tumor tissue sections (5-8 µm) were stained with H & E and images (10X and 20X) were taken using Olympus AX70 Provis microscope (Scotia, NY).

4.4.3. Proliferative activity

To assess the proliferative status of tumors, tissue sections were stained for the proliferation marker, Ki67. Quantitative evaluation of immunofluorescence indicated a higher tumor proliferation rate of tumor cells in mice immunized with CpG-NP-Blank NPs and NP-Tag as compared to mice immunized with our test sample "bacteriomimetic" CpG-NP-Tag NPs (Fig. 7A and 7B).

4.4.4. Apoptosis Assay

Cell death presumably by immune-mediated host responses due to immunization should involve tumor killing. To verify if the decrease in proliferation rate observed in CpG-NP-Tag tumors correlated with cell death, we performed TUNEL assay. The number of apoptotic nuclei was significantly higher in our test sample CpG-NP-Tag as compared to CpG-NP-Blank and NP-Tag ($p < 0.05$) (Fig. 8A and 8B). These findings demonstrate that conjugation of CpG on Tag encapsulating NPs functions in additive manner where the apoptotic effect can't be achieved by using them individually.

Figure 7

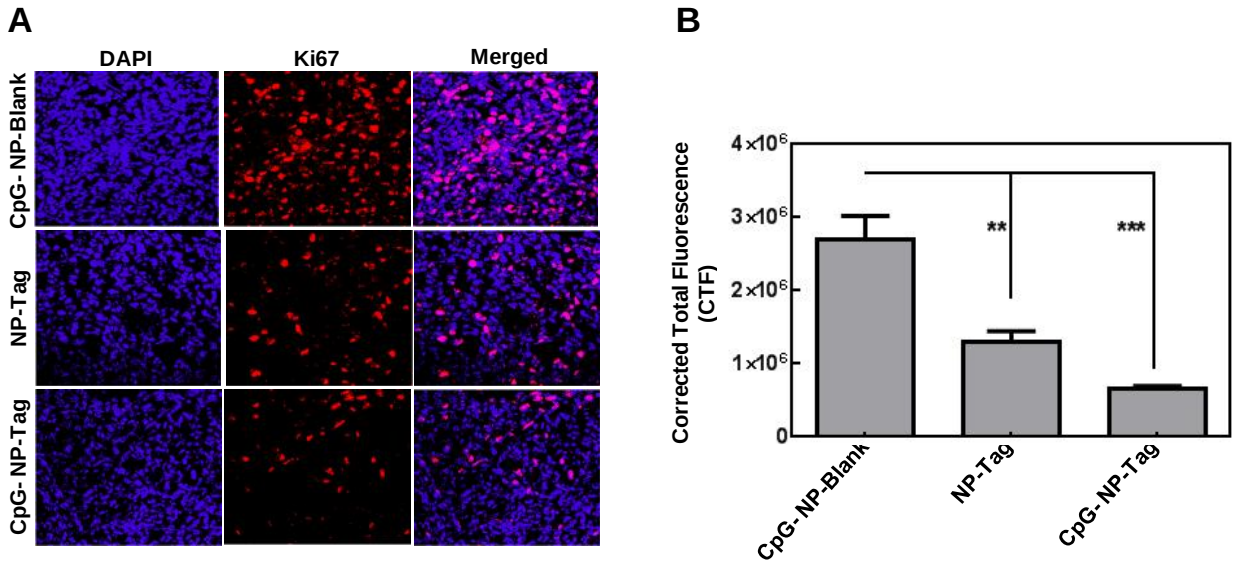
A
DAPI
Ki67
Merged
CpG- NP-Blank
NP-Tag
CpG- NP-Tag
B
Corrected Total Fluorescence (CTF)
4×10^6
3×10^6
2×10^6
1×10^6
0
**
***
CpG- NP-Blank
NP-Tag
CpG- NP-Tag

Figure 7: Effect of NP immunization on tumor cell proliferation. A) Representative images (40X) of Ki67 stained tumor tissues sections showing rate of tumor proliferation. **B)** Quantitative analysis indicating proliferation rate of the tumor tissue harvested from the different groups analyzed using NIH ImageJ software (**$p < 0.01$; ***$p < 0.001$)

Figure 8

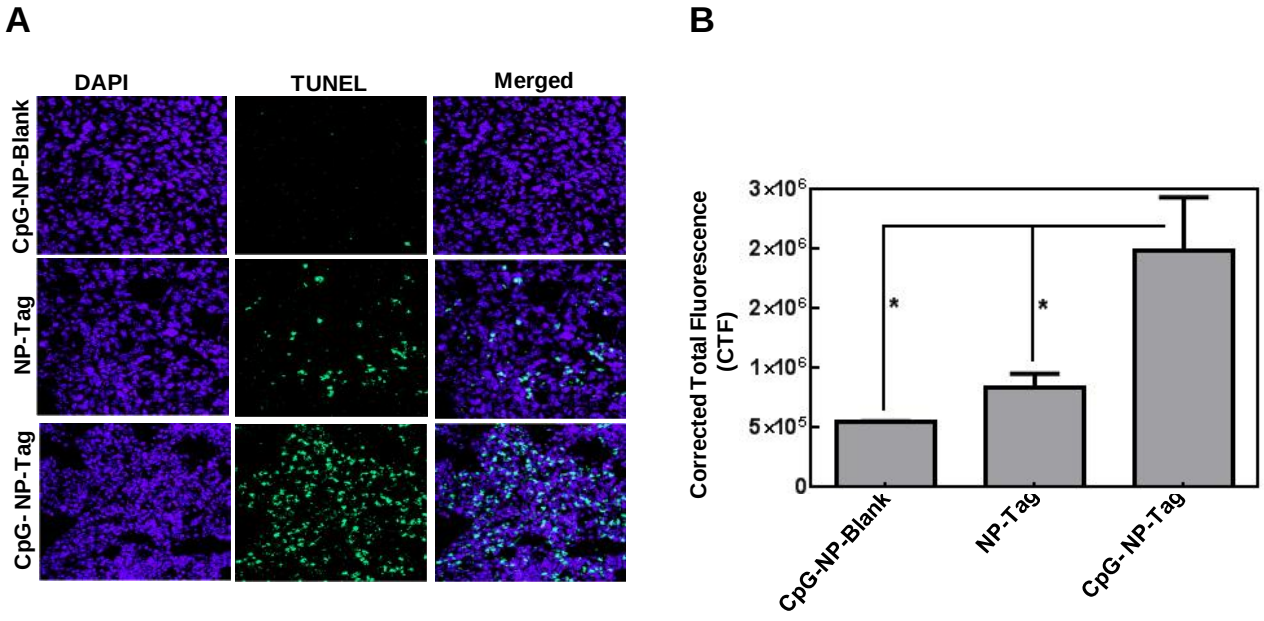
A
DAPI
TUNEL
Merged
CpG-NP-Blank
NP-Tag
CpG- NP-Tag
B
Corrected Total Fluorescence (CTF)
3×10^6
2×10^6
2×10^6
1×10^6
5×10^5
0
*
*
CpG-NP-Blank
NP-Tag
CpG- NP-Tag

Figure 8: Effect of NP immunization on tumor cell survival. A) Representative images of TUNEL staining of the tumor sections showing the induction of apoptosis. **B)** Quantitative analysis of the apoptotic activity using TUNEL assay analyzed using NIH ImageJ software (*$p < 0.05$).

4.5. Immunostimulatory efficacy of "bacteriomimetic" CpG-NP-Tag NPs

4.5.1. $CD4^+$ and $CD8^+$ T cell infiltration of primary tumor

To evaluate if our test formulation CpG-NP-Tag NPs enhanced T lymphocyte infiltration, we assessed the presence of $CD4^+$ and $CD8^+$ T cell infiltrates within subcutaneous tumors isolated on day 14. CpG-NP-Tag tumors demonstrated a significant infiltration of $CD4^+$ (Fig. 9A) as well as $CD8^+$ T cells (Fig. 9B) relative to tumor of controls NP-Tag and CpG-NP-Blank-treated mice ($p < 0.05$).

4.5.2. IFN-γ in primary tumor tissue

IFN-γ is an essential cytokine mediator of immune cell-mediated tumor cell cytotoxicity [71,72,91]. We investigated the presence of IFN-γ by intracellular staining of tissue sections. CpG-NP-Tag tumors demonstrated higher levels of IFN-γ as compared to NP-Tag and CpG-NP-Blank tumors ($p < 0.05$) (Fig. 10A and 10B).

Figure 9

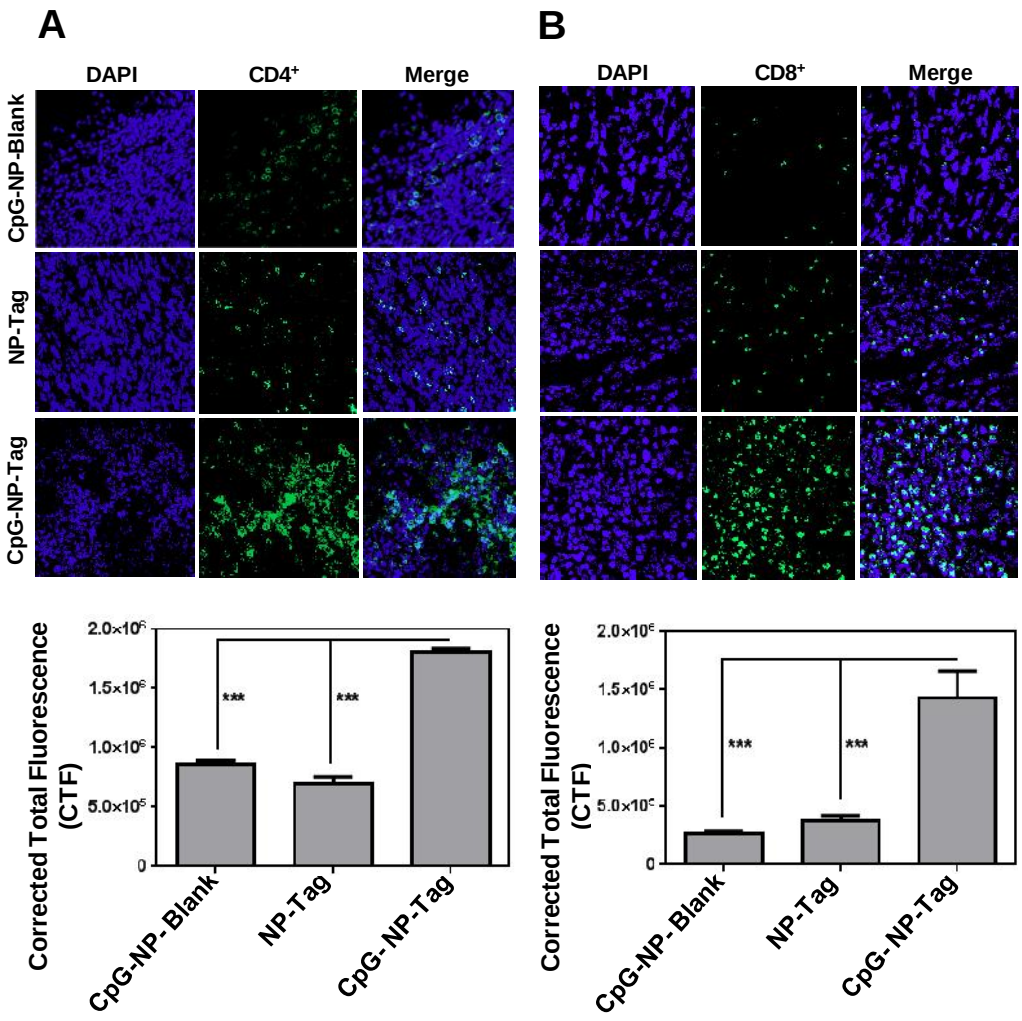
A
B
DAPI
CD4+
Merge
DAPI
CD8+
Merge
CpG-NP-Blank
NP-Tag
CpG-NP-Tag
Corrected Total Fluorescence (CTF)
2.0×10^6
1.5×10^6
1.0×10^6
5.0×10^5
0
***
***
CpG-NP-Blank
NP-Tag
CpG-NP-Tag
Corrected Total Fluorescence (CTF)
2.0×10^6
1.5×10^6
1.0×10^6
5.0×10^5
0
***
***
CpG-NP-Blank
NP-Tag
CpG-NP-Tag

Figure 9: A) Representative images (40X) of $CD4^+$ T cell infiltration at tumor site indicating immunostimulatory potential of CpG-NP-Tag NPs and Quantification of tumor $CD4^+$ T cell infiltration analyzed using NIH ImageJ software (***$p < 0.001$). **B)** Representative images of $CD8^+$ T cell infiltration at tumor site indicating immunostimulatory potential of CpG-NP-Tag NPs and Quantification of tumor $CD8^+$ T cell infiltration analyzed using NIH ImageJ software (***$p < 0.001$).

Figure 10

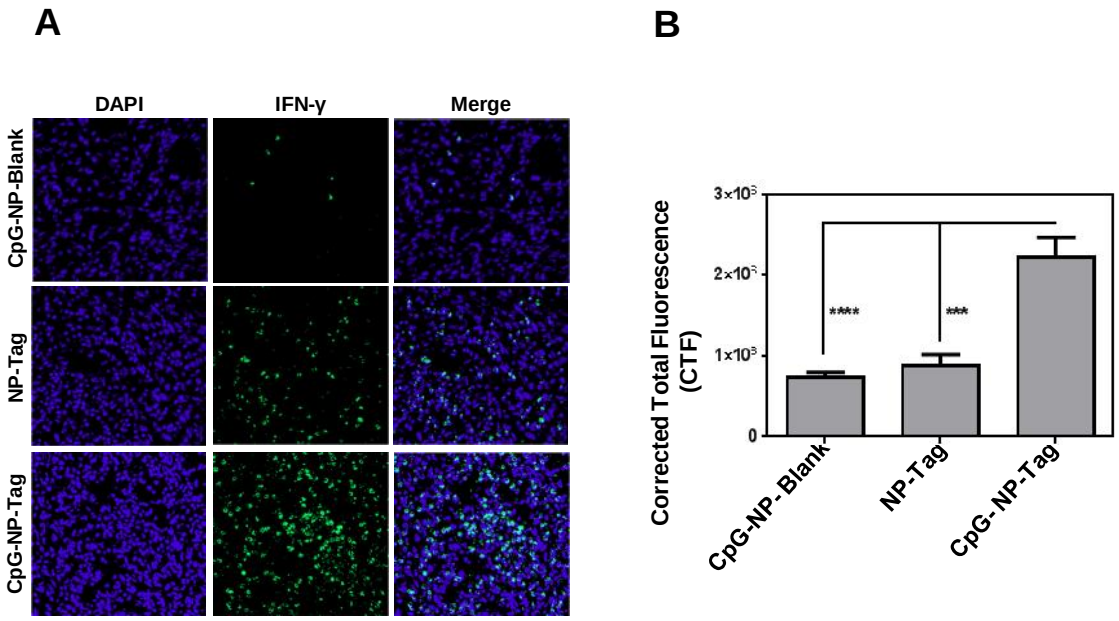
A
DAPI
IFN-γ
Merge
CpG-NP-Blank
NP-Tag
CpG-NP-Tag
B
Corrected Total Fluorescence (CTF)
3×10⁸
2×10⁸
1×10⁸
0
****
***
CpG-NP-Blank
NP-Tag
CpG- NP-Tag

Figure 10: A) Representative images of IFN-γ intracellular staining at tumor site.

B) Quantification of tumor IFN-γ levels analyzed using NIH ImageJ software (***$p < 0.001$; ****$p < 0.0001$).

5. DISCUSSION

Deficits in immune surveillance against cancer caused by inherent tumor escape mechanisms or by toxicities due to cancer treatment (e.g. chemo-radio-therapy) have raised interests in developing novel immune-based therapies. Most notable are tumor antigen-based cancer vaccines employed to trigger tumor-specific immune responses [59,92]. Such vaccines have taken advantage of nanotechnology to produce nanoparticulate delivery systems capable of anchoring vaccine components including tumor-associated antigens (TAAs), tumor lysates, plasmid DNA and immune stimulants such as TLR agonists to strengthen immune responses against various tumor malignances [41].

NP technology has advanced drug delivery by providing enhanced stability and protection of target antigens from proteolytic degradation. In addition, NPs offers the advantage of co-delivery of antigen along with immune adjuvants. This benefits optimal induction of immune responses by simultaneous targeted delivery to APCs, which is paramount for effective induction of tumor-specific immunity [55,61,93]. Studies conducted by *Blander and Medzhitov et al*; *Schlosser et al*; emphasize the importance of co-delivery in improving vaccine efficacy [93,94]. The submicron size of NPs offers many benefits over microparticles including higher uptake, increased surface to volume ratio, and decreased clearance of particulate vaccines by the reticular system that would negatively impact immune recognition [41]. Additionally, it has been reported that co-delivery of adjuvant moieties such as CpG and antigen (on separate NPs) enhances DC cross-presentation compared to free adjuvant [87]. In contrast, we have utilized PLGA-based NP system for co-delivery of CpG and tumor antigen (on the same NP) to test the immunostimulatory potential of Tag encapsulated CpG surface functionalized (CpG-NP-Tag) NPs in a prophylactic murine breast cancer model.

"Bacteriomimetic" (CpG-NP-Tag) NPs were engineered by decorating the surface of NPs with a bacterial ligand CpG, a commonly used adjuvant in cancer vaccines (Fig. 2). CpG surface functionalization was confirmed using FCS (Fig. 3D). FCS autocorrelation function analyzes translational diffusion of a fluorescent species through a con-focal volume of very dilute sample (nanomolar concentration). It is understood that small molecular size bio-molecules will diffuse faster than high molecular weight bio-molecules. Hence we hypothesized that free CpG will diffuse faster and will have a large diffusion coefficient (bigger number) than when it is bound to a NPs. We observed that free CpG has diffusion coefficient of about 250 $\mu M^2/s$ and bound CpG has 3 $\mu M^2/s$, showing successful conjugation to NP surface.

Electric charge properties influence cellular interactions as well as NP stability. We observed that CpG-NP-Tag and CpG-NP-Blank particles were slightly negatively charged as compared to uncoated NP-Tag particles (Table 1). The shift towards negative charge is due to surface coating with negatively charged CpG DNA. The negative shift is beneficial for the internalization of the NPs by APCs while neutral or positive charge is not favorable for phagocytic or endocytic activity [43]. Studies conducted by *Kasturi et al* suggest that NPs up to 300 nm are capable of inducing a potent T cell-mediated ($CD4^+$ and $CD8^+$) immune response and protect mice against influenza infection [95]. It is also known that particles less than 500 nm are efficiently endocytosed by DCs [41] either actively (> 200 nm) or passively (≤ 200nm) whereas the larger particles (≥ 500 nm) are preferentially cleared by macrophages of reticuloendothelial system (RES) [89]. Particle size of CpG-NP-Tag NPs was in the range of 200-220 nm (Fig. 3B) and PDI of 0.03 indicating monodispersity of the NP formulation. Encapsulation efficiency was found to be approximately 32 %. For hydrophilic drugs, peptide or protein encapsulation efficiency is relatively lower as compared to hydrophobic substances in PLGA matrix.

Specifically, encapsulation efficiency of hydrophilic species lies in the range of 30-60% compared to a range of 80-90 % encapsulation efficiency of hydrophobic species [96]. Taking into consideration that co-encapsulation of Tag and CpG might compromise the encapsulation efficiency of both components; we prepared surface functionalized activated NPs using BS3 crosslinker for CpG ligand attachment.

CpG-ODNs are known to generate antigen specific memory immune responses [37]. In our studies we found that administration of CpG alone prior to a single CpG-NP-Tag immunization was conducive for promoting an effective immune response leading to slower tumor progression. In contrast, multiple CpG-NP-Tag administration typical of traditional immunization protocols demonstrated significantly faster tumor growth compared to our method of immunization (data not shown). This finding suggests that exposure of CpG combined with NP-Tag could promote immune-tolerogenic responses and that priming with CpG alone followed by administration of a booster dose of the "bacteriomimetic" NPs construct is optimal for inducing anti-tumor immune responses. Previous reports show that CpG-ODN as a single agent is also efficient in reducing progression of tumors [37,97]. However, in those studies the CpG-ODN was given repeatedly over the duration of tumor growth monitoring. Our study shows that a single dose of CpG-ODN followed by the administration of a booster dose of CpG-NP-Tag NPs before tumor challenge can significantly reduce tumor progression. Whereas, administration of a CpG pre-dose followed by booster dose of CpG-NP-Blank, does not provide the same response (data not shown). This suggests that the effect seen in CpG-NP-Tag mice is not only due to CpG, but also the Tag encapsulated in NPs leading to tumor specific immune response. We also monitored the weight of the animals after CpG preimmunization, NP immunization, post tumor challenge until day 14. We found that the weight of the animals was not affected significantly over the entire duration of

the study indicating that the CpG preimmunization as well as NP immunization was safe and did not lead to any adverse effects or toxicities (Supplementary Fig. S4). Based on our findings, it will be prudent to understand how various vaccination models using various NPs vaccine constructs provide optimal tumor defenses.

To avoid non-specific immune-stimulation, we used 4T1 mouse carcinoma cells for preparation of Tag instead of human cancer cell line depicting a syngeneic BALB/c murine model as summarized in Fig. 1. The growth of subcutaneous 4T1 tumors was monitored over time. *In vivo* tumor growth rate was significantly ($p<0.05$) decreased in CpG-NP-Tag immunized mice than CpG-NP-Blank mice (Fig. 4A and 4B). Post tumor harvest, it was evident that CpG-NP-Tag tumors were significantly smaller in size as well as weight than respective control groups (Fig. 5B) & C). Further validation by H & E staining showed CpG-NP-Tag treated mice tumors were well differentiated and less aggressive (less nuclear staining) (Fig. 6). To confirm this, tumor sections were stained for the proliferation marker, Ki67. As expected, tumors from CpG-NP-Tag group showed significantly less proliferative activity (Fig. 7A and 7B). Furthermore, the decreased proliferation of CpG-NP-Tag tumors may be a consequence of cell death via apoptosis. We performed TUNEL assay on tumor tissue sections and found that CpG-NP-Tag NPs induce apoptotic tumor cell death (Fig. 8A and 8B). Thus, CpG-NP-Tag NPs were found to be effective in attenuating tumor growth by inhibiting the proliferation and inducing apoptotic death of tumor cells.

Considering the importance of cell-mediated immunity in antitumor defense mechanisms, vaccine strategies aim toward activating tumor specific $CD8^+$ T cell (CTLs). A number of studies also substantiate the central role of $CD4^+$ T cells in mounting an effective immune response [98,99]. As Helper T cells, $CD4^+$ T cells contribute to antitumor activity by releasing a range of cytokines

such as interleukin-2 (IL-2) and interferon-gamma (IFN-γ) and hence are critical in optimal activation and priming of CTLs. Furthermore, $CD4^+$ T cells are known to help in clonal expansion of CTLs and thus help in maintenance of immune memory leading to prolonged tumor protection [98,99]. Not only overall production of $CD4^+$ cells, but also its infiltration at the site of disease is of importance. The cytokines produced by $CD4^+$ cells help in potentiation of cytotoxic effect and increases survival of $CD8^+$ cells [99-102]. Uptake of NPs by receptor mediated endocytosis as well as by other mechanisms by APCs such as dendritic cells leads to both cytosolic and endosomal delivery of antigen leading to cross-presentation, capable of production of both $CD4^+$ and $CD8^+$ T cells [41,103]. We found that CpG-NP-Tag tumors showed higher infiltration of $CD4^+$ and $CD8^+$ T cells (Fig. 9A and 9B) as compared to NP-Tag and CpG-NP-Blank tumors. Moreover, spleen flow cytometric analysis (refer Supplementary methods section 1.3) also showed a higher $CD4^+$ and $CD8^+$ T cell response in CpG-NP-Tag immunized mice (Supplementary Fig. S5). We observed higher IFN-γ levels within the CpG-NP-Tag tumor tissue as compared to NP-Tag and CpG-NP-Blank tumors (Fig. 10A and 10B). IFN-γ is known to induce MHC Class I expression of cancer cells and thereby potentiates tumor specific immune responses [91]. Thus, CpG-NP-Tag NPs induce a potent $CD4^+$ T cell response as well as higher levels of IFN-γ which potentially aids in triggering a stronger $CD8^+$ T cell response leading to apoptotic death of tumor cells.

Ligation of the intracellular TLR-9 receptor by CpG results in the up-regulation of MHC molecules (MHC I and II), co-stimulatory surface molecules (CD80 and CD86) and increased cytokine production by APCs required for optimal induction of antigen-specific $CD4^+$ and $CD8^+$ T cell responses [73] resulting in tumorlytic responses by $CD8^+$ and $CD4^+$ T cells [101]. The current study demonstrated, significantly higher infiltrating $CD4^+$ and $CD8^+$ T cells, as well as increased

IFN-γ levels within the tumor microenvironment. These findings were associated with increased tumor cell death by apoptosis.

T cell mediated mechanisms are critical in vaccine-based therapies. In addition, humoral antibody responses mainly through the induction of antibody-dependent cell cytotoxicity (ADCC) are also known to mediate anti-tumor immune responses [104]. Thus, we also measured serum IgG antibody titers (refer Supplementary methods section 1.4) of NP-treated tumor bearing mice. CpG-NP-Tag as well as NP-Tag mice showed significantly higher total serum IgG levels as compared to CpG-NP-Blank mice supporting the efficacy of CpG-NP-Tag NPs to trigger humoral immune responses along with cell mediated immunity (Supplementary Fig. S6). Collectively, these studies indicate that CpG-NP-Tag ("bacteriomimetic") NPs have an inhibitory effect on tumor proliferation and possess immunostimulatory potential indicated by their ability to stimulate $CD4^+$ and $CD8^+$ T cell mediated response which might aid the apoptotic killing of tumor cells as well as promote a higher antibody response.

6. CONCLUSION

In this study, our goal was to engineer CpG surface functionalized Tag containing "bacteriomimetic" NPs (CpG-NP-Tag) and to investigate their immune potentiating ability against breast tumor. We formulated and characterized CpG-NP-Tag NPs and tested their immunostimulatory efficacy *in vivo* in a murine breast cancer model. Our results indicate that a combined approach of Tag encapsulation and CpG surface functionalization of PLGA NPs, with a pre-dose of CpG enhances antitumor immunity of NPs. We believe that NP mediated vaccination strategies could be efficiently used as adjuvant therapy along with surgery, radiation and chemotherapy [105,106]. This study also suggests that vaccination strategies whereby coating of

well-known immunogenic antigens such as bacterial antigen such as CpG on NPs could be used to enhance anti-tumor responses. In our future studies, we plan to delineate the mechanistic details involved in enhancement of antitumor immunity imparted by the “bacteriomimetic” NPs. Further validation of this system in a therapeutic model and delineation of anti-tumor mechanisms associated with NP-based delivery approaches will be of translational significance for cancer immunotherapy.

7. SUPPLEMENTARY MATERIALS AND METHODS

7.1. Preparation of CpG-NP-Tag NPs using solvent evaporation technique

Briefly, 70 mg of PLGA polymer was dissolved in 1 ml of ethyl acetate which constitutes the organic phase (o). BS3 (0.5 mg/ml) was dissolved in 1.1% polyvinyl alcohol (PVA) which forms the aqueous phase (w). Primary emulsion (w/o) was prepared by vortexing a 200 µl of Tag solution (1 µg/µl) with organic phase. The primary emulsion (w/o) was added to BS3 solution in PVA (a). The mixture was sonicated on ice using an ultrasonic processor UP200H system (Hielscher ultrasonics Gmb, Germany) at 40% amplitude for 1 minute) in continuous mode to form activated NPs. The separated NPs were washed by resuspending NPs in 0.01% sucrose solution 3 times (14000 rpm for 20 minutes) and subsequently lyophilized on ATR FD 3.0 system. Activated NPs were stored at 4 °C until further use. For conjugation of CpG on the surface of NPs briefly a desired amount of lyophilized NPs were weighed and suspended in 500 µl PBS at room temperature. CpG ligand (1:200 w/w ratio) and resuspended NPs were incubated on an orbital shaker for 1-2 hours at room temperature for optimal ligand binding. After incubation, excess ligand was removed by centrifugation followed by washing with PBS to finally obtain CpG coated Tag containing "bacteriomimetic" NPs (CpG-NP-Tag) which were characterized and subsequently used for *in vivo* studies.

7.2. Stable transfection of 4T1 murine carcinoma cells

4T1 murine mammary carcinoma cell line was purchased from American Type Culture Collection (ATCC) and their authentication included viability testing, trypan blue dye-exclusion assay, morphological appearance for recovery and growth while isoenzymology for species confirmation. 4T1 cells were further transfected with pGL4.5 [*luc2*/Hygro] Vector (Promega, Madison, WI, USA) using Lipofectamine™ 2000 (Grand Island, NY, USA) following standard

protocol reported previously. Stably transfected clones were isolated under Hygromycin selection pressure (400 µg/ml) (Supplementary Fig. S1).

7.3. Flow Cytometry

For evaluating $CD4^+$ and $CD8^+$ T cell response, spleens were harvested from immunized mice at different time points after tumor challenge. Splenocytes were isolated using established protocol as reported elsewhere [107] and were subsequently stained with anti-CD4 and anti-CD8 antibody conjugated to Alexa flour 488 followed by flow cytometric analysis. Flow cytometry was conducted using a Beckman Coulter Cytomics FC 500 Flow Cytometer from core facility.

7.4. Serum Total IgG levels

For the quantitative detection of mouse total IgG, ELISA was performed using Mouse IgG total Ready-SET-Go kit (eBioscience, San Diego, California, USA) on the serum samples collected on day 14 after tumor challenge.

8. Supplementary Data

Figure S1

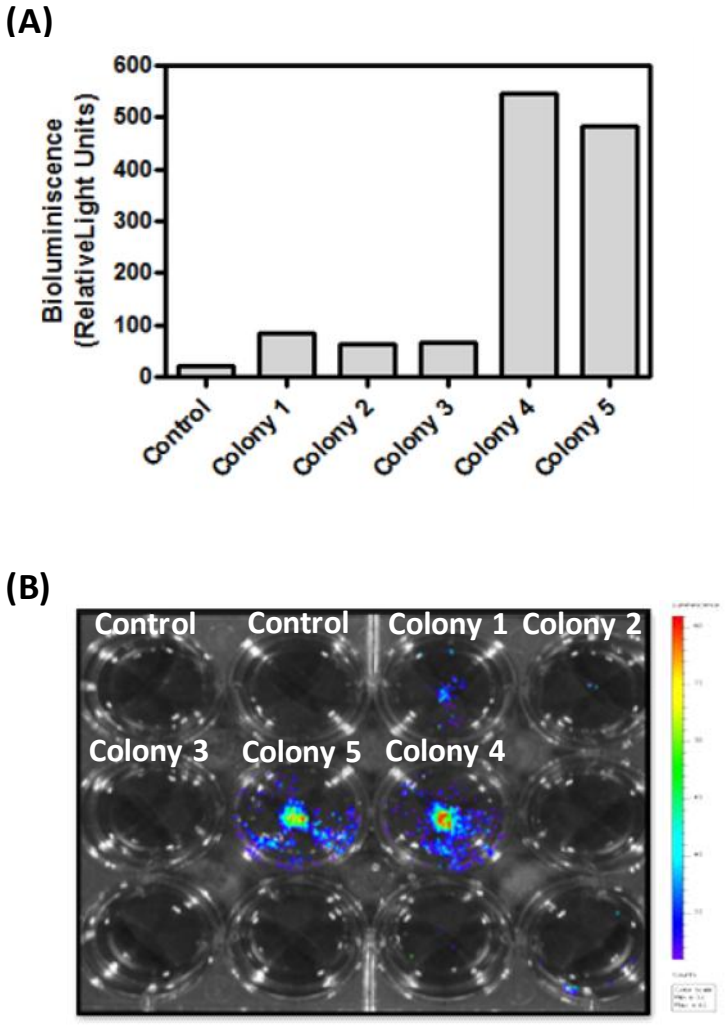

Figure S1: Stable transfection of 4T1 cells with Luciferase. A) Luciferase reporter assay for evaluating the transfected clones. B) Bioluminiscence imaging to isolate stably transfected clones of 4T1 cells.

Figure S2

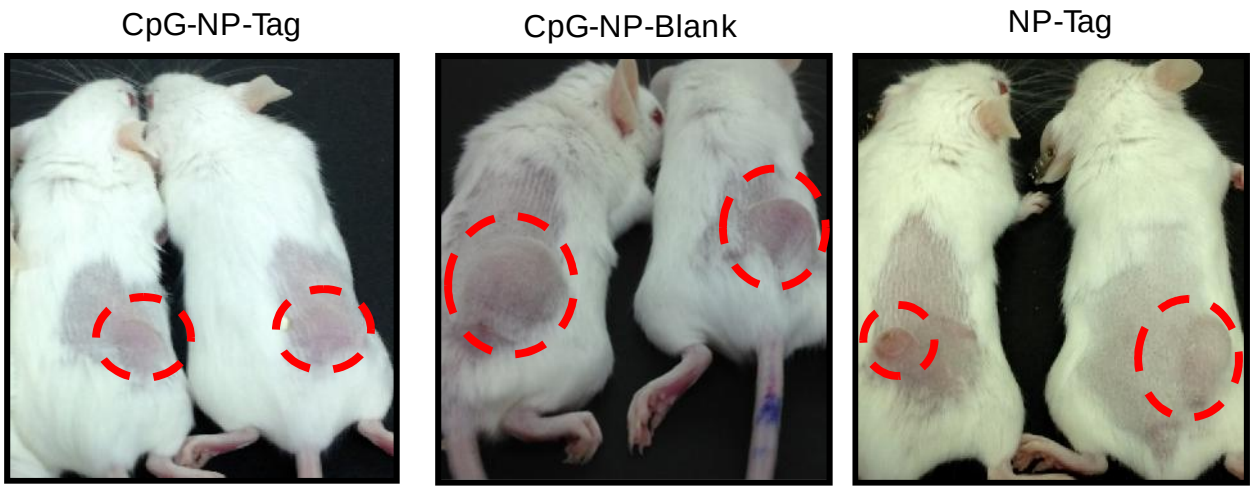

Figure S2: Representative images of tumor bearing mice at day 14 after immunization with the respective groups of nanoparticles.

Figure S3

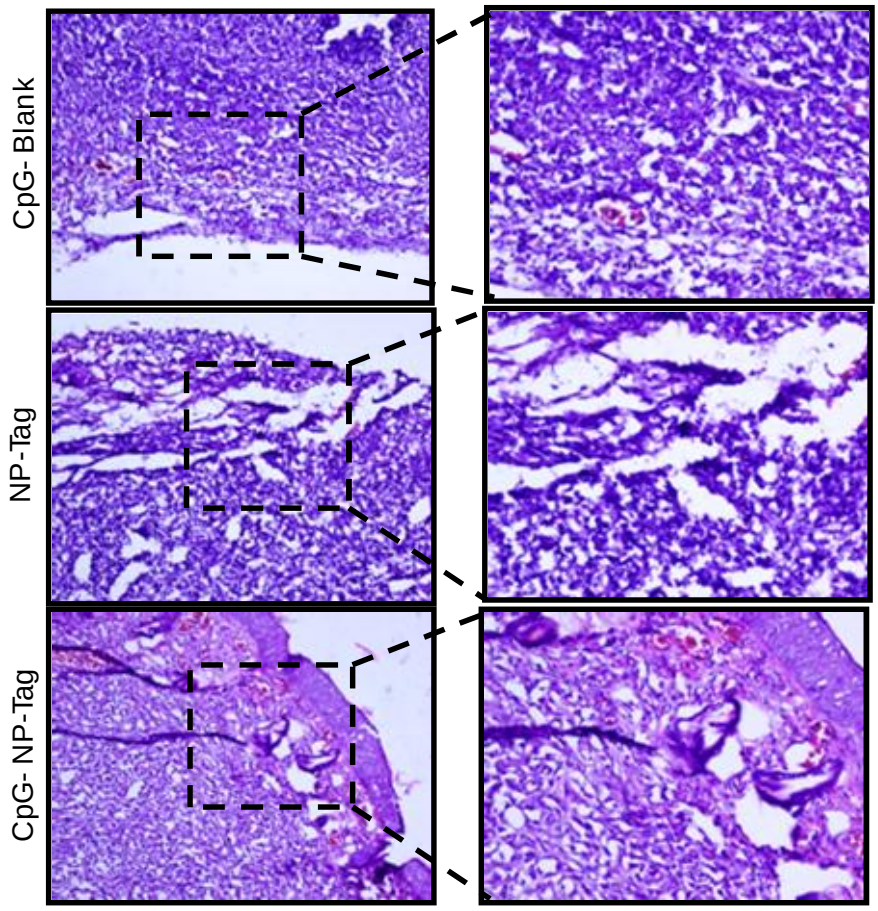

Figure S3: Histological sections showing the periphery of tumor tissue by H & E staining.

Figure S4

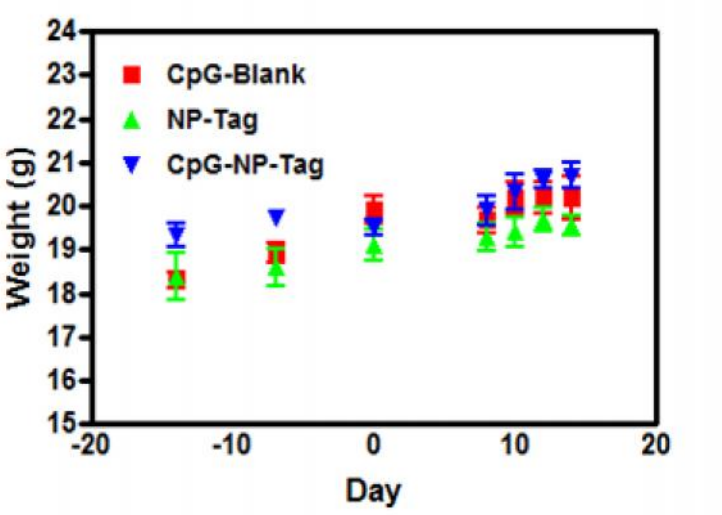

Figure S4: Effect of CpG preimmunization and NP immunization on animal weight before and after tumor challenge. Day -14 indicates CpG preimmunization, day -7 indicates NP immunization and day 0 is the day of tumor challenge. Weight (g) was measured post tumor challenge until day 14 before sacrificing the animals.

Figure S5

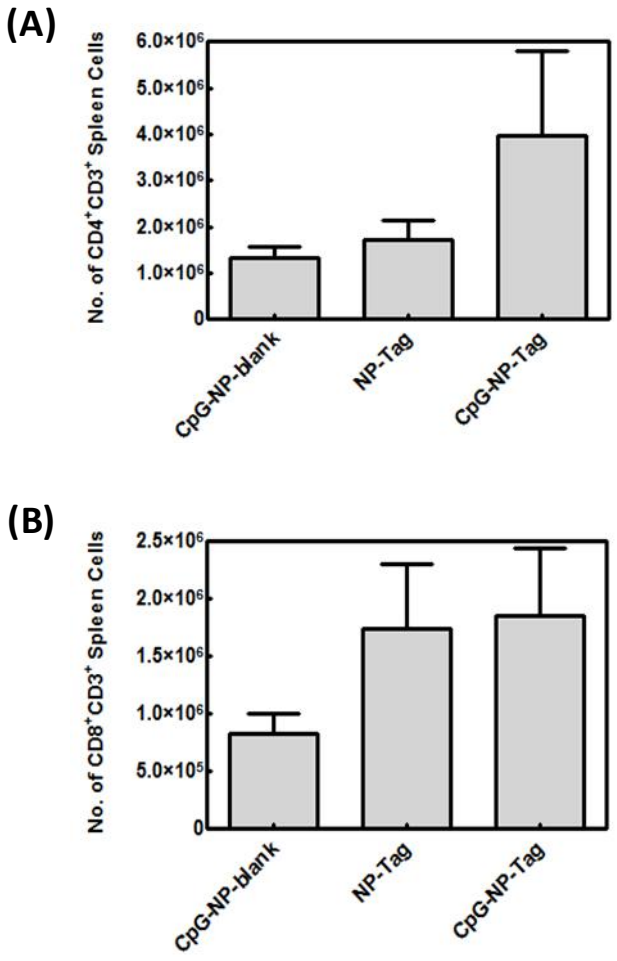

Figure S5: T cell response in spleen. 8A) and B) Splenocytes were isolated from immunized mice (n=4) on day 7 and flow cytometry was conducted for $CD4^+$ and $CD8^+$ T lymphocytes respectively.

Figure 6

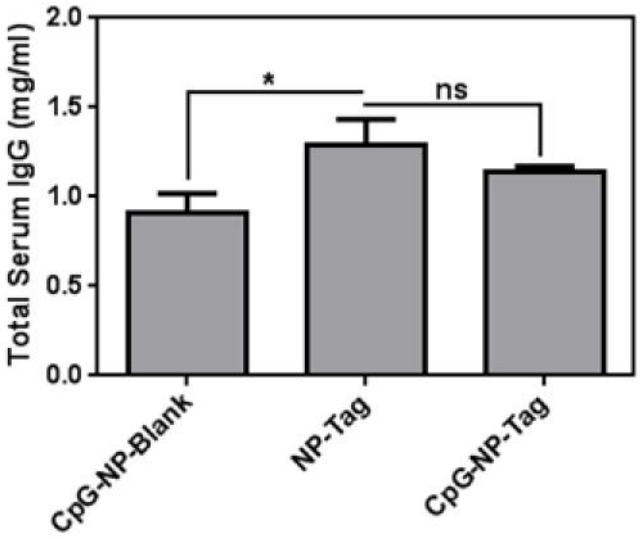

Figure S6: Serum total Immunoglobulin (IgG) levels. Serum was collected from NP-immunized tumor bearing mice on day 14 prior to the sacrifice and ELISA was conducted to measure the antibody titers (*$p<0.05$, ns= non-significant).

CHAPTER III

RATIONALIZING THE USE OF FUNCTIONALIZED PLGA NANOPARTICLES FOR DENDRITIC CELL TARGETED ANTICANCER THERAPY

Rutika A. Kokate[1,2], Pankaj Chaudhary[1,2], Xiangle Sun[3], Sanjay I. Thamake[1,2,#], Sayantan Maji[1,2], Rahul Chib[3], Jamboor K. Vishwanatha[1,2] and Harlan P. Jones*[1,2]

[1] *Department of Molecular and Medical Genetics, University of North Texas Health Science Center (UNTHSC), Fort Worth, TX 76107, USA*

[2] *Institute of Cancer Research, UNTHSC, Fort Worth, TX 76107, USA*

[3] *Department of Cell Biology and Immunology, University of North Texas Health Science Center (UNTHSC), Fort Worth, TX 76107, USA*

[#] *Current Address:*

RadioMedix Inc., Houston, TX 77042, USA

* Corresponding Authors: Department of Molecular and Medical Genetics, UNTHSC, 3500 Camp Bowie Blvd, Fort Worth, TX 76107, USA.

E-mail address: Harlan P. Jones (Harlan.Jones@unthsc.edu) Phone: 817-735-2448/0494

1. ABSTRACT

Poly(lactide-coglycolide) (PLGA) nanoparticles (NPs) encapsulating tumor antigen (Tag) have been successfully used to induce cell mediated immunity in animal models. Delivery of polymeric PLGA based biodegradable NPs to APCs, particularly DCs, has potential for Cancer Immunotherapy. However, the mechanisms through which PLGA NPs impart antitumor effects remain elusive. Using our established NP antitumor vaccine construct, In the current study characterized its efficacy model in rationalizing *in vivo* and *in vitro* use. Our results demonstrate attenuation of tumor growth and angiogenesis in vivo as well as induction of potent tumor-specific cytotoxic T-lymphocyte (CTL) responses. Since PLGA based vaccines are known to operate through DCs, we alsotested the efficacy of our NP construct to stimulate DCs in an *ex vivo* model using bone marrow derived dendritic cells (BMDCs). Our findings demonstrate that CpG-NP-Tag NPs were avidly taken up by BMDCs and exhibited an elevated maturation and activation status. Specifically, CpG-NP-Tag NPs were found to be engulfed preferentially by BMDCs in significantly higher amounts and exclusively localized in the endosomal compartment. CpG-NP-Tag pulsed BMDCs showed higher percent of CD80 and CD86 expressing sub population of BMDCs as well as higher IL12 secretion relative to controls. Collectively, all these results portray that apart from inhibiting tumor growth CpG-NP-Tag NPs possess antitangiogenic and immunostimulatory properties *in vivo* as well as ability to stimulate DCs ex vivo. Studies conducted with CpG-NP-Tag NPs could form a stepping stone for the development of *ex vivo/in vivo* DC based NP vaccines in future.

KEYWORDS: Nanoparticle (NP), Cancer Vaccines, Dendritic Cells (DCs).

2. INTRODUCTION

Cancer is the major cause of morbidity and mortality in western countries [108]. Traditional treatment regimens such as chemotherapy, radiotherapy and surgery are partially successful is limiting primary tumors, but due to the heterogeneous nature of disease (e.g. metastasis), many cancer therapies have low therapeutic indices and are accompanied by multiple non-specific toxicities or side effects [43]. Thus, there is a need to develop effective adjuvant therapies that could be combined with the current treatment to target primary tumors as well as the residual disease [39].

An increased understanding of immune responses against cancer has led to major breakthroughs is cancer research, yielding a growing field of cancer immunotherapy [109,110]. Targeting patients' immune system to identify and kill tumor cells has proven to reduce primary and metastatic cancers while minimizing detrimental effects to non-cancerous cells [110]. Also, the ability to manipulate immune responses for the induction of tumor-specific immunological memory holds promise for cancer vaccines [111]. Such therapies akin to the FDA approved dendritic cell (DC) vaccine, Sipuleucel-T for metastatic prostate cancer, exemplify the potential for immunotherapy as adjunctive cancer therapy [112]. The emergence of immune-based cancer treatments however, are not without considerable limitations including, immune suppression caused by current radio-chemo-therapy [113,114], dose toxicity of immune adjuvants (e.g. IL-2) [115], and immune penetrance and targeting of primary tumors [116,117]. Therefore, further research is critical to fully recognize the potential efficacy of safe, non-toxic, clinically relevant immunotherapies.

Delivery vehicles for such vaccines are of prime interest in the success of immune-based cancer therapies. Nanocarrier systems for the delivery of anticancer therapeutics have prompted

special interests for the field of immunotherapy. In addition to loading chemotherapeutic drug candidates, the ability to encapsulate Tumor Associated Antigens (TAAs) or peptide conjugates as immune stimulants is currently being pursued as primary cargo for nanocarrier systems [10]. Use of nanoparticles (NPs) is thought to increase the antigenic properties of encapsulated soluble antigens by increasing uptake by antigen presenting cells, particularly dendritic cells (DCs) [112,118](Luis J. Cruz). Also, the large surface to volume ratio provided by NPs allows efficient surface functionalization which could be used for cellular targeting purposes or secondary cargo loading. A majority of TAAs are weakly immunonogenic and result in weak vaccines [119]. To circumvent poor tumor-specific immunogenicity, NPs could provide an additive immunogenic effect coupled with immune stimulants thus making co-delivery of multiple agents possible [112].

NP synthesis and surface fabrication can be customized to yield desired optimal properties [112]. In particular, Poly(lactide-coglycolide) (PLGA) based nanoparticles have been extensively studied for developing antigen based vaccines with controlled release properties. Biodegradable PLGA NPs have been designed to encapsulate both antigen and adjuvant inside the nanoparticle or surface functionalization [41]. The main advantage of using PLGA NPs from a vaccine perspective is that they serve as a safe, non-toxic mode of co-delivery of Ag and adjuvant for a sustained period of time [39,120,121].

In our studies we have used PLGA NP system for delivery of breast tumor antigen (Tag: membrane lysate of 4T1 murine mammary carcinoma cells) and surface functionalized bacterial ligand CpG (immune stimulant) using BS3 cross linker resulting in the "bacteriomimetic" CpG-NP-Tag NP formulation. Previous studies conducted and published recently *(article in press)* by our group indicate that CpG-NP-Tag NPs were able to inhibit cancer cell proliferation, growth, and promote apoptotic cancer cell death *in vivo*. CpG-NP-Tag NPs showed immunostimulatory

potential by increasing both $CD4^+$ and $CD8^+$ T cell infiltration in tumor tissue. The studies described in this project indicate that CpG-NP-Tag NPs were not only able to inhibit growth but had significant anti-angiogenic properties. Our next goal was to probe into the mechanistic details of CpG-NP-Tag NPs which is currently elusive in nature in case of most particulate vaccines.

The majority of literature claims that DCs the "professional Antigen presenting Cells (APCs)" of the immune system are the prominent initiators of antigen Ag-specific immune responses and therefore are the key components of cancer vaccines [118]. Vaccination models involving DCs have been developed owing to their unique properties [47,122]. For the induction of DC-based immune responses it is essential that Ag is engulfed by DCs. The final goal of DC vaccination is to produce potent effector response that will lead to tumor eradication and that produce immunological memory for the purpose of controlling tumor relapse [31,123,124]. For this purpose the encounter of DC and Tag is crucial. This can be achieved *ex vivo* by pulsing DCs (derived from patient) with Tag along with immune stimulants (such as GM-CSF or TLR agonists that induce DC maturation) and then injecting cells back into patient. Preliminary studies using *ex vivo* pulsed DCs have shown positive outcomes in some cancer patients but clinical trials in general show poor efficacy [55]. Another route could be by inducing DCs *in vivo* to engulf Tag. Possible limitation of such a route could be development of a clinically relevant delivery system to deliver the Ag load in sufficient amounts to generate potent cytotoxic T cell (CTL) as well as $CD4^+$ T helper cell responses for tumor immunity [40]. From an immunological perspective it would be desirable to develop a safe and non-toxic carrier system that will preferentially target the "professional APCs" (i.e. DCs) leading to their activation [10,55].

Since NP vaccine systems work mainly via DCs; in the last segment of this project we describe some interesting *ex vivo* studies with bone marrow derived dendritic cells (BMDCs) which portray the capacity of "bacteriomimetic" CpG-NP-Tag NPs to improve DC function and thus serve as optimal candidates for *ex vivo* and possibly *in vivo* DC based vaccines in future.

3. MATERIALS AND METHODS

3.1. Materials

Poly (D,L-lactide-co-glycolide) 50:50; inherent viscosity 0.7-0.9 dL/g; mw 50,000 was purchased from Lakeshore Biomaterials (Birmingham, AL). Polyvinyl alcohol (PVA; mw 30,000–70,000; alcoholysis degree 88 ~ 99.9 (mol / mol) %) was purchased from Sigma Aldrich (St Louis, MO). BS3 was purchased from Thermo Fisher Scientific (Indianapolis, IL). CpG-ODN 1826 (Class B CpG Oligonucleotide-Murine TLR9 ligand) was obtained from InvivoGen (San Diego, CA). RPMI 1640 media, Penicillin-Streptomycin (Pen-Strep), fetal bovine serum (FBS) were obtained from Invitrogen (Carlsbad, CA). Anti-Mouse IFN-γ Alexa fluor 488, CD31 (PECAM-1) eFluor® 650NC, CD80 (B7-1) FITC, CD86 (B7-2) APC and CD107α Alexa fluor 488 purchased from ebioscience, Inc. (San Diego, CA).

3.2. Cell Line

4T1 murine mammary carcinoma cell line was purchased from American Type Culture Collection (ATCC), [Manassas, VA] and was grown until seventy percent confluent in RPMI media supplemented with 10% FBS and 1% Pen-Strep.

3.3. Mice

Adult female BALB/c AnNHsd mice (5-6 weeks) were obtained from Harlan laboratories, Inc. (Indianapolis IN) and used for all studies. Mice were maintained at UNTHSC animal facility and allowed to acclimatize for a week prior to experimentation to avoid shipping stress. Mice were kept under optimal temperature and humidity conditions and provided with proper care under Institutional Animal Care and Use Committee (IACUC) guidelines. All procedures for the studies were in accordance with the IACUC guidelines at UNTHSC.

3.4. Generation of Bone Marrow Derived Dendritic Cells (BMDCs)

Briefly, mice were sacrificed with anesthesia followed by cervical dislocation, and rare legs were excised with two intact bones (femur-upper bone and tibia-lower bone). Every muscle and flesh was cleaned and the bones were placed in 70% ethanol in a petridish for 10 min. Bones were transferred to wash media (RPMI supplemented with 1% FBS and 1% Pen-Strep). One end of tibia (lower part) was cut and bone marrow cells were flushed out in an 50 ml conical tube using 27G needle and 10 ml syringe. Cells were centrifuged at 200g for 10 min and incubated with 10 ml ACK (ammonium-chloride-potassium) lysis buffer for 10 min to remove the red blood cells. Cells were centrifuged and resuspended in culture media (RPMI media supplemented with 10% FBS, 1% Pen-Strep, 10ng/ml GM-CSF and 10ng/ml IL-4) and passed through mesh boat (to remove any debris) into a 60 mm culture plate containing 14 ml of culture media. On day 7 of the culture, BMDCs were transferred to either 6-well/12/24/96 well plates for different experiments [125].

3.5. Membrane Lysate preparati[125]on:

Membrane fraction of 4T1 cells was prepared using hypotonic buffer and dounce homogenizer followed by centrifugation at 5,000 x g at 4°C for 15 minutes to pellet cell debris.

Supernatant was collected and further centrifuged at 100,000 g for 1 hr at 4°C using N55 rotor to obtain the membrane lysate pellet. Final membrane fraction was washed with PBS and resuspended in 100-150 µl of RIPA buffer. Pierce™ BCA protein assay kit (Thermo Scientific, Rockford, IL) was used to estimate the protein concentration.

3.6. Formulation of CpG-NP-Tag NPs:

CpG-NP-Tag NPs were prepared using water-in-oil-in-water (w/o/w) double emulsion method employing solvent evaporation technique reported in our previous studies (article in press). Briefly, primary emulsion (w/o) was prepared by vortexing a 200 µl of Tag solution (1 µg/µl) with organic phase (PLGA in ethylacetate). The primary emulsion (w/o) was added to aqueous phase (BS3 solution in PVA). The mixture was sonicated on ice using an ultrasonic processor UP200H system (Hielscher ultrasonics Gmb, Germany) for 1 minute) to form activated NPs. After washing with 0.01% sucrose solution 3 times these NPs were lyophilized on ATR FD 3.0 system and stored at -20 °C until further use. For optimal conjugation of CpG, CpG ligand (1:200 w/w ratio) and resuspended NPs were incubated on an orbital shaker for 1-2 hours at room temperature. After removal of excess ligand with PBS washes, CpG coated Tag containing "bacteriomimetic" NPs (CpG-NP-Tag) were obtained. CpG-NP-Tag NPs were characterized and subsequently used for *in vivo* and *ex vivo* studies.

3.7. Characterization of NPs

3.7.1. Particle size, Polydispersity Index (PDI), Zeta Potential and Encapsulation efficiency:

Particle size, PDI and was measured using Zetasizer (Malvern Instruments Ltd.). A known quantity of NPs (0.25- 0.5 mg) were resuspended in 1m distilled water and further

diluted 10 times before measuring particle size and zeta potential. Tag encapsulation efficiency was confirmed based on the amount of Tag (protein) extracted after degrading a fixed amount of NPs. 5 mg of NPs were degraded using 500 µl Acetonitrile (Sigma-Aldrich, St. Louis, MO) by incubating at 37° C on a shaker (6-8 hrs). Samples were further centrifuged at 11,000 g at 4° C for 10 minutes and the supernatants were tested for their protein content using Bicinchonic acid (BCA) protein assay kit (Thermo Scientific, Rockford, IL) as per manufacturer's instructions [126]. Encapsulation efficiency was calculated as follows: Amount of protein encapsulated / amount of protein used in encapsulation * 100%.

3.7.2. Scanning electron microscopy (SEM):

SEM images were taken using Sigma VP Field Emission Scanning Electron Microscope manufactured by Carl Zeiss Microscopy Ltd. NP Samples were coated with a Cressington 108 Sputter Coater for thirty seconds. Target used for coating was an Au-Pd target.

3.7.3. Ligand Binding Efficiency:

For evaluating CpG ligand binding efficiency, 0.5 mg of NPs were resuspended in distilled water and incubated with 7 µg of CpG-FITC for 60-90 min followed centrifugation and washing at 11,000 g for 15 min to remove excess CpG ligand. Flow cytometry was conducted using a Beckman Coulter Cytomics FC 500 Flow Cytometer from core facility to determine the binding efficiency.

3.8. Enzyme Linked Immunoabsorbent Assay (ELISA)

BMDCs were obtained and cultured as described above in section 2.4 of materials and methods. On day 6, BMDCs (approx. $1*10^4$) were plated in 96 well round bottom plates

and were pulsed with 0.5-1mg of NPs for 24 and 48 hr respectively. Supernatants were collected at both time points and IL12 levels in the supernatants collected were measured using Mouse IL-12 p70 ELISA Ready-SET-Go! reagent set from ebioscience as per manufacturer's instructions. Briefly, 96-well flat bottom plates were coated with optimal concentrations of capture antibody and blocked later with assay diluent (provided in the kit). Standards/supernatant samples were incubated overnight at 4° C following incubation with biotin-conjugated detection antibody and Avidin-HRP (horseradish peroxidase). Tetramethylbenzidine (TMB) peroxide substrate solution from the kit was added and the concentration of IL12 cytokine in the samples was determined based on the standard curved generated for the cytokine. Readings were taken at wavelength of 450 nm using colorimetric plate reader (Biotek Instruments Inc. Winooski, VT).

3.9. Syngenic breast cancer BALB/c mice model

Mice were pre-immunized intraperitoneally with CpG (600 µg/kg) and subsequently immunized with the respective NPs (as listed in Table 1) 7 days before tumor challenge. The required dose of NPs (6mg) was calculated based on the encapsulation efficiency. Mice immunized with the CpG-NP-Tag NPs (n=7) comprised the treatment group while the control group consisted of mice immunized with CpG-NP-Blank NPs (n=7) and NP-Tag (n=7). Seven days post NP immunization mice were challenged with $1*10^5$ 4T1 cells. Primary tumor size was monitored over the course of 21 days following tumor challenge. After sacrificing animals on day 21, spleens and primary tumors were procured for further studies (Fig. 1).

Figure 1

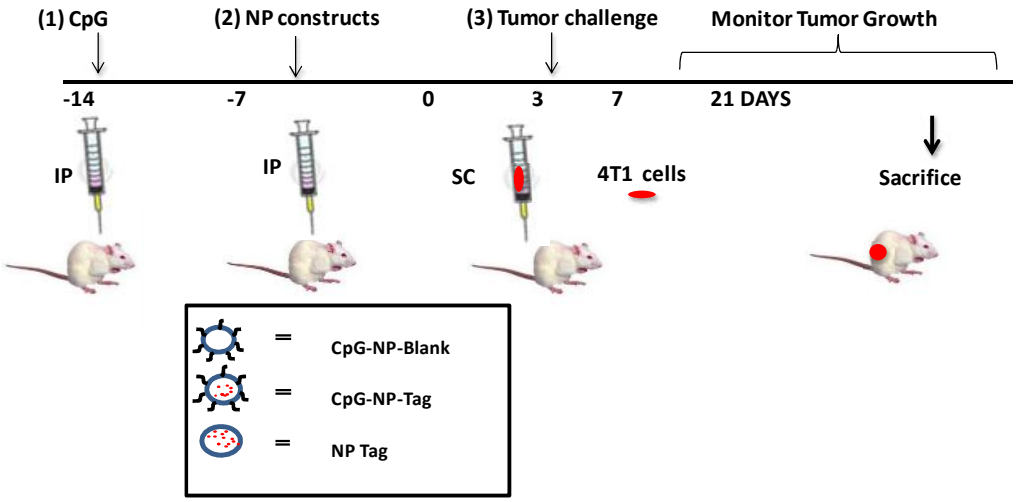
(1) CpG
(2) NP constructs
(3) Tumor challenge
Monitor Tumor Growth
-14
-7
0
3
7
21 DAYS
IP
IP
SC
4T1 cells
Sacrifice
=
CpG-NP-Blank
=
CpG-NP-Tag
=
NP Tag

Figure 1: Schematic of the study timeline followed for the *in vivo* model. 5-6 weeks female BALB/c mice (n=7) were preimmunized intraperitoneally (IP) with CpG 14 days before tumor challenge followed by IP immunization (7days after CpG preimmunization) with the respective groups of NPs. Mice were challenged subcutaneously (SC) with 10^5 4T1 mammary carcinoma cells and the effect of NP immunization was evaluated on the rate of tumor growth and immune response for 21 days.

3.9.1. Rate of tumor growth and animal weight:

Tumor size and animal weight were measured until day 21 at different time intervals using vernier caliper and calibrated weighing balance respectively. Tumor volume (mm^3) was calculated for all the animals using the below mentioned formula [88]. Tumor volume (mm^3) = $\pi/6$ (length *breadth*height).

3.9.2. Histological analysis of tumors:

Tissues were fixed in 4% paraformaldehyde, embedded in Optimum Cutting Temperature (O.C.T) compound (Tissue-Tek, Sakura Fine-Tek, Torrance, CA) and sectioned using cryostat to obtain 5-8 µm thin sections. Frozen sections were stored at -80° C and used subsequently for Immunofluorescence staining.

3.9.3. Hemoglobin estimation by Drabkin's reagent:

To quantify the formation of functional vasculature in the tumor, the amount of hemoglobin was measured using a Drabkin reagent kit 525 (sigma, St. Louis, MO) following the Drabkin and Austin method. Briefly, the excised tumors were chopped and homogenized in a Dounce homogenizer in presence of 0.5 ml deionized water and allowed to stand overnight at 4 ºC. The lysate was centrifuged at 5000 g for 10 mins and the supernatant was collected. 0.3 ml of each sample was mixed with 0.5 ml of Drabkin's reagent and allowed to stand for 15 mins at room temperature. The absorbance was read at 540 nm by using Drabkin's reagent solution as blank. A standard curve was constructed by using known concentrations of hemoglobin and the concentrations of the samples were obtained from the standard curve [127].

3.10. BMDC NP uptake and Intracellular Localization:

To evaluate uptake of the NPs flow cytometry was conducted using nile red stained NPs. BMDCs (approx. $5 * 10^4$) were plated in 6-well plates on day 6, and pulsed on day 7 with the respective groups of NPs (1-2 mg) for 60 min and processed for flow cytometric analysis. Briefly, cells were washed twice post NP incubation and trypsinized using 0.25% trypsin (Hyclone Laboratoroes, UT). Cells were washed with staining buffer (1X PBS and 1% FBS) and centrifuged for 10 min at 200g. Cells were fixed using 4% paraformaldehyde in dark for 20 min and analyzed the next day for NP uptake .Flow cytometry was conducted using a Beckman Coulter Cytomics FC 500 Flow Cytometer from core facility. For the purpose of intracellular (Endosomal) localization, Immunocytochemistry was conducted. Briefly, BMDCs were grown on cover slips in a 6- well plate and pulsed with a fixed quantity (1-2 mg) of nile red stained NPs for 1 hr. Cells were washed twice with PBS and were incubated with an early endosome marker, EEA1 (primary) antibody overnight. Cells were washed thrice with PBS and incubated with secondary antibody conjugated to alexa fluor 488 for 1 hr. Cells were fixed with 4% paraformaldehyde and mounted in a medium containing 1.5µg/ml DAPI and confocal microscopy was used to study intracellular Endosomal localization. Confocal microscopy was conducted utilizing LSM 510 META (Carl Zeiss).

3.11. Immunostimulatory efficacy of bacteriomimetic NPs

Immunostimulatory potential was evaluated by quantifying IFN-γ cytokine production in tumor using Immunofluorescence staining technique. CD107α assay was performed to evaluate CTL activity. Maturation markers CD80/86 were determined using flow cytometric analysis.

3.11.1. BMDC activation and maturation

To evaluate the effect of NP immunization on APCs, BMDCs were derived from BALB/c mice as described above in section 2.4 in materials and methods. At day 7 of the culture, BMDCs were pulsed with a fixed amount (1-2 mg) of different groups of NPs for 48 hrs. At day 9, BMDCs were processed for flow cytometry to determine the expression of maturation markers, CD80/86. Briefly, cells were washed twice post NP incubation and trypsinized using 0.25% trypsin (Hyclone Laboratoroes, Utah). Cells were washed with staining buffer (1X PBS and 1% FBS) and centrifuged for 10 min at 200g. Cells were incubated with antimouse CD80 FITC and CD86-APC antibodies for 1 hr in dark. After washing with staining buffer, cells were fixed using 4% paraformaldehyde in dark for 20 min and analyzed the next day for maturation markers CD80 and CD86 .Flow cytometry was conducted using a Beckman Coulter Cytomics FC 500 Flow Cytometer from core facility.

3.11.2. Cd107α Assay

For this assay, we followed the same study time-line as mentioned before (Figure 2). After CpG pre-immunization and NP immunization, animals were sacrificed day 21 post tumor challenge and spleens were harvested to obtain the splenocytes (effector cell population: E). For stimulation, splenocytes (primed *in vivo* due to NP immunization) stained with alexa 488 conjugated anti-CD107α were co-cultured with target 4T1 cells (T) at different E: T (1:1; 5:1; 10:1; 20:1) ratios for 4-6 hours. Flow cytometric analysis was conducted to measure the population of CD107a expressing CTLs.

3.12. Statistical analysis

GraphPad Prism 6 version was utilized for analyzing biological assays. One way ANOVA and unpaired Student's t test ($p<0.05$) were used to analyze the *in vivo* and *ex vivo* data.

4. RESULTS

4.1. Formulation and characterization of nanoparticles

CpG-NP-Tag NPs were prepared using our previously established modified double emulsion technique followed by solvent evaporation. Three groups of NPs were formulated as shown in Figure.1. CpG-NP-Blank and NP-Tag NPs served as control groups for all our experiments along with the test CpG-NP-Tag formulation. We successfully incorporated Tag (membrane lysate of 4T1 tumor cells) in the nanoparticle core and docked CpG ligand on the surface employing BS3 crosslinker. These NPs were characterized for particle size, Polydispersity index (PDI), zeta potential, surface morphology, CpG ligand binding efficiency and Tag encapsulation efficiency. The particle size of non-coated NP-Tag particles and coated CpG-NP-Blank and CpG-NP-Tag NPs was found to be 227.3 ± 0.07 nm, 230.6 ± 0.78 nm and 229.2 ± 0.71 nm respectively (Fig. 2A and Table 1). Surface zeta potential was found to be, -1.14 ± 0.56 mV for CpG-NP-Blank, -0.51 ± 0.59 for NP-Tag and -1.18 ± 0.39 for CpG-NP-Tag NPs (Fig. 2B and Table 1). PDI and encapsulation efficiency for the respective NP formulations are listed in Table 1. SEM images of the particles confirmed the particle size as well as morphology. Particles were found to be uniform in size, spherical and non-agglomerated with smooth surface (Fig. 2C).The CpG ligand binding efficiency tested by flow cytometry was found to be around 12-14 percent (Figure 3A and 3B).

Table 1. Physicochemical Characterization of NPs

Sr. no.	NP-Construct	Particle Size (nm± SD)	Zeta potential (mV ± SD)	PDI	Encapsulation efficiency (%)
1.	CpG-NP-Blank	230.6 ± 0.78	-1.14 ± 0.56	0.134	
2.	NP-Tag	227.3 ± 0.07	-0.51 ± 0.59	0.166	37.45 ± 8.38
3.	CpG-NP-Tag	229.2 ± 0.71	-1.18 ± 0.39	0.13	37.45 ± 8.38

NPs: Nanoparticles
NP-Construct: Nanoparticle Construct
PDI: Polydispersity Index
PLC: Protein (Tag) Loading Content

Figure 2

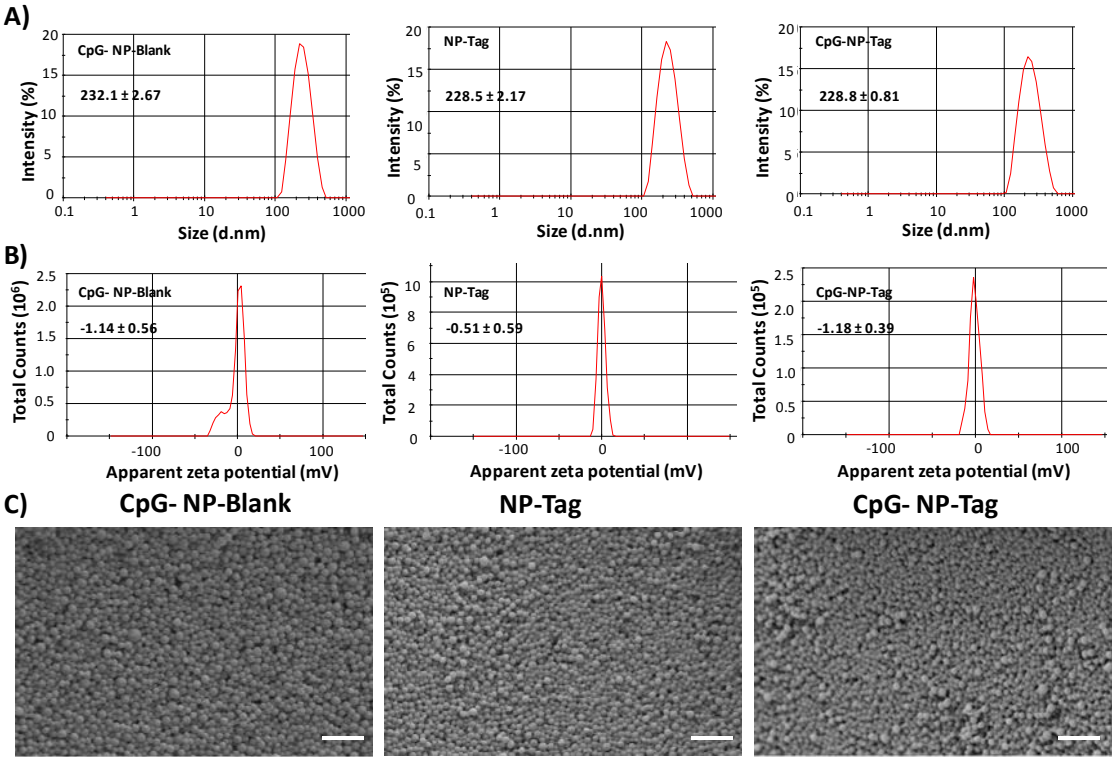
A)
CpG- NP-Blank
232.1 ± 2.67
NP-Tag
228.5 ± 2.17
CpG-NP-Tag
228.8 ± 0.81
Intensity (%)
Size (d.nm)
B)
CpG- NP-Blank
-1.14 ± 0.56
NP-Tag
-0.51 ± 0.59
CpG-NP-Tag
-1.18 ± 0.39
Total Counts (10^6)
Total Counts (10^5)
Apparent zeta potential (mV)
C)
CpG- NP-Blank
NP-Tag
CpG- NP-Tag

Figure 2: Characterization of Nanoparticles (NPs). A) Particle size distribution of CpG-Blank (i), NP-Tag (ii) and CpG-NP-Tag (iii) NPs obtained from dynamic light scattering (DLS) measurements. **B)** Surface zeta potential graphs for CpG-Blank, NP-Tag and CpG-NP-Tag NPs **C)** Scanning Electron Micrographs of CpG-Blank, NP-Tag and CpG-NP-Tag NPs (Scale, bar: 1μm).

Figure 3

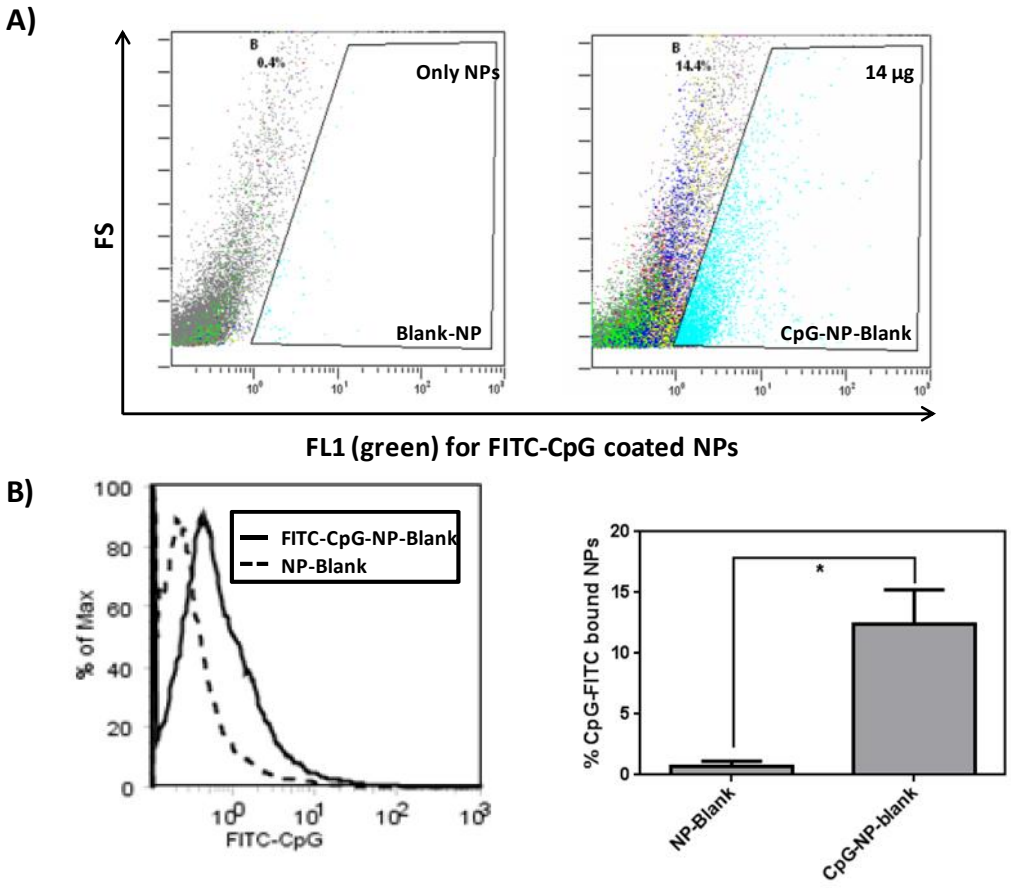
A)
B
0.4%
Only NPs
Blank-NP
B
14.4%
14 µg
CpG-NP-Blank
FS
FL1 (green) for FITC-CpG coated NPs
B)
100
80
60
40
20
0
% of Max
FITC-CpG-NP-Blank
NP-Blank
FITC-CpG
20
15
10
5
0
% CpG-FITC bound NPs
*
NP-Blank
CpG-NP-blank

Figure 3: CpG Ligand Binding Efficiency. A) Percentage of CpG bound Nanoparticles (NPs). 1mg /ml of NPs were incubated with 14 µg of CpG-FITC and percent of CpG bound NPs was determined using flow cytometry. **B)** Histograms of blank NPs and CpG-FITC bound NPs (FITC-CpG-NP-Blank) indicating shift in fluorescence for the CpG-FITC bound NPs. **C)** Quantification of the ligand binding efficiency data obtained from flow cytometric measurements (*$p < 0.05$).

4.2. In vivo antitumor efficacy of CpG-NP-Tag NPs

For *in vivo* model, we followed the study timeline described in section 2.9 and Fig.1. To test the efficacy of CpG-NP-Tag as vaccine carriers in vivo, we first monitored the tumor growth physically by measuring the tumor dimensions at different time points using vernier caliper until day 21. After sacrificing mice, spleens, tumors and serum were collected for further analysis.

4.2.1. Tumor growth

Using the dimensions obtained from vernier caliper readings, tumor volume was calculated using formula mentioned in section 2.9.1. Tumor volume was found to be significantly higher in case of control groups as compared to CpG-NP-Tag immunized mice ($p=0.01$) (Fig.4A).

Fold change in tumor volume over the 21 day period was also found to be relatively slightly greater in case of control groups as compared to CpG-NP-Tag immunized group (Fig.4B). Animals were sacrificed and tumors were excised on day 21 for ex vivo studies. *Ex vivo* examination revealed that the tumors from CpG-NP-Tag immunized mice were significantly smaller in size as compared to controls (Fig.4C).

Figure 4

A)

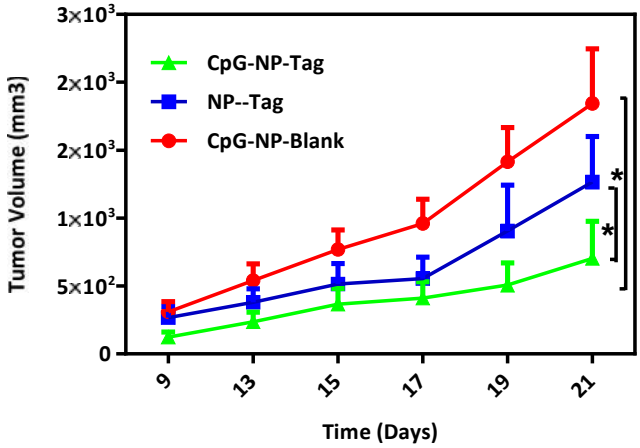
3×10³
2×10³
2×10³
1×10³
5×10²
0
Tumor Volume (mm3)
CpG-NP-Tag
NP--Tag
CpG-NP-Blank
*
*
9
13
15
17
19
21
Time (Days)

B)

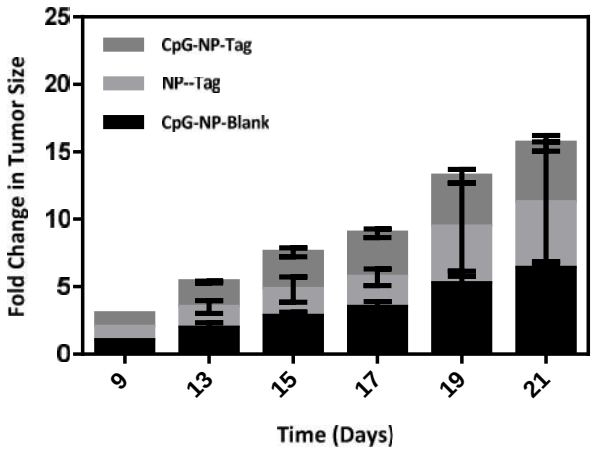
25
20
15
10
5
0
Fold Change in Tumor Size
CpG-NP-Tag
NP--Tag
CpG-NP-Blank
9
13
15
17
19
21
Time (Days)

C)

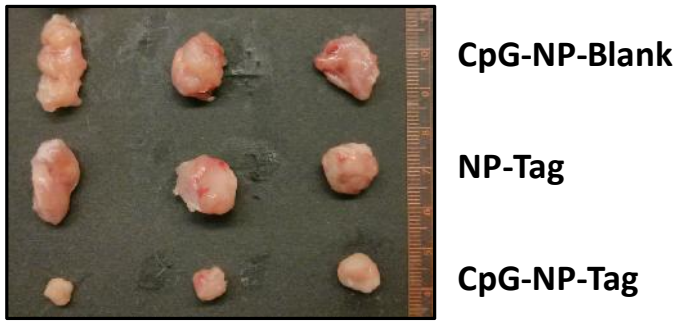
CpG-NP-Blank
NP-Tag
CpG-NP-Tag

Figure 4: A) Tumor volume (mm^3) measured in mice treated with different NP formulations (*$p < 0.05$). **B)** Fold change in tumor volume (mm^3) as compared to Day 9 post-tumor challenge, in mice treated with different NP formulations. **C)** Tumor tissue of animals immunized with respective groups of NPs harvested on day 21 after tumor challenge.

For NP toxicity study weight of the animals was also tracked during the entire study at different time points, right from the start of the study (baseline), prior to CpG-preimmunization, post-preimmunization, post- NP immunization, before and after tumor challenge. As shown in graph in Fig. 5 the weight of the animals remained stable and did not change (lessen or increase) significantly during the course study.

Figure 5

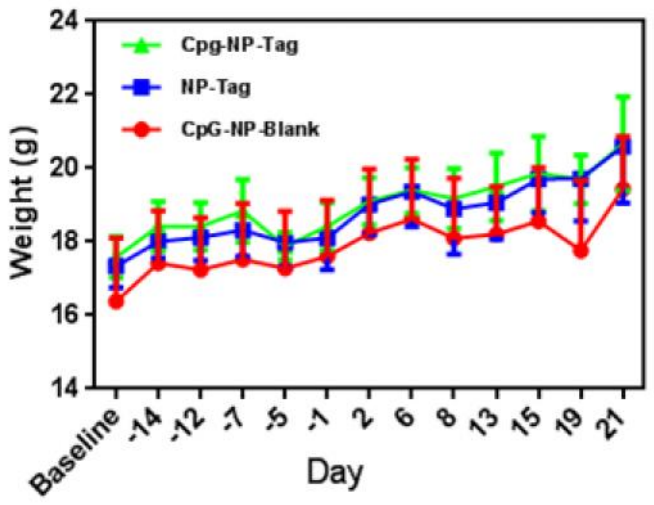
Cpg-NP-Tag
NP-Tag
CpG-NP-Blank
Weight (g)
24
22
20
18
16
14
Baseline
-14
-12
-7
-5
-1
2
6
8
13
15
19
21
Day

Figure 5: Effect of CpG preimmunization and NP immunization on animal weight before and after tumor challenge.

4.2.2. Angiogenic Activity:

During primary tumor excision on day 21, the site of tumor was visually examined to observe any anatomical changes. Dense vascularization was observed in case of control tumors as compared to CpG-NP-Tag mice tumors (Fig. 6A)

To confirm and quantify the angiogenic activity the excised tumors were subjected to biochemical analysis using Drapkins reagents to test the Haemoglobin (Hb) levels which serve as an indirect marker of angiogenesis. CpG-NP-Blank as well as NP-Tag control tumors as expected showed high Hb levels as compared to CpG-NP-Tag tumors ($p= 0.03$) (Fig. 6B).

Figure 6

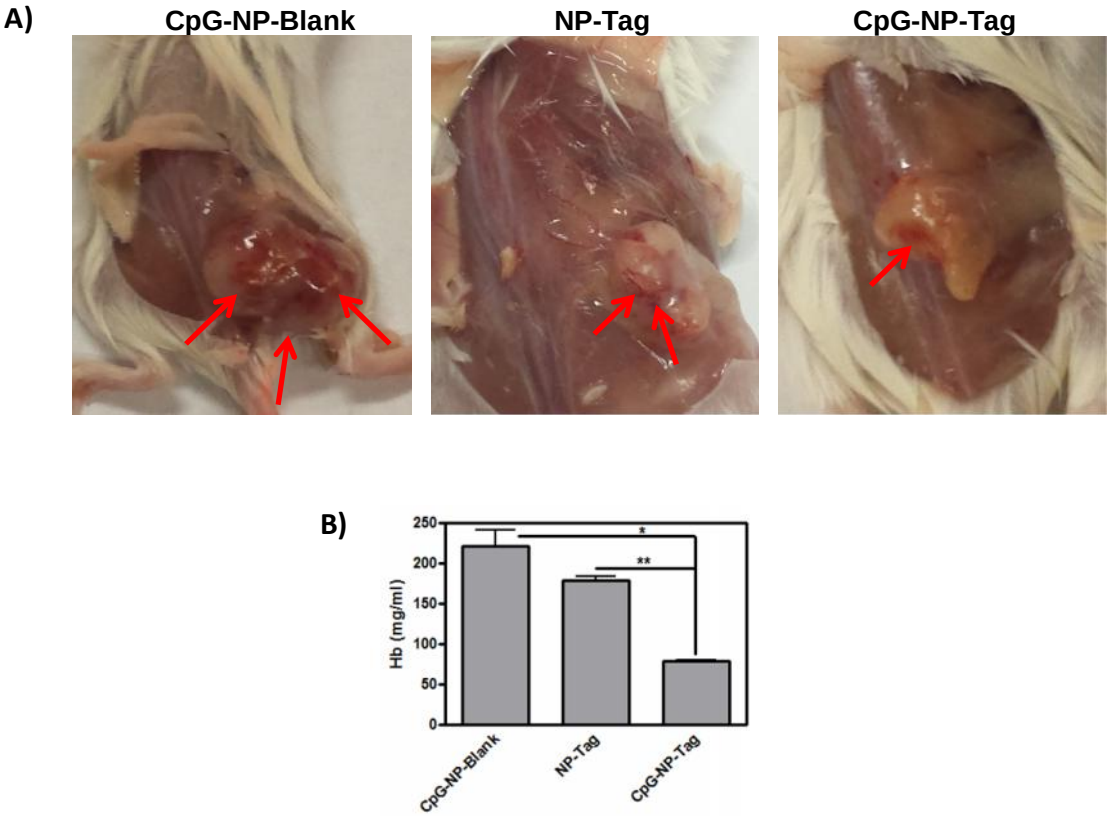
A)
CpG-NP-Blank
NP-Tag
CpG-NP-Tag
B)
Hb (mg/ml)
250
200
150
100
50
0
*
**
CpG-NP-Blank
NP-Tag
CpG-NP-Tag

Figure 6: Effect of Nanoparticle (NP) Immunization on Tumor Vasculature.

A) Representative images of blood vessel vascularization surrounding the primary tumor tissue in tumor bearing mice prior to resection of tumor. **B)** Haemoglobin (Hb) estimation for quantification of blood vascularization (angiogenesis) in tumors harvested from NP immunized mice (*$p < 0.05$; **$p < 0.01$).

The tumors were fixed in 4% paraformaldehyde and embedded in O.C.T and frozen sections were used for further investigation. Immunofluorescence images for CD31 or Platelet endothelial cell adhesion molecule (PECAM-1), a known angiogenesis marker, indicated a significantly high degree of angiogenesis in case of control CpG-NP-Blank as well as NP-Tag tumors relative to CpG-NP-Tag tumors ($p=0.0011$) (Fig. 7A and 7B).

In previous studies, we also determined the local production of cytokine IFN-γ which is known for its antiangiogenic activities via intracellular staining in the tumor sections. We found that IFN-γ levels correlated well the CD31 as well as Hb estimation results in control and treatment group. We observed low levels of IFN-γ in tumor microenvironment correlating to high Hb levels as well as higher CD31 staining in case of control groups while high local production of IFN-γ was seen in CpG-NP-Tag tumors which correlating to low Hb levels and CD31 staining (Fig 6B, 7A, 7B and Supplementary Fig. 1).

Figure 7

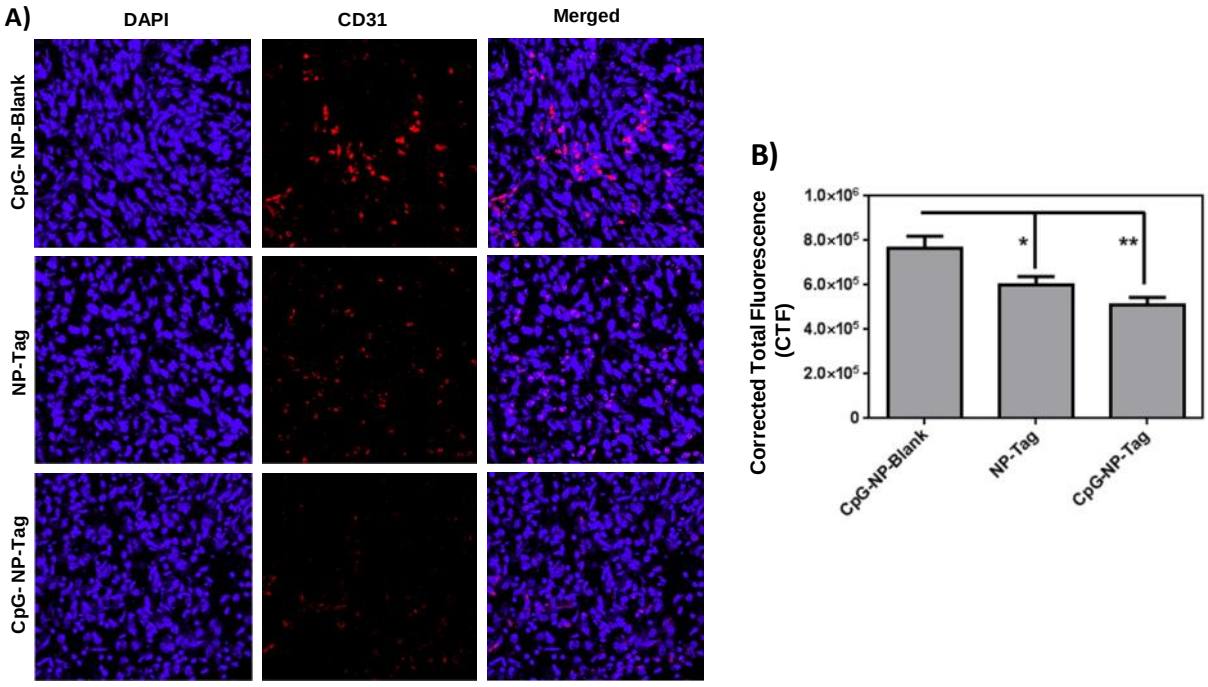
A)
DAPI
CD31
Merged
CpG- NP-Blank
NP-Tag
CpG- NP-Tag
B)
Corrected Total Fluorescence (CTF)
1.0×10⁶
8.0×10⁵
6.0×10⁵
4.0×10⁵
2.0×10⁵
0
*
**
CpG-NP-Blank
NP-Tag
CpG-NP-Tag

Figure 7: Effect of Nanoparticle (NP) Immunization on Angiogenesis.

A) Representative images (40X) of CD31 stained tumor tissues sections showing the angiogenic blood vascularization **B)** Quantitative analysis indicating angiogenic activity surrounding the tumor tissue harvested from the different groups analyzed using NIH ImageJ software (*$p < 0.05$; **$p < 0.01$).

4.2.3. CTL activity

$CD8^+$ T cells are the major effector cell population involved in tumor cell killing. To evaluate the CTL activity of these T lymphocytes we used CD107α assay. For this experiment we used the entire splenocytes population obtained from immunized tumor bearing mice and cocultured it with target 4T1 tumor cells (section 2.11.3). The experiment was conducted at different effector: target ratios and CTL activity was quantified further using flow cytometry. Results from the killing assay indicate that splenocytes from the CpG-NP-Tag immunized mice displayed higher percentage of CD107a+ population as compared to control mice implying enhanced CTL function (Fig. 8).

Figure 8

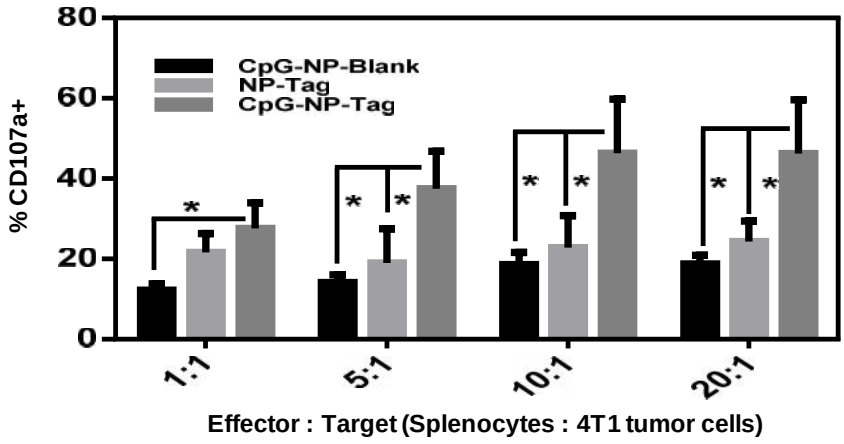
80
60
40
20
0
% CD107a+
CpG-NP-Blank
NP-Tag
CpG-NP-Tag
*
1:1
5:1
10:1
20:1
Effector : Target (Splenocytes : 4T1 tumor cells)

Figure 8: Quantification of Cytotoxic CD8+ T lymphocyte (CTL) activity. CTL activity was measured using CD107α assay. Splenocytes (primed *in vivo* due to NP immunization) obtained from tumor bearing mice a day 21 were stained with alexa 488 conjugated anti-CD107α and subsequently co-cultured with target 4T1 cells (T) at different E: T (1:1; 5:1; 10:1; 20:1) ratios for 4-6 hours. Flow cytometric analysis was conducted to measure the population of CD107a expressing CTLs (*$p < 0.05$).

4.3. Ex vivo immunostimulatory efficacy of CpG-NP-Tag NPs

4.3.1. Dendritic cell uptake and intracellular localization

The uptake of nanoparticle by APCs was checked in BMDCs obtained from female Balb/c mice as described in section 2.3. Cells were cultured on 6 well plates in RPMI 1640 media supplemented with 10% FBS, 1% Pen-Strep, 10ng/ml GM-CSF and 10ng/ml IL-4 until day 7. On day 7, cells were pulsed with nile stained NPs (CpG-NP-Blank, NP-Tag, CpG-NP-Tag) for 60 min and processed for flow cytometric analysis.

The percentage of cells with nanoparticles as well as the Mean Fluorescence Intensity (MFI) data was collected from this experiment. Percent of cells that had engulfed CpG-NP-Tag was found to be slightly greater than control NP-Tag NPs and significantly greater than control CpG-NP-Blank NPs (Fig.9A). MFI data indicated CpG-NP-Tag NPs have significantly higher uptake as compared to control groups ($p=0.0057$) (Fig. 9B).

Figure 9

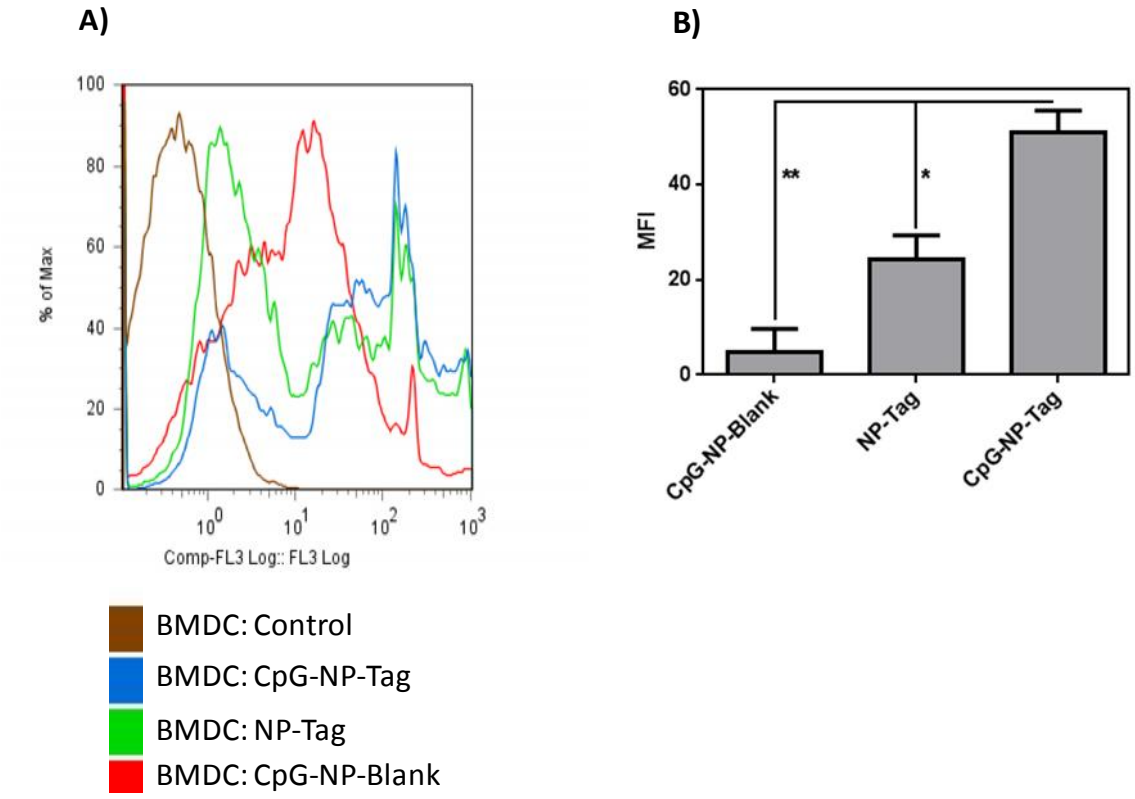
A)
B)
100
80
60
40
20
0
% of Max
10^0
10^1
10^2
10^3
Comp-FL3 Log:: FL3 Log
BMDC: Control
BMDC: CpG-NP-Tag
BMDC: NP-Tag
BMDC: CpG-NP-Blank
60
40
20
0
MFI
**
*
CpG-NP-Blank
NP-Tag
CpG-NP-Tag

Figure 9: Uptake of Nanoparticles (NPs) in Bone Marrow Derived Dendritic Cells (BMDCs). **A)** Percentage of BMDCs positive for the respective nile red stained NPs as determined by flow cytometry. **B)** Mean Fluorescence Intensity (MFI) values indicating uptake of respective NPs in BMDCs (*$p < 0.05$; **$p < 0.01$).

CpG ODN is a TLR9 ligand that is expressed intracellularly in the endocytic compartment. Thus, to check Endosomal localization of the CpG coated NPs (CpG-NP-Blank and CpG-NP-Tag) we used confocal microscopy. We pulsed the BMDCs on day 7 with the respective nile red stained NP formulations for 1 hr and processed the cells for Immunocytochemistry as described in section 2.10. Confocal images revealed that CpG-NP-Blank and CpG-NP-Tag NPs (red) were largely accumulated in Endosomal compartment (green) as compared to non-coated ones (NP-Tag) (Fig.10A). Percent co-localization calculation also indicated higher number of nile red stained coated (CpG-NP-Blank and CpG-NP-Tag) particles (red) co-localized (yellow) with the early Endosomal compartment (green) (Fig. 10A and 10B).

Uptake and intracellular localization for coated (CpG-NP-Blank) and uncoated (NP-Blank) was also analyzed in JAWSII cell line (immature dendritic cells) in another setting and the same trend was observed. Cells showed preferential uptake and Endosomal localization for CpG-NP-Blank NPs compared to uncoated (NP-Blank) ones. (Refer Supplementary Fig. S3 and S4)

Figure 10

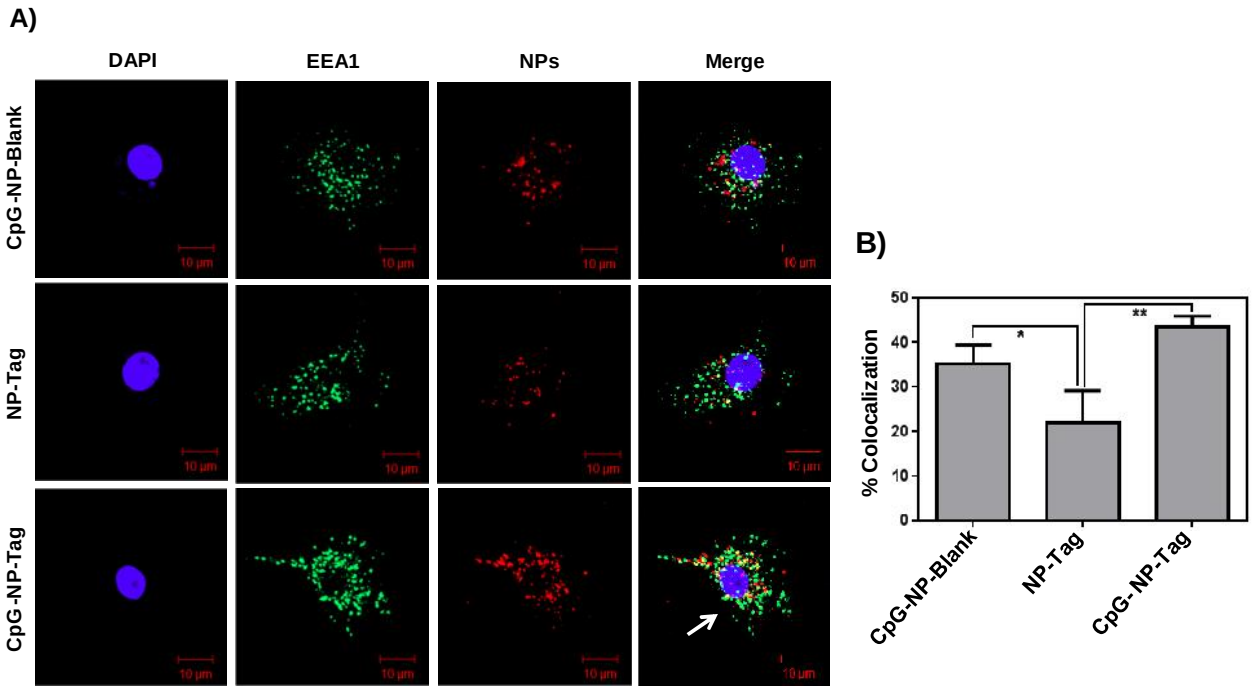
A)
DAPI
EEA1
NPs
Merge
CpG-NP-Blank
NP-Tag
CpG-NP-Tag
10 µm
B)
% Colocalization
50
40
30
20
10
0
*
**
CpG-NP-Blank
NP-Tag
CpG-NP-Tag

Figure 10: NP BMDC intracellular Localization. A) Representative images (40X) showing the Endosomal (green) co-localization (yellow) of the different nile red stained nanoparticles (NPs) in BMDCs **B)** Percent co-localization determined in NP pulsed BMDCs. Imaged show Nile red stained particles (red) co-localized (yellow) with the early Endosomal compartment (green; EEA1) (*$p < 0.05$; **$p < 0.01$).

4.3.2. BMDC activation and maturation

DC based immune induction involves pathogen recognition and uptake, migration, activation and maturation [128]. As potential vaccine delivery system NPs must be engulfed in sufficient amounts leading to subsequent activation and maturation of DCs. After evaluating the uptake, we determined the capability of NPs to induce DC activation and maturation by checking for maturation markers CD80/86 and cytokine IL12. BMDCs were pulsed with respective groups of NPs for 48 hrs and the cells were processed and tested for maturation markers CD80/86 by flow cytometry.

Percent of CD80 and CD86 positive cells were calculated and it was found to be significantly higher in case of CpG-NP-Tag pulsed BMDCs as compared to controls ($p<0.0001$) (Figure 11A and 11B). Supernatants were collected for IL12 ELISA from NP pulsed BMDCs as described in section 2.8. CpG-NP-Tag and CpG-NP-Blank pulsed BMDCs secreted significantly high levels of IL12 as compared to non-coated NP-Tag NPs ($p<0.0001$) (Figure 11C).

Figure 11

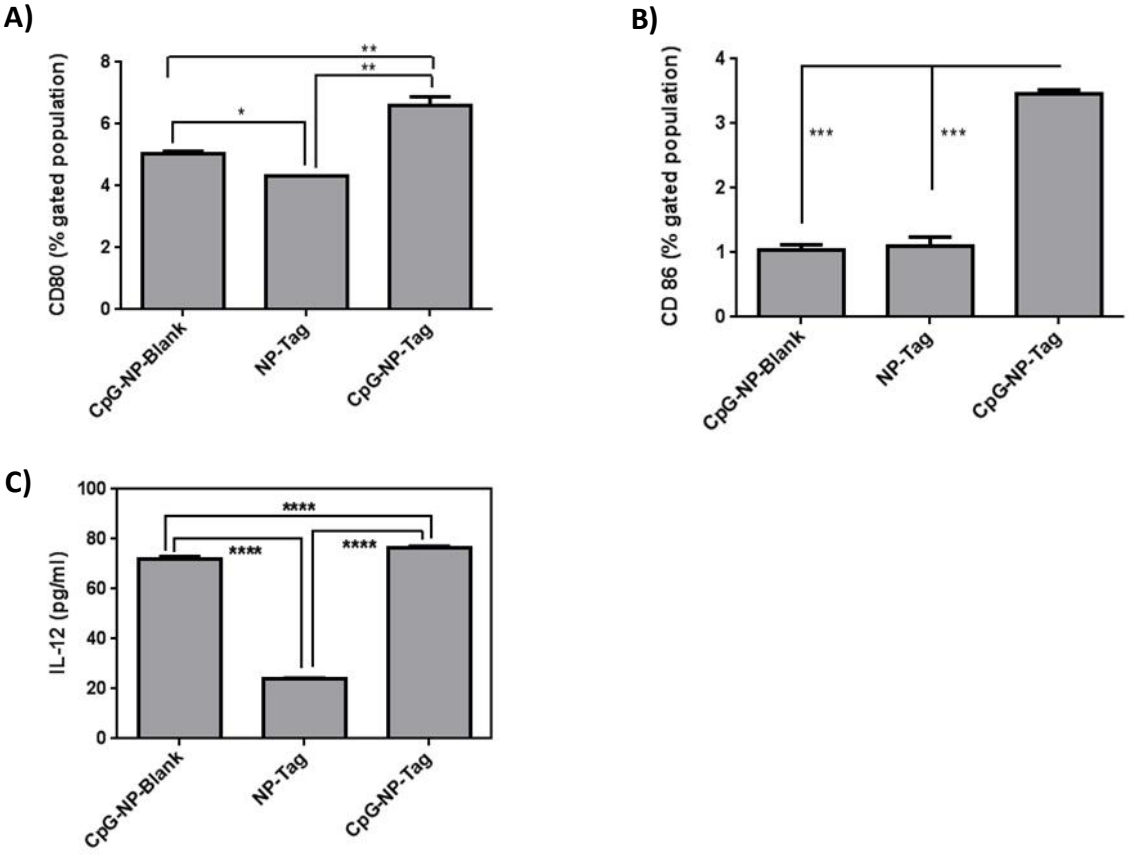
A)
CD80 (% gated population)
8
6
4
2
0
**
**
*
CpG-NP-Blank
NP-Tag
CpG-NP-Tag
B)
CD 86 (% gated population)
4
3
2
1
0
***
***
CpG-NP-Blank
NP-Tag
CpG-NP-Tag
C)
IL-12 (pg/ml)
100
80
60
40
20
0
****
****
****
CpG-NP-Blank
NP-Tag
CpG-NP-Tag

Figure 11: Effect of NPs on BMDC activation and maturation. A) Percentage of NP pulsed BMDCs expressing CD80. B) Percentage of NP pulsed BMDCs expressing CD86 C) IL12 cytokine levels (pg/ml) in supernatants collected from NP pulsed BMDCs post 48 hrs measured by ELISA (****$p < 0.0001$).

5. DISCUSSION

Multifunctional nanosystems (dendrimers, polymeric NPs, metallic NPs) allows use of different technologies (surface attachment, encapsulation, labeled NPs) for site specific, simultaneous or sequential delivery of multiple components (antigens, adjuvants, peptides, tracking agents/dyes) to antigen presenting cells, particularly DCs as they are key immune based regulators [10,47]. One of the challenges in using this technology in cancer immunotherapy is the development of a suitable delivery vehicle which is clinically safe and toxic. PLGA is an FDA approved biodegradable polymer that has been employed in several studies to fabricate micro or nanoparticles [39,120]. These NPs can encapsulate wide variety of biologically active compounds ranging from anticancer drugs to peptides or hormones. Many such products are in market or under clinical investigation [118]. PLGA NPs are good candidates for vaccine delivery. A variety of antigenic substances (proteins, peptides, plasmid DNA, viruses) have been successfully delivered using PLGA particles. Apart from protecting the encapsulated cargo from degradation these NPs are mainly engulfed by phagocytic DCs restricting entry of Ag in systemic circulation [54,55].

In this study we have reported successful formulation of a multi-component PLGA NP particulate vaccine (CpG-NP-Tag) and tested the efficacy of this formulation to induce CTL response and impart antitumor immunity *in vivo* in a syngenic prophylactic 4T1 murine breast cancer BALB/c model (section 2.3). We also conducted some *ex vivo* studies using the BMDCs from the same mice to evaluate the ability of these NPs to interact with the most efficient APCs, DCs, as most of the particulate vaccine responses are modulated via DCs [118,122,129].

We have successfully engineered CpG coated Tag containing PLGA NPs using solvent evaporation technique within a particle size ranging from 200-230 nm (Fig. 2A, Table 1) which is desirable for preferential DC uptake as compared to macrophages. It has been reported than

PLGA NPs lesser than 500nm in size are more effective in generating CTL responses in vivo relative to microparticles (>2μm) [130].

Surface zeta potential and particle size of colloidal nanosytems has a major impact on cellular uptake as well as intracellular trafficking. As mentioned earlier it is known that phagocytic DCs prefer smaller size particles (in viral size range) while macrophages ingest bigger particles. In addition to this, negatively charged particles are known to have better phagocytic rate compared to neutral and highly positive charged particles [43,131]. The routes of uptake essentially do not differ for positively or negatively charged particles but definitely higher uptake is directly linked to better biological responses, specifically a better immune response in our case [132,133]. Neutrally charged or negatively charged particles localize in Endosomal compartment where Ag processing machinery resides to generate effective $CD4^+$ T cell response. Some of these particles are known to escape Endosomal compartment into cytosol through unknown mechanisms which facilitates cross-presentation and to trigger CTL responses [129]. In our study we found that the NPs were mostly negatively charged and coated particles (CpG-NP-Tag and CpG-NP-Blank) were slightly more negative (-1.18±0.39 mV and -1.14±0.56 mV) than uncoated ones (NP-Tag; -0.51±0.59 mV) (Fig.2B and Table 1). SEM images show uniform, smooth, spherical particles in nano size range (Fig. 2C). Since we are encapsulating hydrophilic Tag (4T1 membrane lysate in RIPA buffer) the maximum encapsulation efficiency obtained was not as much as it is observed in case of hydrophobic core ingredients. We were able to attain encapsulation efficiency of approximately 37% [96]. PDI is an important parameter in NP preparation as it indicates the variability in size of the prepared formulation. PDI close to zero is optimal as it indicates uniform size distribution [134]. PDI of the particles prepared was in the desirable range of 0.13-0.16

(Table 1). Ligand binding efficiency quantified using flow cytometry was found to be around 12-14 percent (Fig. 3A and 3B).

Our group recently published *(article in press)* a study demonstrating the antitumor effects of CpG-NP-Tag NPs after *in vivo* administration in a prophylactic setting. The results of this study indicated that CpG-NP-Tag NPs had an overall inhibitory effect on tumor growth, proliferation, and induced apoptotic cell death. CpG-NP-Tag were able to boost the immune system and enhance antitumor immune response which was evident from the increased tumor $CD4^+/CD8^+$ T cell infiltration and local IFN-γ production (article in press). In the previous study we observed the above mentioned effects until day 14, in the studies conducted in this project, we observed the same effects until day 21. Tumor growth was drastically inhibited indicated by small tumor volume observed in case of CpG-NP-Tag immunized mice ($p<0.05$) compared to CpG-NP-Blank and NP-Tag controls (Fig 4A). Fold change in tumor size monitored over the 21 day time scale also confirmed slower tumor growth in CpG-NP-Tag immunized mice compared to controls (Fig. 4B). *Ex vivo* examination of harvested tumors from the respective NP groups displaying significant differences in morphology (size and volume) also supported the tumor volume and fold change data (Fig 4C). We also measured the weight of animals of the animals during the course of the study including pre- and post NP immunization. No significant changes in the body weight were noticed post NP immunization confirming that NP dosage was safe and non-toxic (Fig 5).

IFN-γ is an extensively studied cytokine in vaccine therapy. This cytokine is known to have a protective role and mediate its antitumor effects via (i) affecting tumor growth/survival cell proliferation (ii) inhibiting angiogenesis and (iii) enhancing innate and adaptive immune functions [135]. In our previous paper *(article in press)*, we have shown a high local production of

IFN-γ in tumor environment in CpG-NP-Tag immunized mice, along with attenuation of tumor growth/proliferation, induction of apoptosis, as well high T cell infiltration in the tumor region. In the studies conducted in this project, we were able to replicate the above mentioned effects and interestingly found noticeable visual differences in vasculature surrounding the primary tumor. CpG-NP-Blank and NP-Tag tumors showed dense blood vessel vascularization as compared to CpG-NP-Tag mice (Fig. 6A). We estimated Hb levels which would serve as a semi-quantitative method in order to measure the angiogenic activity. As expected, we found high Hb levels in case of control groups as compared to CpG-NP-Tag tumors (Fig. 6B) which was also in accordance with dense the blood vessel CD31 staining in control groups (Fig. 7A and 7B). Interestingly, these results concerted with the high IFN-γ in our previous studies (Supplementary Fig 1). Thus, there is likelihood that antiangiogenic effect seen may be mediated due to local production of IFN-γ in the tumor microenvironment. IFN-γ also originally known as "macrophage activating factor" is an important stimuli for the activation of macrophages which further induce direct antitumor effects as well as upregulate antigen presentation (Schroder). Additionally, IFN-γ polarizes macrophages towards the inflammatory M1 phenotype thus helping in tumor eradication [136]. We were able to see a significant increased macrophage infiltration in CpG-NP-Tag tumors as compared to control tumors (Refer Supplementary Fig. S2). Further investigation in this direction will be needed to characterize the phenotype of these infiltrating macrophages.

The ultimate goal of cancer vaccines is to evoke robust CTL responses. Nevertheless, it has been reported by many groups that both $CD4^+$ and $CD8^+$ T cell act synergistically to finely tune and regulate antitumor immune responses [99,101,137,138]. Thus, we isolated the splenocytes (consisting majorly of CD4 and CD8 T lymphocytes) and performed the

CTL assay to evaluate the cytotoxic ability of the primed T cells against the target 4T1 cells. We found that splenocytes from CpG-NP-Tag immunized mice generated most potent CTL responses as compared to rest of the control groups at all effector: target ratios (Fig 8).

The role of DCs in promoting CTL based immunity is well established [31,100,123,124,139]. The development of protocols for isolation and in vitro culture of DCs has revolutionized the field of DC based vaccines. Two main strategies are in picture currently with respect to DC vaccination models: *ex vivo* loading and *in vivo* targeting. Ex vivo approach involves isolation of monocytes from the patient and culturing them appropriately in presence of GM-CSF and IL4 to obtain immature DCs. These immature DCs further pulsed with tumor antigen or tumor cell lysates and adjuvant costimulatory molecules (IL6, PGE2) are transferred back to patient. Such approaches have been studies in several clinical trials. These studies indicate that such a strategy is safe, non-toxic, well tolerated in patients and is capable of generating cellular immunity [31]. In the last segment of our project, we show studies conducted in order to test the efficacy of CpG-NP-Tag NPs to serve as candidates for *ex vivo* based DC vaccines. Sufficient uptake of NPs is a prerequisite to render effective DC based immune responses. For all our experiments we used BMDCs obtained from female BALB/c mice. In uptake studies, we found that uptake of CpG-NP-Tag NPs was significantly higher in BMDCs compared to CpG-NP-Blank or NP-Tag NPs. (Fig. 9A and 9B). We attribute the higher uptake to the presence of both CpG and Tag. We also checked the intracellular localization of the respective NPs. We found greater percent Colocalization within the Endosomal compartment for CpG coated NPs (CpG-NP-Blank and CpG-NP-Tag) than the uncoated ones (NP-Tag) (Figure 10A and 10B). We believe CpG being a TLR 9 ligand will preferentially route the coated NPs to Endosome where the TLR9 receptors are located. To confirm DC activation and function which is crucial for transport of processed

antigen loaded MHC complexes to cell surface we probed for maturation markers (CD80/B7-1 and CD86/B7-2) as well as IL12 secretion. The transport of MHC-peptide complex to cell surface is accompanied with increased expression of co-stimulatory molecules (CD80/86). These are known to play a key role in the amplification of T cell receptor (TCR) signaling and thereby T cell activation [140]. Our studies indicated a higher percentage of BMDCs expressing CD80 and CD86 molecules for CpG-NP-Tag pulsed BMDCs compared to control groups (Fig. 11A and 11B). Function of DCs was evaluated by comparing IL12 secretion amongst the NP pulsed BMDCs. IL12 is naturally produced by DCs in response to antigenic stimulation and typically aids in the growth, function and CTL activity of $CD8^+$ T lymphocytes. IL12 is also known to have antiangiogenic role which it mediates via increasing secretion of IFN-γ. Interestingly, IL12 levels were seen to be higher in case of BMDCs pulsed with coated NPs (CpG-NP-Blank and CpG-NP-Tag) as compared to uncoated ones (NP-Tag) (Fig. 11C). We believe that this might be due to the presence of CpG which promoted IL12 secretion. Although presence of CpG might facilitate increased Endosomal localization and IL 12 secretion (as seen in case of CpG-NP-Blank NPs) incorporating Tag in the formulation CpG-NP-Tag) is essential in avoiding non-specific immune responses and generating tumor specific T cell responses. Thus, above exciting results indicate that CpG-NP-Tag NPs could be studies further in the directions of *ex vivo* targeted DC vaccines. Collectively, all the studies conducted in this project delineate that CpG-NP-Tag NPs are able to attenuate tumor growth as well as angiogenesis in a syngeneic model of breast cancer by enhancing CTL mediated immune responses. Moreover, CpG-NP-Tag NPs were able to stimulate DCs *ex vivo* thus indicating the dual role (*in vivo* and *ex vivo*) CpG-NP-Tag in vaccination models.

6. CONCLUSION

From the studies conducted with "bacteriomimetic" NPs (CpG-NP-Tag) until now we show the dual use of these NPs – (i) *in vivo* to attenuate tumor growth, proliferation, angiogenesis, and to induce apoptotic death of tumor cells possibly due to the induction of optimal antitumor CTL responses and (ii) *ex vivo* to increase the efficacy of DCs by inducing the expression of maturation markers (CD80/CD86) as well as IL12 secretion which in turn will aid T cell responses. Based on these results it is hard to sideline the plausibility that DCs might orchestrate the *in vivo* effects of CpG-NP-Tag NPs. Thus, we plan to conduct some more experiments in future in order to investigate role of CpG-NP-Tag in the *in vivo* and *ex vivo* targeting of DCs.

7. SUPPLEMENTARY DATA

Figure S1

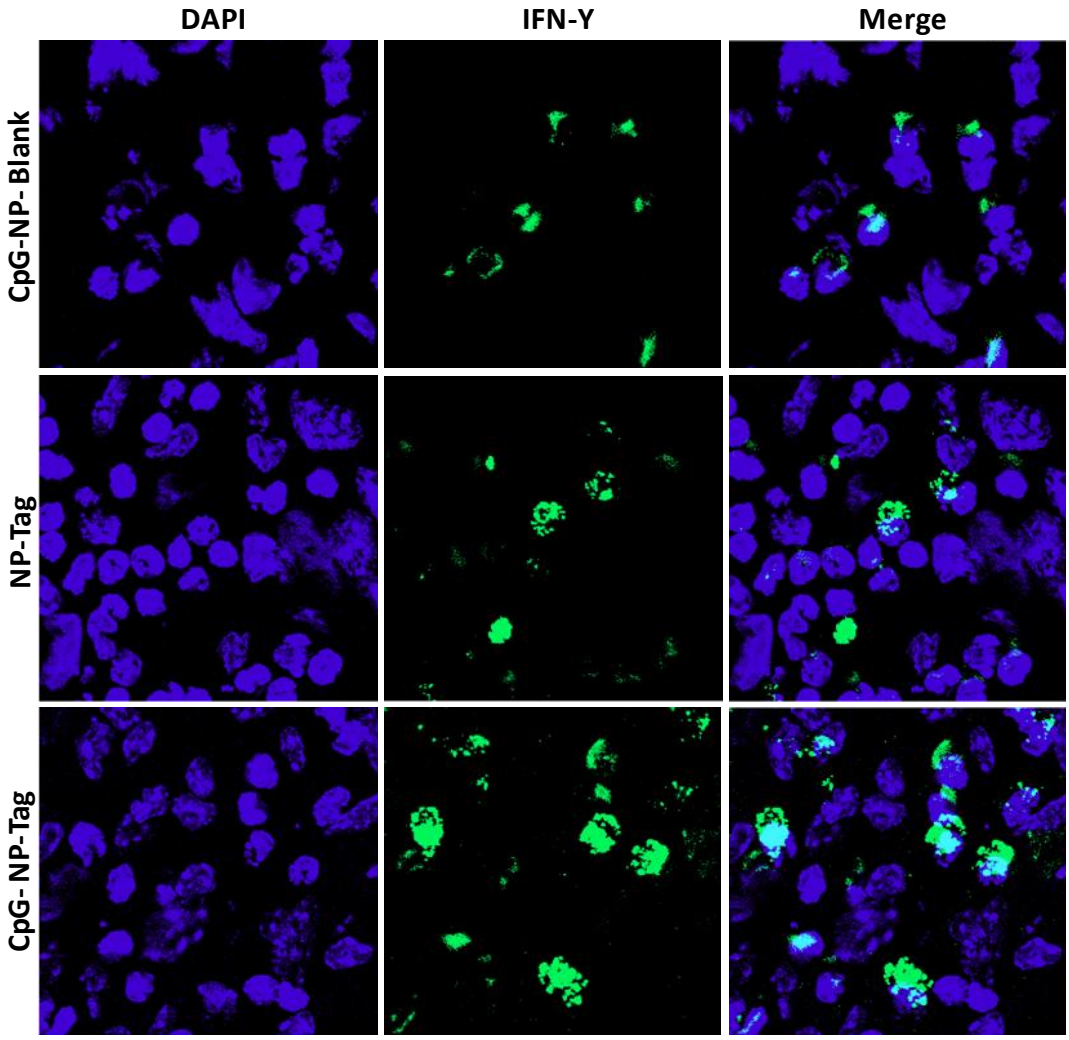

Figure S1: Representative images (40X) of IFN-γ produced in tumor tissues. To evaluate the IFN-γ levels 5-7 µm tumor sections were permeabilized using 0.5% Triton-X and stained for IFN-γ using anti- IFN-γ antibody conjugated to Alexa fluor 488 and immunofluorescence was observed using confocal microscopy.

Figure S2

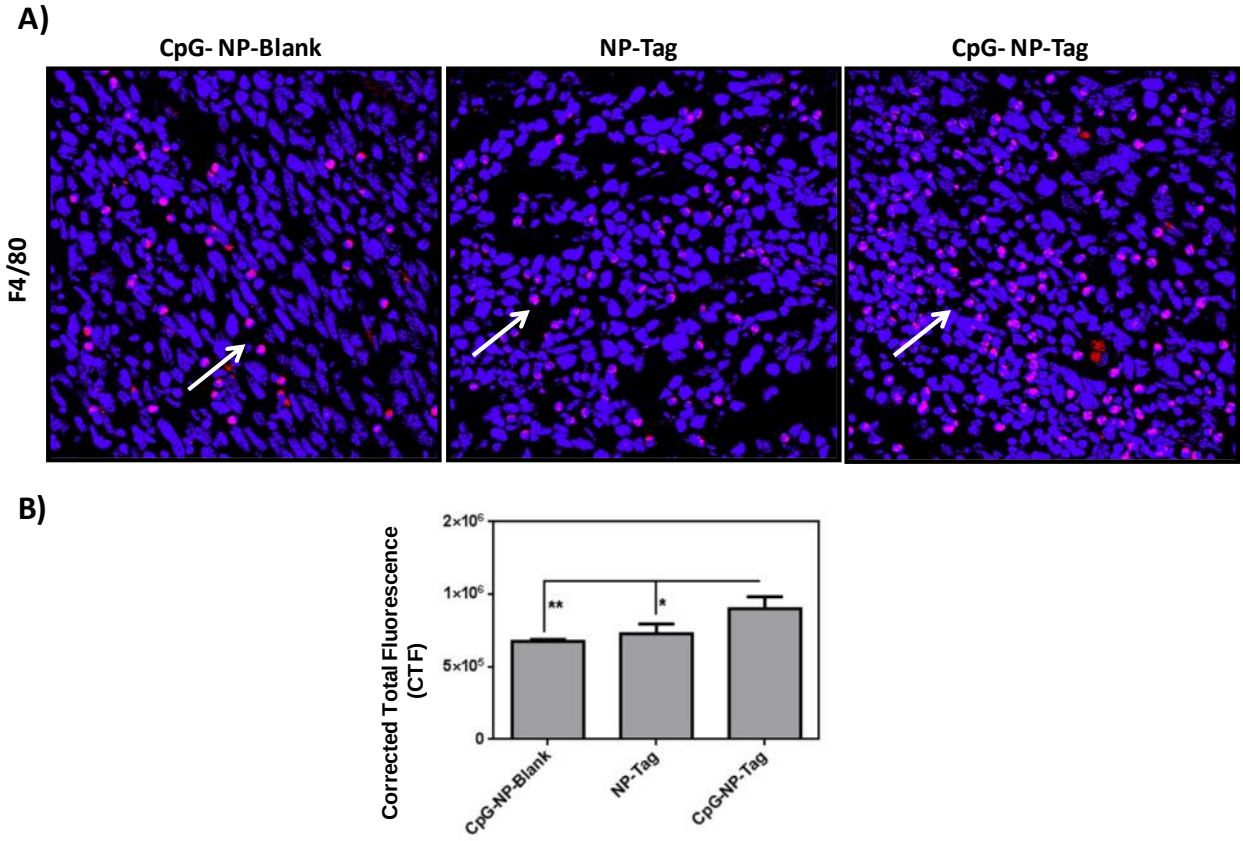

Figure S2: Macrophage infiltration in tumor microenvironment. A) Representative images (40X) of F4/80 stained tumor tissues sections showing the macrophage infiltration **B)** Quantitative analysis of the macrophage infiltration in the tumor tissue harvested from the different groups analyzed using NIH ImageJ software (*$p < 0.05$; **$p < 0.01$).

Figure S3

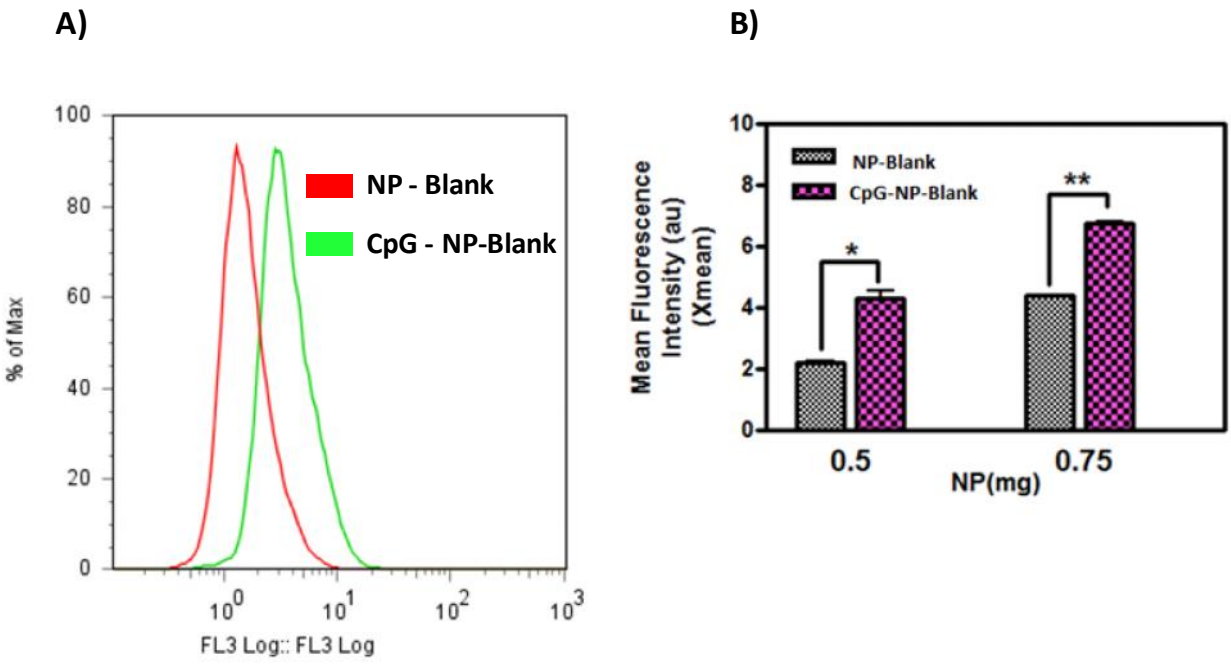

Figure S3: Preferential uptake of CpG coated NPs by JAWSII (immature dendritic) cells. Cells were pulsed with 0.5-1 mg of nile red stained NP formulations (NP-Blank and CpG-NP-Blank) and the uptake was analysed using flow cytometry.

Figure S4

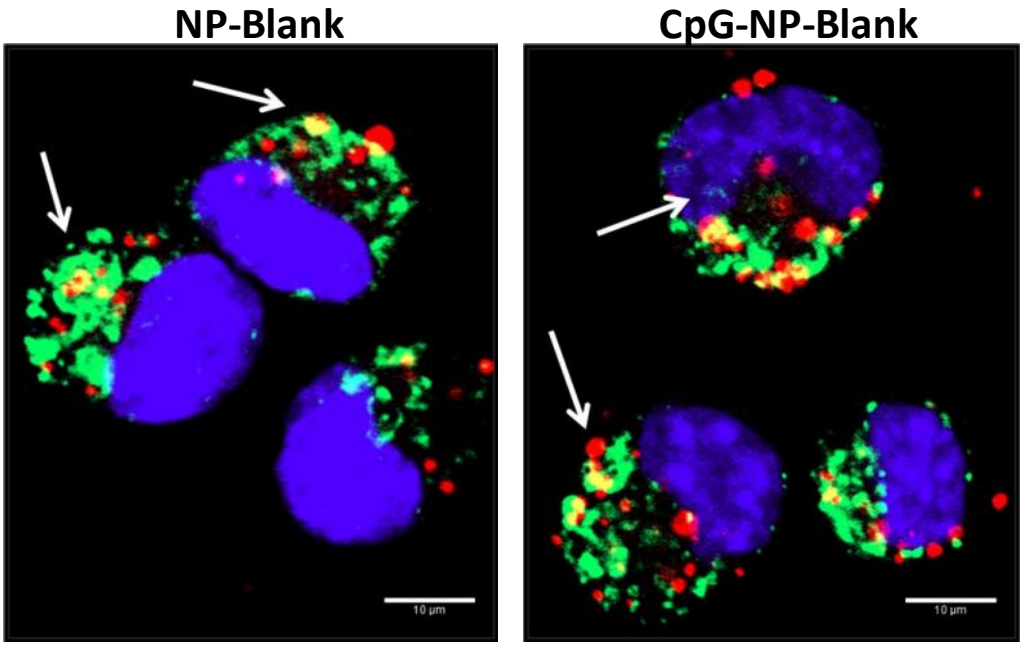

Figure S4: Trafficking of NPs in endosomal compartment of JAW SII cells (immature dendritic cells). Cells were pulsed with 0.5-1 mg of nile red stained NP formulations (NP-Blank and CpG-NP-Blank) and the endosomal Colocalization (yellow) was observed in images (40X) using confocal microscopy. Early endosome was stained using EEA1 and DAPI (4',6-diamidino-2-phenylindole) was used to stain nucleus.

CHAPTER IV

SUMMARY, CONCLUSIONS AND FUTURE PERSPECTIVE

The long-term goal of this dissertation was to establish an experimental basis to advance immunotherapy useful as a future therapeutic option for cancer treatment. Our central hypothesis was that co-delivery of tumor-antigen with an immunostimulatory factor would increase tumor immune defense. We addressed this hypothesis by focusing on the following two main objectives: 1) To formulate polymer based "bacteriomimetic nanoparticles" and 2) To validate bacteriomimetic nanoparticles potential by enhancing tumor immunity *in vivo* and secondly by determining whether DCs are plausible targets for inducing anti-tumor immune responses. Recent literature suggests polymeric nanoparticle (NP) based vaccines are known to overcome limitations of inherent instability of soluble antigen (Ag), accompanied with low internalization and poor cross-presentation [141]. These systems are popular in cancer vaccines due to their low immunogenicity, low toxicity, bio-degradable and bio-compatible nature. Studies show that vaccine antigen could either be encapsulated within or conjugated on surface of NPs by chemical modification. Reports also suggest that vaccines administered concomitantly with immune adjuvants (stimulants) provide better clinical efficacy. However, there are very few studies in literature focusing on co-delivery of antigen and adjuvant in a single NP formulation. Co-encapsulation of antigen and adjuvant would compromise the encapsulation efficiency of hydrophilic antigens while delivering Ag and adjuvant on separate NPs (as tried in some models) might not affirm delivery to same APC [46]. Reports suggest presence of microbial ligands (TLR agonists) leads to receptor mediated endocytosis and induces DC maturation thus achieving both uptake and immune cell activation. Use of multifunctional particles such as "CpG-NP-Tag" will

allow co-delivery of Ag and adjuvant (CpG: TLR9 agonist) to APCs (specifically DC), sufficient uptake and activation, maturation, appropriate MHC presentation leading to an enhanced CTL response.

DC based vaccination schemes have been successful in delivering vaccine Ag to lymphatic tissues and enhance CTL response. However, DC vaccines have shown poor clinical efficacy due to insufficient Ag uptake by DCs. Therefore to improve Ag uptake, NP based delivery system have been explored [40,52,142]. Studies reported that particulate PLGA vaccines could enhance uptake of Ag and adjuvants by DCs resulting in improved immune responses [141]. Thus, fabrication of NPs with "danger signals" such as TLR agonists or PAMPs (pathogen associated molecular patterns) on surface could activate APCs and stimulate NP uptake. Multivalent presentation of PAMPs through surface modifications renders repetitive presentation of pathogens "mimicking" infection and promoting better immune response through receptor cross linking and immune cell activation [143].

Studies conducted with PLGA based CpG-NP-Tag NPs are of translational value since these could be fabricated in future for *in vivo* DC targeting. Overall, we propose that PLGA based CpG-NP-Tag NPs will be preferentially engulfed by DCs which will lead to activation and maturation of DCs. Tag will further be processed in the Endosomal compartment to be presented as MHCII-Tag complex to trigger a $CD4^+$ T cell response. These cells traditionally being "helper" in nature will aid in tumor killing by enhancing the activity of effector CD8+ T lymphocytes (CTLs) via the release of pro-inflammatory cytokines such as IFN-γ. Since DCs are "professional APCs" they are known to be capable of cross-presentation to initiate a CD8+ T cell response. We believe that a part of Tag will escape the Endosomal compartment to be cross-presented for generation of a $CD8^+$ T cell response (Fig 16).

Figure 1

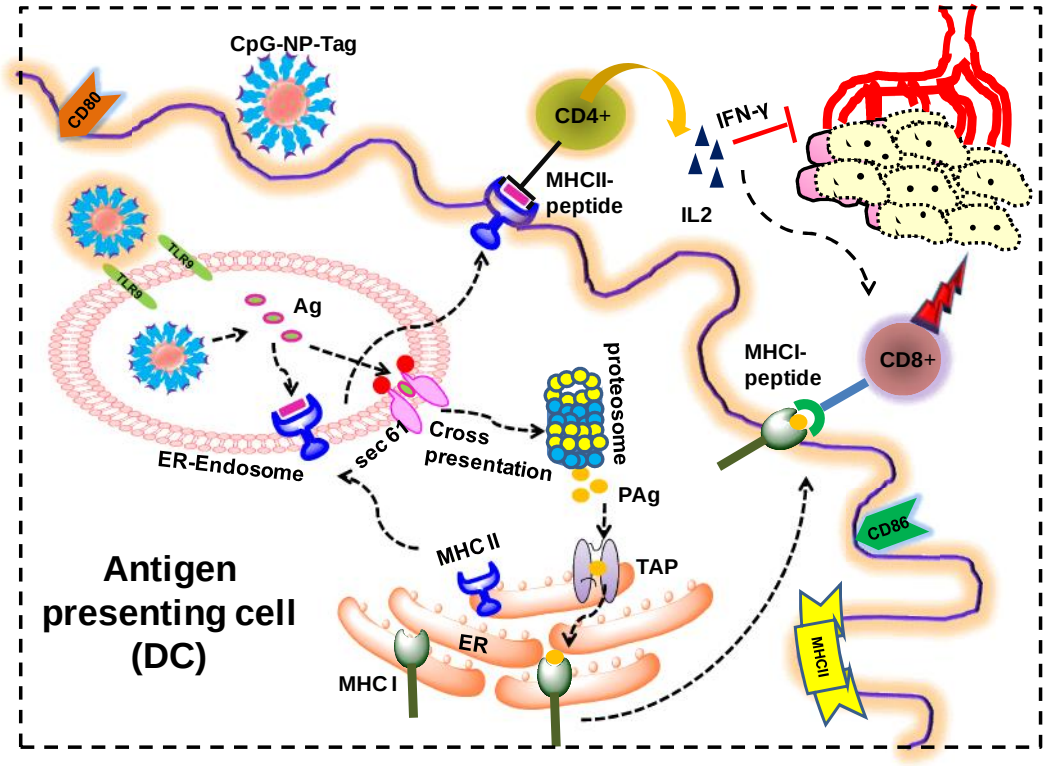

Figure 1: Predicted mechanism for the immunostimulatory efficacy of "bacteriomimetic" nanoparticles (CpG-NP-Tag). CpG-NP-Tag NPs will be preferentially engulfed by dendritic cells with subsequent localization in the Endosomal compartment leading to activation maturation of DCs indicated by expression of maturation markers CD80, CD86 and MHCII. CpG-NP-Tag NPs will be processed in the Endosome to present Tag as MHC-peptide complex that will trigger "helper" CD4+ T cell response. A part of Ag will escape via sec 61 translocon, degraded by cytoplasmic proteosomes and the processed Ag (Pag) transported to endoplasmic reticulum (ER) through the TAP (transporter associated with antigen processing) proteins will be presented to cell surface as MHCI-Ag peptide complex to trigger CD8+ T cell response. IFN-γ released by helper cells will enhance effector cytotoxic CD8+ T cell response eventually leading to tumor cell death via apoptosis.

Proof-of-concept studies from this project will aid to development of nanoparticulate immunotherapy agents for prophylactic as well as therapeutic applications. The use of CpG coated tumor antigen containing "bacteriomimetic" NPs will serve as a novel technique to evoke a dual immune response – non-specific immune stimulation by the use of common bacterial/viral antigens such as CpG / HA peptide and Tag specific T cell mediated response eventually providing a robust and a long-lasting immune response. Thus, "bacteriomimetic" NPs will serve as a platform for the development of immune based therapeutic vaccines in future which could be efficiently used as an adjuvant therapy along with surgery, radiation and chemotherapy. Validation of this system in mice model will be of translational importance for breast cancer therapy as well as other cancer models. Recent advances in molecular characterization of tumor for personalized therapy can help to identify a particular tumor associated antigen (TAA) in patients. Such information about antigens and proposed model of bacteriomimetic drug delivery system can be implemented for personalized vaccination/immune therapy.

Personalized preventive/therapeutic *ex vivo* DC vaccines have been studied extensively and shown successful results in mice models and many investigators have started clinical trials with Ag loaded DCs. Although *ex vivo* DC vaccines were able to generate effective CTL response and tumor regression in murine models currently they show poor clinical efficacy in human trial due to poor migratory capacity or inability to overpower the immunosuppressive tumor microenvironment. Nevertheless, these studies were important as proof of principle that DCs sufficiently loaded with Tag, optimally activated and properly migrated to lymph nodes were able to initiate tumor specific $CD4^+$ and $CD8^+$ T cell responses. Additional studies will be required to understand and enhance the therapeutic potential of such *ex vivo* based vaccines in

humans. These *ex vivo* studies will definitely help build a novel approach for successfully delivering the Tag directly to DCs *in vivo* and thereby achieve meaningful therapeutic responses. In our studies, we stress on dual role of CpG-NP-Tag NPs – *in vivo* as well as *ex vivo*. We strongly believe that particulate vaccines such as CpG-NP-Tag NPs have the capacity to overcome majority of the above mentioned clinical problems. With the use of such products clinical intervention will be limited to mode of administration/dosage frequency. Overall, studies conducted with CpG-NP-Tag NPs in this project and *in vivo* DC targeting studies which we intend to conduct in future are of translational significance which will help to tailor particulate vaccines to evolve as an attractive approach to develop large scale cost effective cancer vaccines that could benefit larger subsets of patients unlike personalized therapy. Understanding the mechanism through which these NPs work could provide more insight in the area of such nanocarrier vaccines. Such technology can be readily translated into humans by using a commonly used vaccine component, such as flu vaccine, on the surface of NPs encapsulating established tumor associated antigen (TAAs) to produce strong immune response against tumor. In future this strategy could be extended to other models such as infectious/viral diseases including HIV.

BIBLIOGRAPHY

1. Siegel R, Naishadham D, Jemal A. Cancer statistics for hispanics/latinos, 2012. *CA: a cancer journal for clinicians*. 2012;62(5):283-298.

2. Jabir NR, Tabrez S, Ashraf GM, Shakil S, Damanhouri GA, Kamal MA. Nanotechnology-based approaches in anticancer research. *International journal of nanomedicine*. 2012;7:4391.

3. Subbiah R, Veerapandian M, S Yun K. Nanoparticles: Functionalization and multifunctional applications in biomedical sciences. *Curr Med Chem*. 2010;17(36):4559-4577.

4. McCarthy EF. The toxins of william B. coley and the treatment of bone and soft-tissue sarcomas. *Iowa Orthop J*. 2006;26:154-158.

5. Richardson MA, Ramirez T, Russell NC, Moye LA. Coley toxins immunotherapy: A retrospective review. *Altern Ther Health Med*. 1999;5(3):42-47.

6. Snook AE, Waldman SA. Advances in cancer immunotherapy. *Discov Med*. 2013;15(81):120-125.

7. Rosenberg SA. Cell transfer immunotherapy for metastatic solid cancer—what clinicians need to know. *Nature reviews Clinical oncology*. 2011;8(10):577-585.

8. Knuth A, Wölfel T, zum Büschenfelde KM. Cellular and humoral immune responses against cancer: Implications for cancer vaccines. *Curr Opin Immunol*. 1991;3(5):659-664.

9. Elgert KD. *Immunology: Understanding the immune system.* John Wiley & Sons; 2009.

10. Conniot J, Silva JM, Fernandes JG, et al. Cancer immunotherapy: Nanodelivery approaches for immune cell targeting and tracking. *Frontiers in chemistry*. 2014;2.

11. Junker U, Knoefel B, Nuske K, et al. Transforming growth factor beta 1 is significantly elevated in plasma of patients suffering from renal cell carcinoma. *Cytokine*. 1996;8(10):794-798.

12. Noguera R, Nieto OA, Tadeo I, Farinas F, Alvaro T. Extracellular matrix, biotensegrity and tumor microenvironment. an update and overview. *Histol Histopathol*. 2012;27(6):693-705.

13. Types of biological cancer immunotherapy. http://www.cel-sci.com/types_of_cancer_immunotherapy.html. Accessed 02/21, 2015.

14. Igney FH, Krammer PH. Immune escape of tumors: Apoptosis resistance and tumor counterattack. *J Leukoc Biol*. 2002;71(6):907-920.

15. Scott AM, Wolchok JD, Old LJ. Antibody therapy of cancer. *Nature Reviews Cancer*. 2012;12(4):278-287.

16. Vanneman M, Dranoff G. Combining immunotherapy and targeted therapies in cancer treatment. *Nature Reviews Cancer*. 2012;12(4):237-251.

17. Rosenberg SA, Yang JC, Restifo NP. Cancer immunotherapy: Moving beyond current vaccines. *Nat Med*. 2004;10(9):909-915.

18. Baluna R, Vitetta ES. Vascular leak syndrome: A side effect of immunotherapy. *Immunopharmacology*. 1997;37(2):117-132.

19. Cancer immunotherapy. http://www.cancer.org/treatment/treatmentsandsideeffects/treatmenttypes/immunotherapy/immunotherapy-cancer-vaccines. Updated 2014. Accessed 02/21, 2015.

20. Guilhot F, Roy L, Guilhot J, Millot F. Interferon therapy in chronic myelogenous leukemia. *Hematol Oncol Clin North Am*. 2004;18(3):585-603.

21. Cancer vaccines. http://www.cancer.gov/cancertopics/factsheet/Therapy/cancer-vaccines. Updated 2011. Accessed 02/23, 2015.

22. Hellstrom KE, Hellstrom I. Novel approaches to therapeutic cancer vaccines. . 2003.

23. Kufe DW, Pollock RE, Weichselbaum RR, Bast RC, Gansler TS. *Holland-frei cancer medicine.* BC Decker; 2006.

24. Lahn M, Köhler G, Schmoor C, et al. Processing of tumor tissues for vaccination with autologous tumor cells. *European surgical research*. 1997;29(4):292-302.

25. Chan AD, Morton DL. Active immunotherapy with allogeneic tumor cell vaccines: Present status. *Semin Oncol*. 1998;25(6):611-622.

26. Schulz M, Zinkernagel RM, Hengartner H. Peptide-induced antiviral protection by cytotoxic T cells. *Proc Natl Acad Sci U S A*. 1991;88(3):991-993.

27. Jäger E, Ringhoffer M, Karbach J, Arand M, Oesch F, Knuth A. Inverse relationship of melanocyte differentiation antigen expression in melanoma tissues and CD8 cytotoxic-T-cell

responses: Evidence for immunoselection of antigen-loss variants in vivo. *International Journal of Cancer*. 1996;66(4):470-476.

28. Holmberg LA, Sandmaier BM. Vaccination with theratope®(STn-KLH) as treatment for breast cancer. . 2004.

29. Marshall J. Carcinoembryonic antigen-based vaccines. . 2003;30:30-36.

30. Xu H, Cao X. Dendritic cell vaccines in cancer immunotherapy: From biology to translational medicine. *Frontiers of medicine*. 2011;5(4):323-332.

31. Palucka K, Banchereau J, Mellman I. Designing vaccines based on biology of human dendritic cell subsets. *Immunity*. 2010;33(4):464-478.

32. Wiemann B, Starnes CO. Coley's toxins, tumor necrosis factor and cancer research: A historical perspective. *Pharmacol Ther*. 1994;64(3):529-564.

33. Mellman I, Coukos G, Dranoff G. Cancer immunotherapy comes of age. *Nature*. 2011;480(7378):480-489.

34. Holmes FF, Wilson J, Blesch KS, Kaesberg PR, Miller R, Sprott R. Biology of cancer and aging. *Cancer*. 1991;68(S11):2525-2526.

35. De Cecco L, Berardi M, Sommariva M, et al. Increased sensitivity to chemotherapy induced by CpG-ODN treatment is mediated by microRNA modulation. *PloS one*. 2013;8(3):e58849.

36. Vallejo R, Hord ED, Barna SA, Santiago-Palma J, Ahmed S. Perioperative immunosuppression in cancer patients. *Journal of environmental pathology, toxicology and oncology*. 2003;22(2).

37. Baines J, Celis E. Immune-mediated tumor regression induced by CpG-containing oligodeoxynucleotides. *Clinical cancer research*. 2003;9(7):2693-2700.

38. Fioretti D, Iurescia S, Fazio VM, Rinaldi M. DNA vaccines: Developing new strategies against cancer. *J Biomed Biotechnol*. 2010;2010:174378. doi: 10.1155/2010/174378 [doi].

39. Krishnamachari Y, Geary SM, Lemke CD, Salem AK. Nanoparticle delivery systems in cancer vaccines. *Pharm Res*. 2011;28(2):215-236.

40. Cho N, Cheong T, Min JH, et al. A multifunctional core-shell nanoparticle for dendritic cell-based cancer immunotherapy. *Nature nanotechnology*. 2011;6(10):675-682.

41. Akagi T, Baba M, Akashi M. Biodegradable nanoparticles as vaccine adjuvants and delivery systems: Regulation of immune responses by nanoparticle-based vaccine. In: *Polymers in nanomedicine.* Springer; 2012:31-64.

42. Kamaly N, Xiao Z, Valencia PM, Radovic-Moreno AF, Farokhzad OC. Targeted polymeric therapeutic nanoparticles: Design, development and clinical translation. *Chem Soc Rev*. 2012;41(7):2971-3010.

43. Thamake SI, Raut SL, Ranjan AP, Gryczynski Z, Vishwanatha JK. Surface functionalization of PLGA nanoparticles by non-covalent insertion of a homo-bifunctional spacer for active

targeting in cancer therapy. *Nanotechnology*. 2011;22(3):035101. doi: 10.1088/0957-4484/22/3/035101.

44. Cheng CJ, Tietjen GT, Saucier-Sawyer JK, Saltzman WM. A holistic approach to targeting disease with polymeric nanoparticles. *Nature Reviews Drug Discovery*. 2015.

45. Elbayoumi T. Nanotechnologies in cancer. .

46. de Titta A, Ballester M, Julier Z, et al. Nanoparticle conjugation of CpG enhances adjuvancy for cellular immunity and memory recall at low dose. *Proc Natl Acad Sci U S A*. 2013;110(49):19902-19907. doi: 10.1073/pnas.1313152110 [doi].

47. Klippstein R, Pozo D. Nanotechnology-based manipulation of dendritic cells for enhanced immunotherapy strategies. *Nanomedicine: Nanotechnology, Biology and Medicine*. 2010;6(4):523-529.

48. Jaganathan K, Vyas SP. Strong systemic and mucosal immune responses to surface-modified PLGA microspheres containing recombinant hepatitis B antigen administered intranasally. *Vaccine*. 2006;24(19):4201-4211.

49. Jaganathan K, Singh P, Prabakaran D, Mishra V, Vyas SP. Development of a single-dose stabilized poly (d, l-lactic-co-glycolic acid) microspheres-based vaccine against hepatitis B. *J Pharm Pharmacol*. 2004;56(10):1243-1250.

50. Gupta PN, Khatri K, Goyal AK, Mishra N, Vyas SP. M-cell targeted biodegradable PLGA nanoparticles for oral immunization against hepatitis B. *J Drug Target*. 2007;15(10):701-713.

51. Feng L, Qi XR, Zhou XJ, et al. Pharmaceutical and immunological evaluation of a single-dose hepatitis B vaccine using PLGA microspheres. *J Controlled Release*. 2006;112(1):35-42.

52. Yuba E, Kojima C, Harada A, Watarai S, Kono K. pH-sensitive fusogenic polymer-modified liposomes as a carrier of antigenic proteins for activation of cellular immunity. *Biomaterials*. 2010;31(5):943-951.

53. Gutierro I, Hernandez R, Igartua M, Gascon A, Pedraz J. Size dependent immune response after subcutaneous, oral and intranasal administration of BSA loaded nanospheres. *Vaccine*. 2002;21(1):67-77.

54. Rosalia RA, Cruz LJ, van Duikeren S, et al. CD40-targeted dendritic cell delivery of PLGA-nanoparticle vaccines induce potent anti-tumor responses. *Biomaterials*. 2015;40:88-97.

55. Hamdy S, Haddadi A, Hung RW, Lavasanifar A. Targeting dendritic cells with nano-particulate PLGA cancer vaccine formulations. *Adv Drug Deliv Rev*. 2011;63(10):943-955.

56. American cancer society: Key statistics about breast cancer. http://www.cancer.org/cancer/breastcancer/detailedguide/breast-cancer-key-statistics. Updated 2012. Accessed 10/23, 2012.

57. National breast cancer foundation. http://www.nationalbreastcancer.org/breast-cancer-treatment. Updated 2012. Accessed 10/23, 2012.

58. Cancer Research Institute. Cancer immunotherapy. http://www.cancerresearch.org/cancer-immunotherapy/what-is-cancer-immunotherapy. Updated 2013. Accessed 08/02, 2013.

59. Erica Jackson, Hatem Soliman. Realizing the promise of breast cancer vaccines. *Vaccine: Development and Therapy*. 2012;2:35-41.

60. Mansoor M . Amiji, ed. *Nanotechnology for cancer therapy.* CRC Pres; 2006.

61. Prasad S, Cody V, Saucier-Sawyer JK, et al. Polymer nanoparticles containing tumor lysates as antigen delivery vehicles for dendritic cell-based antitumor immunotherapy. *Nanomedicine*. 2011;7(1):1-10. doi: 10.1016/j.nano.2010.07.002.

62. Max Schnurr, Peter Galambos, Christoph Scholz, et al. Tumor cell lysate-pulsed human dendritic cells induce a T-cell response against pancreatic carcinoma cells: An in vitro model for the assessment of tumor vaccines. *Cancer research*. 2001;64:6445-6450.

63. Nathalie Machluf RA. Therapeutic MUC1-based cancer vaccine expressed in Flagella—Efficacy in an aggressive model of breast cancer. *World Journal of Vaccines*. 2012;2:109-120.

64. Weinberg RA. Coevolution in the tumor microenvironment. *Nat Genet*. 2008;40(5):494-495.

65. Hanahan D, Weinberg RA. Hallmarks of cancer: The next generation. *Cell*. 2011;144(5):646-674.

66. Liu C, Xu J, Shi X, et al. M2-polarized tumor-associated macrophages promoted epithelial–mesenchymal transition in pancreatic cancer cells, partially through TLR4/IL-10 signaling pathway. *Laboratory Investigation*. 2013.

67. Krieg AM. Toll-like receptor 9 (TLR9) agonists in the treatment of cancer. *Oncogene*. 2008;27(2):161-167.

68. Hayashi T, Raz E. TLR9-based immunotherapy for allergic disease. *Am J Med*. 2006;119(10):897.e1-897.e6. doi: 10.1016/j.amjmed.2005.12.028.

69. Kawai, T and Akira, S. TLR signaling. *Cell Death and Differentiation*. 2006;13:816-825.

70. Kiyoshi Takeda SA. TLR signaling pathways. *Seminars in Immunology*. 2004;16:3-9.

71. Belardelli F, Ferrantini M, Proietti E, Kirkwood JM. Interferon-alpha in tumor immunity and immunotherapy. *Cytokine Growth Factor Rev*. 2002;13(2):119-134.

72. Dunn GP, Koebel CM, Schreiber RD. Interferons, immunity and cancer immunoediting. *Nature Reviews Immunology*. 2006;6(11):836-848.

73. Bode C, Zhao G, Steinhagen F, Kinjo T, Klinman DM. CpG DNA as a vaccine adjuvant. *Expert review of vaccines*. 2011;10(4):499-511.

74. Gregory AE, Titball R, Williamson D. Vaccine delivery using nanoparticles. *Frontiers in cellular and infection microbiology*. 2013;3.

75. Li AV, Moon JJ, Abraham W, et al. Generation of effector memory T cell-based mucosal and systemic immunity with pulmonary nanoparticle vaccination. *Sci Transl Med*. 2013;5(204):204ra130. doi: 10.1126/scitranslmed.3006516; 10.1126/scitranslmed.3006516.

76. Blattman JN, Greenberg PD. Cancer immunotherapy: A treatment for the masses. *Science*. 2004;305(5681):200-205. doi: 10.1126/science.1100369.

77. Krishnamachari Y, Geary SM, Lemke CD, Salem AK. Nanoparticle delivery systems in cancer vaccines. *Pharm Res*. 2011;28(2):215-236.

78. Jaini R, Kesaraju P, Johnson JM, Altuntas CZ, Jane-Wit D, Tuohy VK. An autoimmune-mediated strategy for prophylactic breast cancer vaccination. *Nat Med*. 2010;16(7):799-803. doi: 10.1038/nm.2161.

79. Carpentier A, Laigle-Donadey F, Zohar S, et al. Phase 1 trial of a CpG oligodeoxynucleotide for patients with recurrent glioblastoma. *Neuro-oncology*. 2006;8(1):60-66.

80. Mangsbo SM, Ninalga C, Essand M, Loskog A, Tötterman TH. CpG therapy is superior to BCG in an orthotopic bladder cancer model and generates CD4 T-cell immunity. *Journal of Immunotherapy*. 2008;31(1):34-42.

81. Nikitczuk KP, Schloss RS, Yarmush ML, Lattime EC. PLGA-polymer encapsulating tumor antigen and CpG DNA administered into the tumor microenvironment elicits a systemic antigen-specific IFN-γ response and enhances survival. *Journal of cancer therapy*. 2013;4(1):280.

82. Mueller M, Reichardt W, Koerner J, Groettrup M. Coencapsulation of tumor lysate and CpG-ODN in PLGA-microspheres enables successful immunotherapy of prostate carcinoma in TRAMP mice. *J Controlled Release*. 2012;162(1):159-166.

83. Wang W, Singh M. Selection of adjuvants for enhanced vaccine potency. *World Journal of Vaccines*. 2011;1:33.

84. Abbas AK, Lichtman AH, Pillai S. *Cellular and molecular immunology: With STUDENT CONSULT online access.* Elsevier Health Sciences; 2011.

85. Thamake SI, Raut SL, Gryczynski Z, Ranjan AP, Vishwanatha JK. Alendronate coated poly-lactic-co-glycolic acid (PLGA) nanoparticles for active targeting of metastatic breast cancer. *Biomaterials*. 2012.

86. Ranjan AP, Zeglam K, Mukerjee A, Thamake S, Vishwanatha JK. A sustained release formulation of chitosan modified PLCL: Poloxamer blend nanoparticles loaded with optical agent for animal imaging. *Nanotechnology*. 2011;22(29):295104.

87. Prasad S, Cody V, Saucier-Sawyer JK, et al. Optimization of stability, encapsulation, release, and cross-priming of tumor antigen-containing PLGA nanoparticles. *Pharm Res*. 2012;29(9):2565-2577. doi: 10.1007/s11095-012-0787-4; 10.1007/s11095-012-0787-4.

88. Feldman JP, Goldwasser R, Mark S, Schwartz J, Orion I. A mathematical model for tumor volume evaluation using two-dimensions. *J Appl Quant Methods*. 2009;4:455-462.

89. Manolova V, Flace A, Bauer M, Schwarz K, Saudan P, Bachmann MF. Nanoparticles target distinct dendritic cell populations according to their size. *Eur J Immunol*. 2008;38(5):1404-1413.

90. Basavanhally A, Ganesan S, Feldman M, et al. Multi-field-of-view framework for distinguishing tumor grade in ER breast cancer from entire histopathology slides. . 2013.

91. Martini M, Testi MG, Pasetto M, et al. IFN-γ-mediated upmodulation of MHC class I expression activates tumor-specific immune response in a mouse model of prostate cancer. *Vaccine*. 2010;28(20):3548-3557.

92. Buonaguro L, Petrizzo A, Tornesello ML, Buonaguro FM. Translating tumor antigens into cancer vaccines. *Clinical and Vaccine Immunology*. 2011;18(1):23-34.

93. Blander JM, Medzhitov R. Toll-dependent selection of microbial antigens for presentation by dendritic cells. *Nature*. 2006;440(7085):808-812.

94. Fischer S, Schlosser E, Mueller M, et al. Concomitant delivery of a CTL-restricted peptide antigen and CpG ODN by PLGA microparticles induces cellular immune response. *J Drug Target*. 2009;17(8):652-661.

95. Kasturi SP, Skountzou I, Albrecht RA, et al. Programming the magnitude and persistence of antibody responses with innate immunity. *Nature*. 2011;470(7335):543-547.

96. Pistel K, Kissel T. Effects of salt addition on the microencapsulation of proteins using W/O/W double emulsion technique. *J Microencapsul*. 2000;17(4):467-483.

97. Gnjatic S, Sawhney NB, Bhardwaj N. TLR AGONISTS: Are they good adjuvants? *Cancer J*. 2009;16(4):382-391.

98. Ding Z, Zhou G. Cytotoxic chemotherapy and CD4. *Clinical and Developmental Immunology*. 2012;2012.

99. Ostrand-Rosenberg S. CD4 T lymphocytes: A critical component of antitumor immunity. *Cancer Invest*. 2005;23(5):413-419.

100. Melief CJ. Cancer immunotherapy by dendritic cells. *Immunity*. 2008;29(3):372-383.

101. Zhang S, Zhang H, Zhao J. The role of CD4 T cell help for CD8 CTL activation. *Biochem Biophys Res Commun*. 2009;384(4):405-408.

102. Yo-Ping L, Chung-Jiuan J, Shu-Ching C. The roles of CD4 T cells in tumor immunity. *ISRN Immunology*. 2011;2011.

103. Yu MK, Park J, Jon S. Targeting strategies for multifunctional nanoparticles in cancer imaging and therapy. *Theranostics*. 2012;2(1):3.

104. Dermime S, Armstrong A, Hawkins RE, Stern PL. Cancer vaccines and immunotherapy. *Br Med Bull*. 2002;62(1):149-162.

105. Formenti SC, Demaria S. Combining radiotherapy and cancer immunotherapy: A paradigm shift. *J Natl Cancer Inst*. 2013;105(4):256-265.

106. Hamby LS, McGrath PC. Improved survival with adjuvant immunotherapy after surgical resection in a murine model. *Annals of Surgical Oncology*. 1994;1(4):307-313.

107. Kruisbeek AM. Isolation of mouse mononuclear cells. *Current protocols in immunology*. 2001:3.1. 1-3.1. 5.

108. De Rosa G, Caraglia M, Salmaso S, Elbayoumi T. Nanotechnologies in cancer. *Journal of drug delivery*. 2013;2013.

109. Armstrong AC, Eaton D, Ewing JC. Science, medicine, and the future: Cellular immunotherapy for cancer. *BMJ*. 2001;323(7324):1289-1293.

110. Soliman H. Immunotherapy strategies in the treatment of breast cancer. *Cancer Control*. 2013;20(1):17-21.

111. Esteves-Natal E, Koury S. A review of cancer vaccine. .

112. Savla R, Ivanova V, Minko T. Nanoparticles in the development of therapeutic cancer vaccines. *Pharmaceutical Nanotechnology*. 2014;2(1):2-22.

113. Koido S, Homma S, Takahara A, et al. Current immunotherapeutic approaches in pancreatic cancer. *Clin Dev Immunol*. 2011;2011:267539. doi: 10.1155/2011/267539 [doi].

114. Wong RM, Ianculescu I, Sharma S, et al. Immunotherapy for malignant pleural mesothelioma. current status and future prospects. *American journal of respiratory cell and molecular biology*. 2014;50(5):870-875.

115. Kirkwood JM, Butterfield LH, Tarhini AA, Zarour H, Kalinski P, Ferrone S. Immunotherapy of cancer in 2012. *CA: a cancer journal for clinicians*. 2012;62(5):309-335.

116. Petrulio CA, Kim-Schulze S, Kaufman HL. The tumour microenvironment and implications for cancer immunotherapy. . 2006.

117. Gajewski TF, Woo S, Zha Y, et al. Cancer immunotherapy strategies based on overcoming barriers within the tumor microenvironment. *Curr Opin Immunol*. 2013;25(2):268-276.

118. Cruz LJ, Tacken PJ, Rueda F, Carles Domingo J, Albericio F, Figdor CG. 8 targeting nanoparticles to dendritic cells for immunotherapy. *Meth Enzymol*. 2012;509:143.

119. Müller L, McArdle S, Derhovanessian E, et al. Current strategies for the identification of immunogenic epitopes of tumor antigens. In: *Immunotherapy of cancer.* Springer; 2006:21-44.

120. Krishnamachari Y. PLGA microparticle based vaccine carriers for an improved and efficacious tumor therapy. . 2011.

121. Krishnamachari Y, Salem AK. Innovative strategies for co-delivering antigens and CpG oligonucleotides. *Adv Drug Deliv Rev*. 2009;61(3):205-217.

122. Cruz LJ, Tacken PJ, Fokkink R, et al. Targeted PLGA nano-but not microparticles specifically deliver antigen to human dendritic cells via DC-SIGN in vitro. *J Controlled Release*. 2010;144(2):118-126.

123. Palucka K, Banchereau J. Cancer immunotherapy via dendritic cells. *Nature Reviews Cancer*. 2012;12(4):265-277.

124. Palucka K, Ueno H, Zurawski G, Fay J, Banchereau J. Building on dendritic cell subsets to improve cancer vaccines. *Curr Opin Immunol*. 2010;22(2):258-263.

125. Kim B, Jones HP. Epinephrine-primed murine bone marrow-derived dendritic cells facilitate production of IL-17A and IL-4 but not IFN-γ by CD4< sup> </sup> T cells. *Brain Behav Immun*. 2010;24(7):1126-1136.

126. Manish M, Rahi A, Kaur M, Bhatnagar R, Singh S. A single-dose PLGA encapsulated protective antigen domain 4 nanoformulation protects mice against bacillus anthracis spore challenge. *PloS one*. 2013;8(4):e61885.

127. Drabkin DL, Austin JH. Spectrophotometric studies II. preparations from washed blood cells; nitric oxide hemoglobin and sulfhemoglobin. *J Biol Chem*. 1935;112(1):51-65.

128. Sheng K, Pietersz GA, Wright MD, Apostolopoulos V. Dendritic cells: Activation and maturation-applications for cancer immunotherapy. *Curr Med Chem*. 2005;12(15):1783-1800.

129. Hamdy S, Haddadi A, Hung RW, Lavasanifar A. Targeting dendritic cells with nano-particulate PLGA cancer vaccine formulations. *Adv Drug Deliv Rev*. 2011;63(10):943-955.

130. Nixon DF, Hioe C, Bian Z, et al. Synthetic peptides entrapped in microparticles can elicit cytotoxic T cell activity. *Vaccine*. 1996;14(16):1523-1530.

131. Honary S, Zahir F. Effect of zeta potential on the properties of nano-drug delivery systems-a review (part 2). *Tropical Journal of Pharmaceutical Research*. 2013;12(2):265-273.

132. Fröhlich E. The role of surface charge in cellular uptake and cytotoxicity of medical nanoparticles. *International journal of nanomedicine*. 2012;7:5577.

133. Yue Z, Wei W, Lv P, et al. Surface charge affects cellular uptake and intracellular trafficking of chitosan-based nanoparticles. *Biomacromolecules*. 2011;12(7):2440-2446.

134. Ranjan AP, Mukerjee A, Helson L, Vishwanatha JK. Scale up, optimization and stability analysis of curcumin C3 complex-loaded nanoparticles for cancer therapy. *J Nanobiotechnology*. 2012;10(38):20.

135. Ikeda H, Old LJ, Schreiber RD. The roles of IFNγ in protection against tumor development and cancer immunoediting. *Cytokine Growth Factor Rev*. 2002;13(2):95-109.

136. Lamagna C, Aurrand-Lions M, Imhof BA. Dual role of macrophages in tumor growth and angiogenesis. *J Leukoc Biol*. 2006;80(4):705-713. doi: jlb.1105656 [pii].

137. Melief CJ. " License to kill" reflects joint action of CD4 and CD8 T cells. *Clinical Cancer Research*. 2013.

138. Perez-Diez A, Joncker NT, Choi K, et al. CD4 cells can be more efficient at tumor rejection than CD8 cells. *Blood*. 2007;109(12):5346-5354.

139. Ardavín C, Amigorena S, e Sousa CR. Dendritic cells: Immunobiology and cancer immunotherapy. *Immunity*. 2004;20(1):17-23.

140. Cella M, Sallusto F, Lanzavecchia A. Origin, maturation and antigen presenting function of dendritic cells. *Curr Opin Immunol*. 1997;9(1):10-16.

141. Park Y, Lee SJ, Kim YS, et al. Nanoparticle-based vaccine delivery for cancer immunotherapy. *Immune network*. 2013;13(5):177-183.

142. Noh Y, Hong JH, Shim S, et al. Polymer nanomicelles for efficient mucus delivery and Antigen-Specific high mucosal immunity. *Angewandte Chemie*. 2013;125(30):7838-7843.

143. Reddy ST, van der Vlies, André J, Simeoni E, et al. Exploiting lymphatic transport and complement activation in nanoparticle vaccines. *Nat Biotechnol*. 2007;25(10):1159-1164.